# Exceptional Event Demonstration for Ozone Exceedances in Clark County, Nevada – August 3, 2020

Final Report Prepared for

U.S. EPA Region 9
San Francisco, CA

September 2021

This document contains blank pages to accommodate two-sided printing.

Exceptional Event Demonstration for Ozone Exceedances in Clark County, Nevada – August 3, 2020

Prepared by

Steve Brown, PhD
Crystal McClure, PhD
Cari Gostic
David Miller, PhD
Nathan Pavlovic
Charles Scarborough
Ningxin Wang, PhD

Sonoma Technology
1450 N. McDowell Blvd., Suite 200
Petaluma, CA 94954
Ph 707.665.9900 | F 707.665.9800
sonomatech.com

Prepared for

Clark County Department of Environment
and Sustainability
Division of Air Quality
4701 W. Russell Road, Suite 200
Las Vegas, NV 89118
Ph 702.455.3206
www.clarkcountynv.gov

Cover graphic illustrates the transport of smoke from the Apple Fire to Clark County, Nevada. See Section 3.1.3 for more information.

Contents

Figures

Tables

Executive Summary

On August 3, 2020, Clark County experienced an atypical episode of elevated ambient ozone. During this episode, the 2015 8-hr ozone National Ambient Air Quality Standards (NAAQS) threshold was exceeded at the Paul Meyer, Walter Johnson, Joe Neal, Green Valley, Boulder City, Jean, and Indian Springs monitoring sites. The exceedance at the Paul Meyer, Walter Johnson, and Joe Neal sites could lead to an ozone nonattainment designation for the Clark County area. Air trajectory analysis and air quality modeling results show that emissions from wildfires burning in southern California contributed to the transport to and formation of ozone in Clark County. The U.S. Environmental Protection Agency (EPA) Exceptional Event Rule (U.S. Environmental Protection Agency, 2016) allows air agencies to omit air quality data from the design value calculation if it can be demonstrated that the measurement in question was caused by an exceptional event. This report describes analyses that help to establish a clear causal relationship between wildfire smoke and the August 3, 2020, ozone exceedances at all seven monitoring sites.

The analyses we conducted provide evidence supportive of wildfire smoke and impacts on ozone concentrations in Clark County. We show that (1) smoke was transported from a wildfire in southern California to the surface in the Clark County area in the hours leading up to the exceedance date and on the exceedance date; (2) wildfire smoke impacted the typical diurnal profiles of ground-level pollution measurements, including CO and $PM_{2.5}$, in the Clark County area on August 3; (3) byproducts and tracers of wildfire combustion were present and elevated at the surface in the Clark County area on August 4, the day after the ozone exceedance; and (4) meteorological regression modeling and similar meteorological day analysis both show that ozone observations on August 3 were unusual in the historical record given the meteorological conditions. Sources of evidence used in these analyses include (1) air quality monitor data to show that supporting pollutant trends at the surface were influenced by wildfire smoke; (2) air trajectory analysis to show transport of smoke-laden air to the Clark County area; (3) media coverage of wildfires and smoke impacts; and (4) meteorological regression modeling and meteorologically similar day analysis.

EPA guidance for exceptional event demonstrations (U.S. Environmental Protection Agency, 2016) provides a three-tiered approach. Depending on the complexity of the event, increasingly involved information may be required to demonstrate a causal relationship between wildfire smoke and an exceedance. Here, we provide the results of analyses conducted to address Tier 1, Tier 2, and Tier 3 exceptional event demonstration requirements.

These analyses show that smoke was transported from a wildfire in southern California to the Clark County area over the hours leading up to August 3. Combined with additional evidence, such as meteorological regression modeling and meteorologically similar day analysis, our results provide key evidence to support smoke impacts on ozone concentrations in Clark County on August 3, 2020.

1.   Overview

1.1   Introduction

The 2020 wildfire season in California was unprecedented, with five of the six largest wildfires in California history occurring in either August or September 2020 (https://www.fire.ca.gov/media/11416/top20_acres.pdf). Smoke emissions from California wildfires can affect downwind areas such as Clark County, Nevada. In particular, smoke emissions from a rapidly growing wildfire in southern California (the Apple Fire) reached Clark County on August 3, 2020. On this date, seven of the 14 ozone (O_3) monitoring locations around Clark County recorded an exceedance of the 2015 National Ambient Air Quality Standard (NAAQS) for 8-hour ozone (0.070 ppm).

Emissions from wildfires can affect concentrations of ozone downwind by direct transport of both ozone and precursor gases (i.e., nitrogen oxides [NO_x] and volatile organic compounds [VOCs]). Each mechanism can cause an enhancement in the overall ozone concentration and/or the amount of ozone that could be produced. For example, in a NO_x-rich area, such as an urban area like Las Vegas, the transport of VOCs from wildfire emissions can enhance the amount of ozone that can be produced, potentially driving concentrations above the ozone standard. According to EPA guidance (U.S. Environmental Protection Agency, 2016), exceptional events such as wildfires that affect ozone concentrations can be subject to exclusion from calculations of NAAQS attainment if a clear causal relationship can be established between a specific event and the monitoring exceedance.

For the August 3, 2020, case in Clark County, we describe the clear causal relationship between the event causing the exceedance (the Apple Fire in southern California) and the event's effects on the seven monitoring sites in Clark County that recorded an exceedance of the maximum daily 8-hour ozone average (MDA8). The evidence in this report includes all three tiers of analysis required by EPA's Exceptional Event Guidance: for Tier 1, ground and satellite-based measurement of smoke emissions, transport of smoke from the Apple Fire to Clark County, and media coverage of the smoke event in Clark County; for Tier 2, emission vs. distance analysis, ground and satellite analysis of smoke-related pollutants, and comparison of event and non-event concentrations; and for Tier 3, vertical column analyses and Generalized Additive Statistical Modeling (GAM) of the event. The wildfire that affected ozone concentrations in Clark County could not be reasonably controlled or prevented because it was caused by accidental ignition and is unlikely to recur. Table 1-1 lists the sites affected during the August 3 event, as well as their locations and MDA8 ozone concentrations.

Concurrent with this document, Clark County is submitting documentation for other ozone exceptional events in 2018 and 2020 due to wildfires and stratospheric intrusions. These events are mentioned throughout this report and are referred to as "proposed 2018 and 2020 exceptional events," recognizing that discussion with EPA is still pending. All proposed exceptional events for

Clark County in 2018 and 2020 are listed in Tables 1-2 and 1-3. Wherever possible, we calculated statistics to provide context both including and excluding the proposed exceptional events from 2018 and 2020.

Table 1-1. August 3, 2020, exceptional event information. All monitoring sites in Clark County that exceeded the 2015 NAAQS standard on August 3, 2020, are listed along with AQS Site Codes, location information, and MDA8 ozone concentrations.

AQS Site Code	Site Name	Latitude (degrees N)	Longitude (degrees W)	MDA8 O_3 Concentration (ppb)
320030043	Paul Meyer	36.106	-115.253	78
320030071	Walter Johnson	36.170	-115.263	82
320030075	Joe Neal	36.271	-115.238	81
320030298	Green Valley	36.049	-115.053	72
320030601	Boulder City	35.978	-114.846	72
320031019	Jean	35.786	-115.357	73
320037772	Indian Springs	36.569	-115.677	71

Table 1-2. Proposed Clark County 2018 exceptional events. For each site and date combination where the 2015 NAAQS standard was exceeded, the MDA8 ozone concentration is shown in ppb. Blank cells indicate that there was no exceedance on that site/date combination.

Date	Paul Meyer	Walter Johnson	Green Valley	Jerome Mack	Joe Neal	Palo Verde	Jean	Indian Springs	Apex	Boulder City
6/19/2018	72	72	77	75						
6/20/2018	71	74			72					
6/23/2018	72	76	75	72	72	71	77	73		
6/27/2018	75	76	78	76	72	72	81	78	74	72
7/14/2018	72		78	78						
7/15/2018		71	73	73	78					
7/16/2018	75	79	71	73	80	75				
7/17/2018	74	77				74				
7/25/2018	71	72	72							
7/26/2018	72	75	77	77					71	
7/27/2018	72	74			76					
7/30/2018			73	72						
7/31/2018		73			73					
8/6/2018	79	77	74	71	76	72			74	
8/7/2018	73	74	72	71	74				71	

Table 1-3. Proposed Clark County 2020 exceptional events. For each site and date combination where the 2015 NAAQS standard was exceeded, the MDA8 ozone concentration is shown in ppb. Blank cells indicate that there was no exceedance on that site/date combination.

Date	Walter Johnson	Paul Meyer	Joe Neal	Jerome Mack	Green Valley	Boulder City	Jean	Indian Springs	Apex
5/6/2020	78	77	76	73	72		75		76
5/9/2020	71	74							
5/28/2020	71	76							
6/22/2020	73	74	78						
6/26/2020		73							
8/3/2020	82	78	81		72	72	73	71	
8/7/2020	71		72					72	
8/18/2020	82	79	78						
8/19/2020	74	74	73		71				
8/20/2020			71						
8/21/2020		71							
9/2/2020	75	73							
9/26/2020	71		75						

1.2   Exceptional Event Rule Summary

The "EPA Guidance on the Preparation of Exceptional Events Demonstration for Wildfire Events that May Influence Ozone Concentrations" (U.S. Environmental Protection Agency, 2016) describes a three-tier analysis approach to determine a "clear causal relationship" for exceptional events demonstrations from an air agency. A summary of analysis requirements for each tier is listed in Table 1-4.

- Tier 1 analyses can be used when ozone exceedances are clearly influenced by a wildfire in areas of typically low ozone concentrations, are associated with ozone concentrations higher than non-event-related values, or occur outside of an area's usual ozone season.

- Tier 2 analyses are appropriate for wildfire emission cases where the impacts of the wildfire on ozone levels are less clear and require more supportive documentation than Tier 1 analyses.

- If a more complicated relationship between the wildfire and the ozone exceedance is observed, Tier 3 analyses with additional supportive documentation—such as statistical modeling of the ozone event, vertical profile analysis of smoke in the column, and meteorological analysis—should be used.

In this work, we conduct all the recommended Tier 1, Tier 2 and Tier 3 analyses.

Table 1-4. Tier 1, 2, and 3 exceptional event analysis requirements for evaluating wildfire impacts on ozone exceedances.

Tier	Requirements
1	- Comparison of fire-influenced exceedance with historical concentrations - Key factor: Evidence that fire and monitor meet one of the following criteria: — Seasonality differs from typical season, or — Ozone concentrations are 5-10 ppb higher than non-event-related concentrations - Evidence of transport of fire emissions to monitor: — Trajectories of fire emissions (reaching ground level) — Satellite Images and supporting evidence from surface measurements — Media coverage and photographic evidence of smoke
2	- All Tier 1 requirements - Key Factor #1: Fire emissions and distance of fires - Key Factor #2: Comparison of the event-related ozone concentration with non-event-related high ozone concentrations (high percentile rank over five years/seasons) — Annual and Seasonal Comparison - Evidence that fire emissions affected the monitor (at least one of the following): — Visibility impacts — Changes in supporting measurements — Satellite enhancements of fire-related species (i.e., NO_x, CO, AOD, etc.) — Fire-related enhancement ratios and/or tracer species — Differences in spatial/temporal patterns
3	- All Tier 2 requirements - Evidence of fire emissions effects on monitor: — Multiple analyses from those listed for Tier 2 - Evidence of fire emissions transport to the monitor: — Trajectory or satellite plume analysis, and — Additional discussion of meteorological conditions - Additional evidence such as: — Comparison to ozone concentrations on matching (meteorologically similar) days — Statistical regression modeling — Photochemical modeling of smoke contributions to ozone concentrations

1.3   Demonstration Outline

As discussed in Section 1.2, the "clear causal relationship" analyses involve first comparing the exceedance ozone concentrations to historical values, providing evidence that the event and monitors meet the tier's key factors, providing evidence of transport of wildfire emissions to monitors, and additional analyses such as ground-level measurements and various forms of modeling depending on the complexity of the event. Table 1-5 summarizes the key factors and additional supporting evidence of the tiered approach, and shows the corresponding sections for each analysis in this report.

Table 1-5. Locations of Tier 1, 2, and 3 elements in this report.

Tier	Element	Section of This Report (Analysis Type)
Tier 1	Key Factor: seasonality differs from typical season and/or ozone concentrations are 5-10 ppb higher than non-event-related concentrations	Section 3.1.1 (comparison of event with historical data)
	Evidence of transport of fire emissions to monitor	Sections 3.1.2 (maps of ozone, $PM_{2.5}$ fire, smoke, visible satellite imagery), 3.1.3 (HYSPLIT trajectories)
	Media coverage and photographic evidence of smoke	Section 3.1.4 (Media coverage and Images)
Tier 2	Key Factor #1: fire emissions and distance of fires	Section 3.2.1 (Q/d analysis)
	Key Factor #2: comparison of event concentrations with non-event-related high ozone concentrations	Section 3.2.2 (comparison of event concentrations with non-event concentrations)
	Evidence that the fire emissions affected the monitor	Sections 3.2.3 (visibility impacts, satellite NO_x (and other pollutant) enhancements), 3.2.4 (changes in supporting measurements, differences in spatial/temporal patterns, and tracer measurements)
Tier 3	Evidence of fire emissions transport to the monitor	Section 3.3.1 (trajectory or satellite plume analysis, additional discussion of meteorological conditions, comparison to ozone concentrations on matching [meteorologically similar] days)
	Meteorologically similar matching day analysis	Section 3.3.2 (methodology and analysis for meteorologically similar days)
	Additional evidence	Section 3.3.3 (statistical regression modeling)

The key factor of Tier 1 analyses is the ozone concentration's uniqueness when compared to the typical seasonality and/or levels of ozone exceedance. The EPA guidance (U.S. Environmental Protection Agency, 2016) suggests providing a time series plot of 12 months of ozone concentrations overlaying more than five years of monitored data and describing how typical seasonality differs from ozone in the demonstration. In addition, trajectory analysis, produced by the Hybrid Single-Particle Lagrangian Integrated Trajectory (HYSPLIT) model, together with satellite plume imagery and ground-level measurements of plume components (e.g., $PM_{2.5}$, CO, or organic and elemental carbon) should be used to provide evidence of wildfire emissions being transported to the monitoring sites. We demonstrate the Tier 1 analysis results for the August 3, 2020, event in Section 3.1. We address the key factor in Section 3.1.1, provide evidence of wildfire smoke transport to the Clark County monitoring sites in Sections 3.1.2 and 3.1.3, and discuss the media coverage and show ground images in Section 3.1.4.

The two key factors for Tier 2 analyses are (1) fire emissions and distance of fires to the impacted monitoring sites, and (2) comparison of event-related ozone concentrations with non-event-related high ozone values. In this report, we address the first factor by determining the emissions divided by distance (Q/d) relationship in Section 3.2.1, and we address the second factor in Section 3.2.2 by comparing the 5- and 6-year percentiles and yearly rank-order analysis of ozone concentrations. The Tier 2 analyses also require evidence of wildfire smoke transport to affected monitoring sites. We provide this evidence in Section 3.2.3 with satellite measurements of pollutant concentrations. In Section 3.2.4, we discuss supporting pollutant trends and diurnal patterns of $PM_{2.5}$, CO, NO_x, and total non-methane organic carbon (TNMOC) compared with ozone concentrations and wildfire tracer measurements.

Tier 3 analyses are shown in Section 3.3. We investigated total column information and event-related meteorological conditions (Section 3.3.1), analyzed meteorologically similar days to find typical ozone concentrations for the exceptional event's specific meteorological conditions (Section 3.3.2), and developed a Generalized Additive Statistical Model (GAM) to estimate the wildfire's contribution to ozone concentrations (Section 3.3.3).

Following the EPA's exceptional event guidance, we performed Tier 1, Tier 2 and Tier 3 analyses to show the "clear causal relationship" between the Apple Fire in southern California and the exceedance event in Clark County, Nevada, on August 3, 2020. Focusing on the characterization of the meteorology, smoke, transport, and air quality on the days leading up to the event, we conducted the following specific analyses, the results of which are presented in Section 3:

- Developed time series plots that show the August 3 ozone concentrations in historical context for 2020 and for the past five years at each affected monitoring site

- Compiled maps of ozone and $PM_{2.5}$ concentrations in the area, smoke plumes, and fire locations from satellite data

- Showed the transport patterns via HYSPLIT modeling, and identified where the back trajectory air mass intersected with smoke plumes or passed over or near fires

- Discussed media coverage of the August 3 event and showed ground images

- Quantified total fire emissions and calculated emissions/distance ratio (Q/d) for the fire

- Performed statistical analysis to compare event ozone concentrations to non-event concentrations

- Provided maps showing satellite retrievals of NO_x, Aerosol Optical Depth (AOD), and CO

- Developed plots to show diurnal patterns of ozone and supporting pollutants such as $PM_{2.5}$, CO, NO_x, and TNMOC

- Examined wildfire tracer species and their background concentrations vs. event concentrations

- Assessed vertical transport of smoke using satellite-observed aerosol vertical profiles and ceilometer mixing height retrievals

- Performed meteorologically similar matching ozone day analysis to assess typical concentrations of ozone given meteorological parameters

- Created a GAM model of MDA8 ozone concentrations to assess the enhancement of ozone concentrations due to wildfire influence

1.4   Conceptual Model

The conceptual model for the exceptional event that led to the ozone exceedances at the Paul Meyer, Walter Johnson, Joe Neal, Green Valley, Boulder City, Jean, and Indian Springs monitoring sites on August 3, 2020, is outlined in Table 1-5, which provides the analysis techniques performed and evidence for each Tier. This establishes a weight of evidence for the clear causal relationship between the wildfire emissions in southern California and the August 3 exceptional ozone event. We assert that wildfire emissions from the Apple Fire in southern California on August 1 and 2 led to enhanced ozone concentrations in Clark County on August 3 and the MDA8 ozone exceedances at the seven monitoring sites. In support of this assertion, the key points of evidence for the conceptual model are summarized as follows:

1. The August 3 ozone exceedance occurred during a typical ozone season, but event concentrations at all seven exceedance sites were significantly higher than non-event concentrations. Ozone concentrations at both exceedance sites showed a high percentile rank when compared with the past six years and ozone seasons.

2. Hazard Mapping System (HMS) smoke and fire detections, visible satellite imagery, AOD, and upper-level CO show a consistent picture of wildfire emission plumes from the Apple Fire extending northeastward and impacting Clark County on August 2 and 3.

3. Back and forward trajectories from the near-surface boundary layer at the exceedance sites at the time of maximum ozone concentration show consistent transport patterns passing

over the HMS smoke plumes originating from the Apple Fire. The combination of trajectories intersecting fire locations or their associated smoke plumes and a deep mixed layer over Clark County that favors vertical mixing demonstrate that wildfire emissions were transported to the surface in Clark County by August 2-3, 2020.

4. Meteorological conditions on August 3 did not favor enhanced local ozone production when compared with meteorologically similar ozone season days. Average MDA8 ozone across similar days was well below the ozone NAAQS and 10 ppb lower than the August 3 ozone exceedances.

5. GAM model predictions of MDA8 ozone on August 3 are all well below the 70-ppb ozone NAAQS for each exceptional event (EE)-affected site. Using the 75th-95th quantile of positive residuals (observed MDA8 ozone minus GAM-predicted MDA8 ozone), we find a minimum wildfire effect on ozone of 2-13 ppb in Clark County from an atypical source; in this case, the Apple Fire in southern California.

6. Surface $PM_{2.5}$ concentration enhancements overnight prior to the exceedance event upwind of Clark County, unusual midday peaks of surface $PM_{2.5}$ and CO concentrations on the event date in Clark County, and typical $PM_{10}:PM_{2.5}$ ratios indicate the presence of wildfire emissions of ozone precursors at the surface in Clark County coincident with the wildfire plume arrival on August 2 and 3.

2. Historical and Non-Event Model

2.1 Regional Description

Clark County is located in the southern portion of Nevada and borders California and Arizona. Clark County includes the City of Las Vegas, one of the fastest growing metropolitan areas in the United States with a population of approximately 2 million (U.S. Census Bureau, 2010). Las Vegas is located in a 1,600 km^2 desert valley basin at 500 to 900 m above sea level (Langford et al., 2015). It is surrounded by the Spring Mountains to the west (3,000 m elevation) and the Sheep Mountain Range to the north (2,500 m elevation). Three mountain ranges comprise the southern end of the valley. The valley floor slopes downward from west to east, which influences surface wind, temperature, precipitation, and runoff patterns. The Cajon Pass and I-15 corridor to the east is an important atmospheric transport pathway from the Los Angeles Basin into the Las Vegas Valley (Langford et al., 2015). **Figures 2-1 and 2-2** show the topography of the Clark County area and surrounding areas.
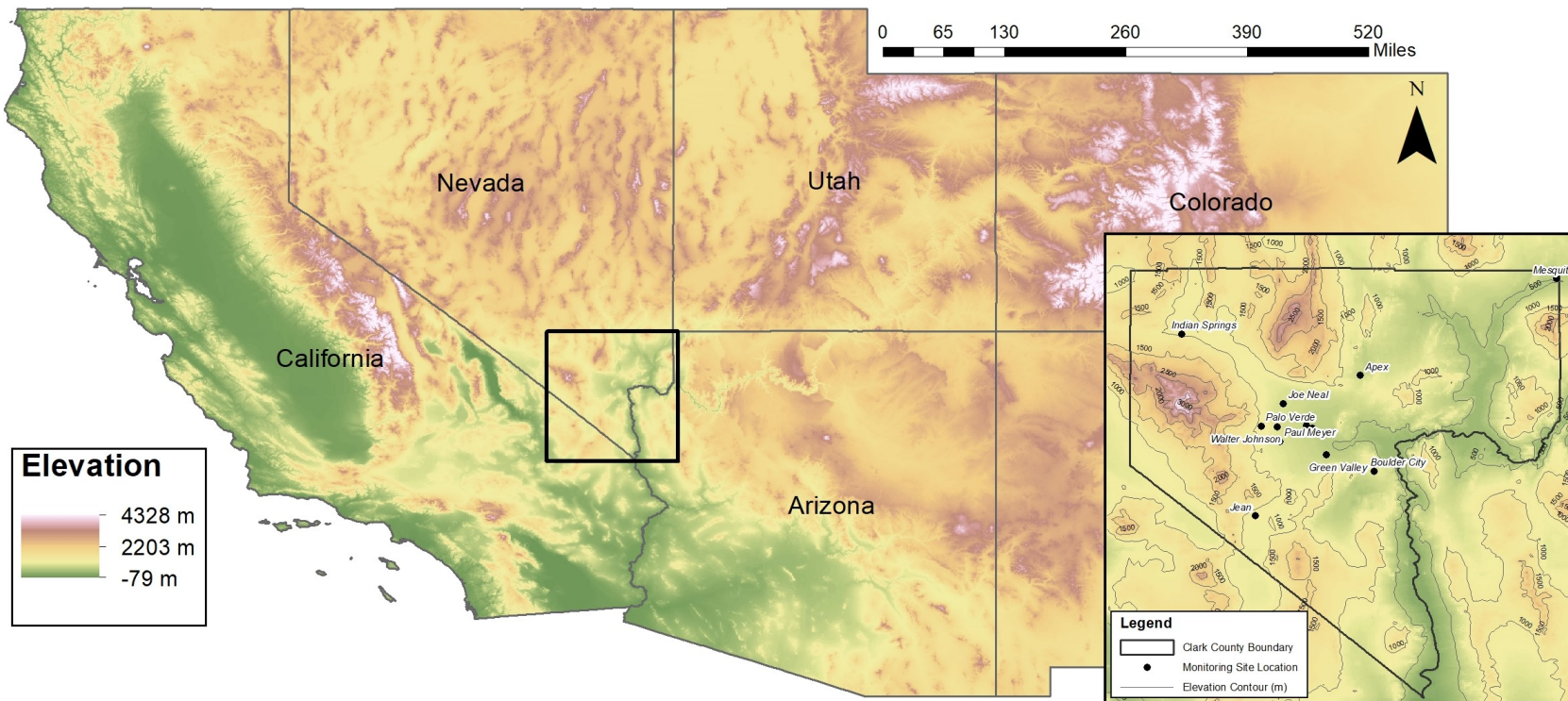
Figure 2-1. Regional topography around Clark County, with an inset showing county boundaries and the air quality monitoring sites analyzed in this report.
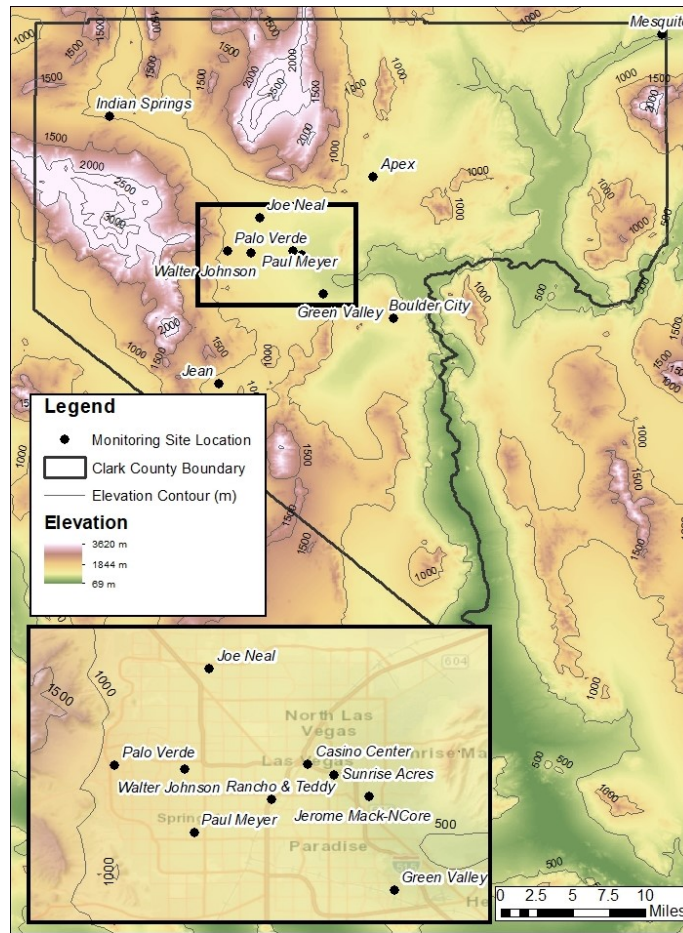
Figure 2-2. Clark County topography, with an inset showing air quality monitoring sites that measure ozone in the Clark County area.

The Las Vegas Valley climatology features abundant sunshine and hot summertime temperatures (average summer month high temperatures of 34°C -40°C). Because of the mountain barriers to moisture inflow, the region experiences dry conditions year-round (~107 mm annual precipitation, 22% of which occurs during the summer monsoon season in July through September). The urban heat island effect in Las Vegas during summer leads to large temperature gradients within the valley, with generally cooler temperatures on the eastern side. During the summer season, monsoon moisture brings high humidity and thunderstorms to the region, typically in July and August (National Weather Service Forecast Office, 2020). Winds in the Las Vegas basin tend to be out of the southwest during spring and summer (Los Angeles is upwind), while winds in the fall and winter tend to be out of the northwest, with air transported between the neighboring mountain ranges and along the valley.

2.2   Overview of Monitoring Network

The Clark County Department of Environment and Sustainability, Division of Air Quality (DAQ) operated 14 ambient air monitoring sites in the region during 2020 (Figure 2-2). These sites measure hourly ozone, particulate matter (PM$_{2.5}$, PM$_{10}$), nitrogen oxides (NO$_x$), TNMOC, and carbon monoxide (CO) concentrations along with meteorological parameters. Table 2-1 presents the monitoring data coverage across time and space for criteria pollutants and surface meteorological parameters (barometric pressure, temperature, wind speed and direction), as well as mixing height. We examined ozone and other criteria pollutants at 11 sites around Clark County to investigate the high ozone event observed on August 3, 2020. DAQ's ambient air monitoring network meets the monitoring requirements for criteria pollutants pursuant to Title 40, Part 58, of the Code of Federal Regulations (CFR), Appendix D. Data are quality-assured in accordance with 40 CFR 58 and submitted to the EPA's Air Quality System (AQS). The spatial distribution of monitoring sites characterizes the regional air quality in Las Vegas, as well as air quality upwind and downwind of the urban valley region (Figure 2-2). The Jean monitoring site along the I-15 corridor is generally upwind such that it captures atmospheric transport into the region and is least impacted by local sources (Figure 2-2).

Table 2-1. Clark County monitoring site data. The available date ranges of all parameters and monitoring sites used in this report for Clark County, Nevada, are shown. Casino Center and RT are near-road sites that are not used for the exceptional event analysis.

Site	AQS Sitecode	O_3	$PM_{2.5}$	CO	NO	NO_2	TNMOC	Temp.	Wind Speed	Wind Direction	Barom. Pressure	Mixing Height
Apex	320030022	2014-2020						2014-2020	2014-2020	2014-2020		
Boulder City	320030601	2014-2020									2014-2016	
Green Valley	320030298	2015-2020	2014-2020	2020				2016-2020	2014-2020	2014-2020	2014-2016	
Indian Springs	320037772	2014-2020										
Jean	320031019	2014-2020	2014-2020					2014-2020	2014-2020	2014-2020	2014-2016	
Jerome Mack	320030540	2014-2020	2014-2020	2015-2020[1,2]	2015-2020	2015-2020	2020	2014-2020	2014-2020	2014-2020	2014-2020	2020
Joe Neal	320030075	2020	2018-2020	2019-2020		2015-2020		2014-2020	2014-2020	2014-2020	2014-2016	
Mesquite	320030023	2014-2020						2014-2020	2014-2020	2014-2020		
Palo Verde	320030073	2014-2020	2020					2014-2020	2014-2020	2014-2020	2014-2016	
Paul Meyer	320030043	2014-2020	2017-2020					2014-2020	2014-2020	2014-2020	2014-2016	
Walter Johnson	320030071	2014-2020	2020					2015-2020	2015-2020	2015-2020	2014-2016	

[1] CO data invalid at Jerome Mack on Sep. 2, 2020

[2] CO data invalid at Jerome Mack Apr. 28, 2020 – May 20, 2020

2.3 Characteristics of Non-Event Historical Ozone Formation

During the ozone season (April–September) in Clark County, Nevada, ozone concentrations are typically influenced by local formation, transport into the region, and on occasion by exceptional events such as wildfires and stratospheric intrusions. Transport from upwind source regions (e.g., Los Angeles Basin, Mojave Desert, Asia) occurs with southwesterly winds, and southerly transport dominates later in the season due to the summer monsoon (Langford et al., 2015; Zhang et al., 2020). Local precursor emissions are present in Clark County, specifically of NO_x and VOCs from mobile sources, NO_x from natural-gas-fueled power generation NO_x sources, and VOCs from biogenic emissions. Based on 2017 Las Vegas emission inventories, on a typical ozone season weekday there are 98 tons of NO_x emissions per day and 238 tons of VOC emissions per day (Clark County Department of Environment and Sustainability, 2020). On-road mobile sources comprise 40% of NO_x emissions and total mobile emissions comprise 88% of total NO_x emissions during the ozone season. In contrast, 52% of VOC emissions originate from biogenic sources within Clark County. Local emissions and/or precursors transported into the region contribute to ozone formation within Clark County (Langford et al., 2015; Clark County Department of Air Quality, 2019).

In this demonstration, we discuss the impacts of wildfire smoke on ozone concentrations in Clark County on August 3, 2020. In order to fully discern the effect of wildfire smoke on ozone concentrations in Clark County on August 3, 2020, we examine the historical ozone record for all affected sites. *Non-event days* refer to all days other than the August 3 event. Because percentile rankings are sensitive to including the relatively large number of potential EE days during 2018 and 2020, we also provide statistics *excluding potential EE days* (i.e., without including the 2018 and 2020 potential EE days as defined in Tables 1-2 and 1-3 in Section 1). The 8-hour ozone design value (DV) is the three-year running average of the fourth-highest daily maximum 8-hour (MDA8) ozone concentration (40 CFR Part 50, Appendix U). Within Clark County, Las Vegas is classified as an EPA Region 9 marginal nonattainment region with a 73 ppb ozone DV for 2017-2019 (U.S. Environmental Protection Agency, 2020).

Ozone EE days were identified as days with significant wildfire or stratospheric intrusion influence in addition to an MDA8 concentration greater than 0.070 ppm. By this criterion, 15 possible EE days in 2018 and 13 possible EE days in 2020 were identified, with no EE days in 2019 identified.

The August 3, 2020, exceptional event occurred late in the ozone season under hot, dry air, upper-level high pressure and surface low-pressure meteorological conditions favoring subsidence and vertical mixing of wildfire smoke-influenced ozone and precursors to ground level (see Section 3.3.1). Compared with a non-event conceptual model of local precursor emissions contributing to ozone formation at ground level under similar conditions, the August 3 conditions indicate additional influence of transported air masses aloft.

Figures 2-3 through 2-16 depict the six-year historical record and seasonality of MDA8 ozone concentrations at each monitoring site, along with the 99th percentile and NAAQS standard ozone concentrations. August 3 ranks in the top 1% for daily maximum ozone concentration in the six-year historical record at six of seven EE affected monitoring sites. For the six-year historical record, August 3 ranks as at least the third highest MDA8 ozone day for all affected sites (see Table 1-1 for a list of August 3 "affected" monitoring sites) and as the highest MDA8 ozone day for the Walter Johnson, Joe Neal, and Boulder City monitoring sites (Figures 2-3 through 2-16). **Figure 2-17** depicts a two-week ozone diurnal cycle beginning one week before the August 3 event and ending one week after. On August 3, daily maximum ozone concentrations were highest during this two-week period at five of the 11 monitoring sites shown. Hourly ozone concentrations on August 3 are 3 to 10 ppb higher than the next highest non-event ozone daily maximum during the two-week period depicted.
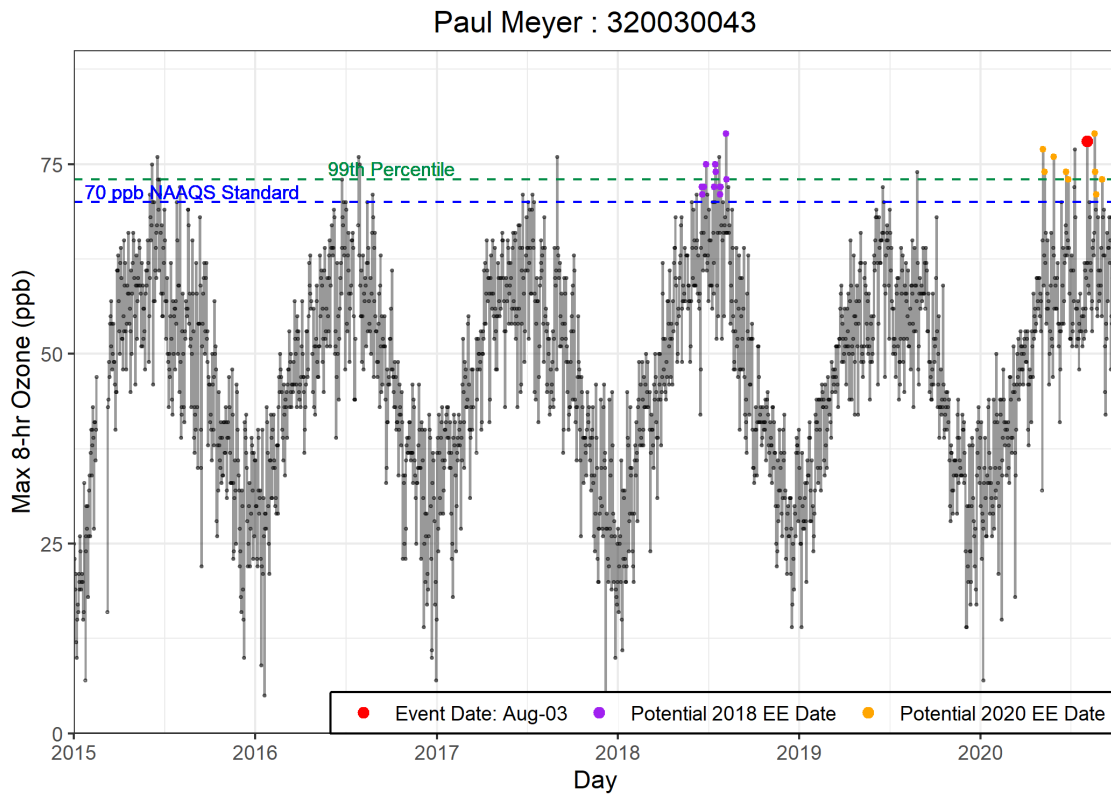
Figure 2-3. Time series of 2015-2020 ozone concentrations at Paul Meyer.
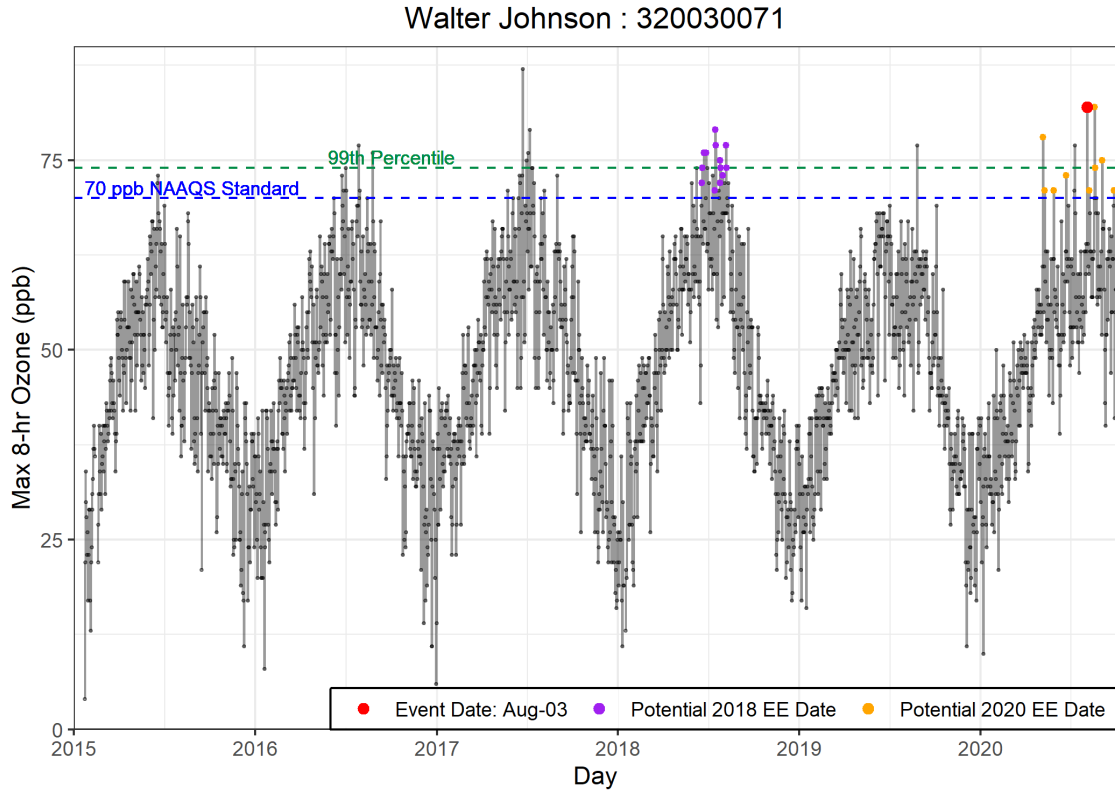
Figure 2-4. Time series of 2015–2020 ozone concentrations at Walter Johnson.
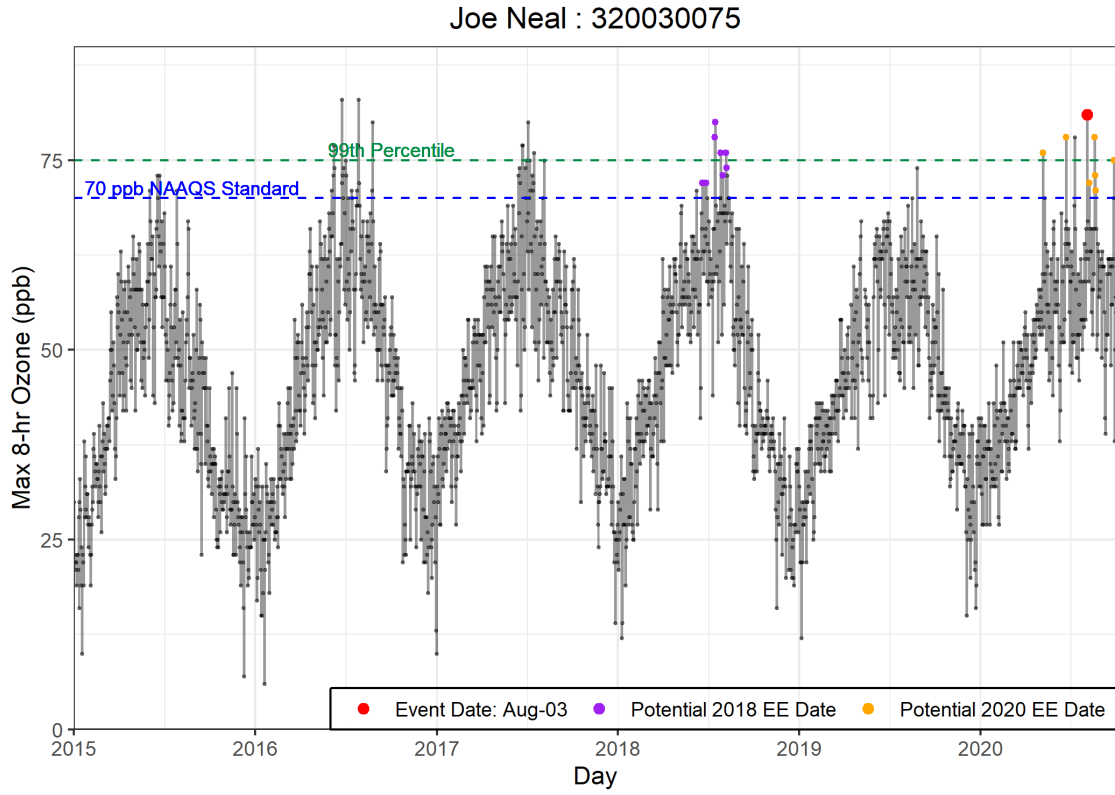
Figure 2-5. Time series of 2015-2020 ozone concentrations at Joe Neal.
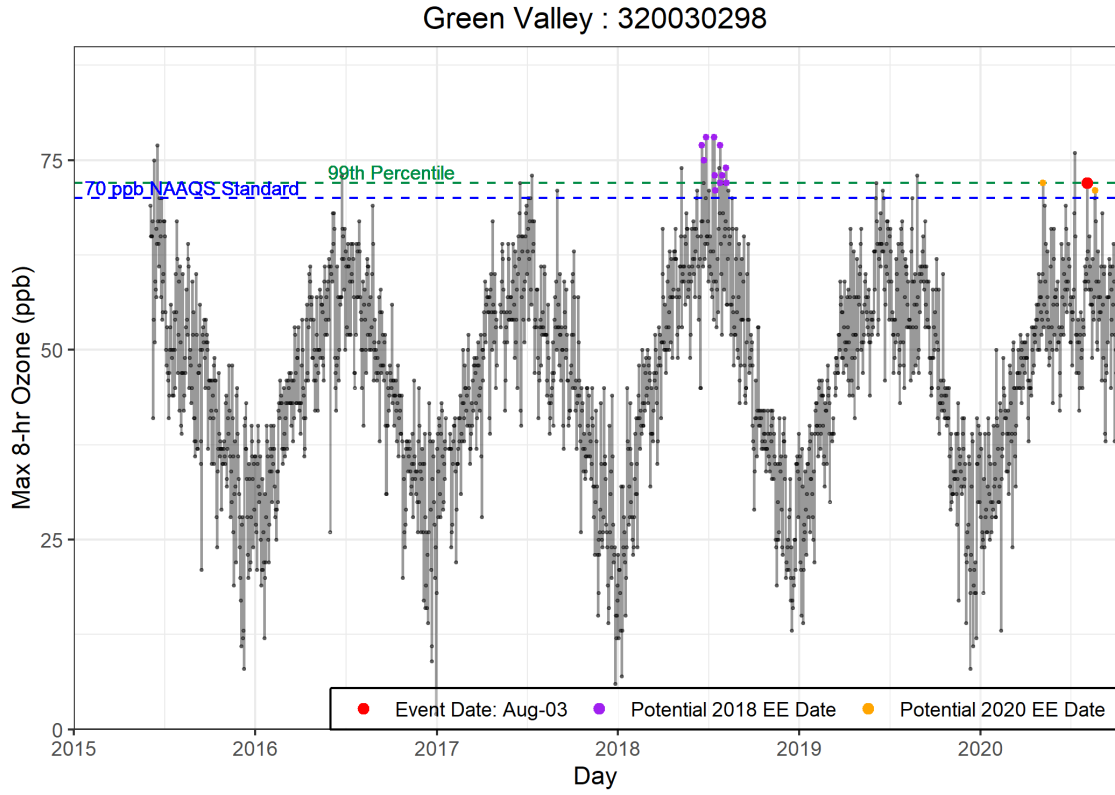
Figure 2-6. Time series of 2015-2020 ozone concentrations at Green Valley.
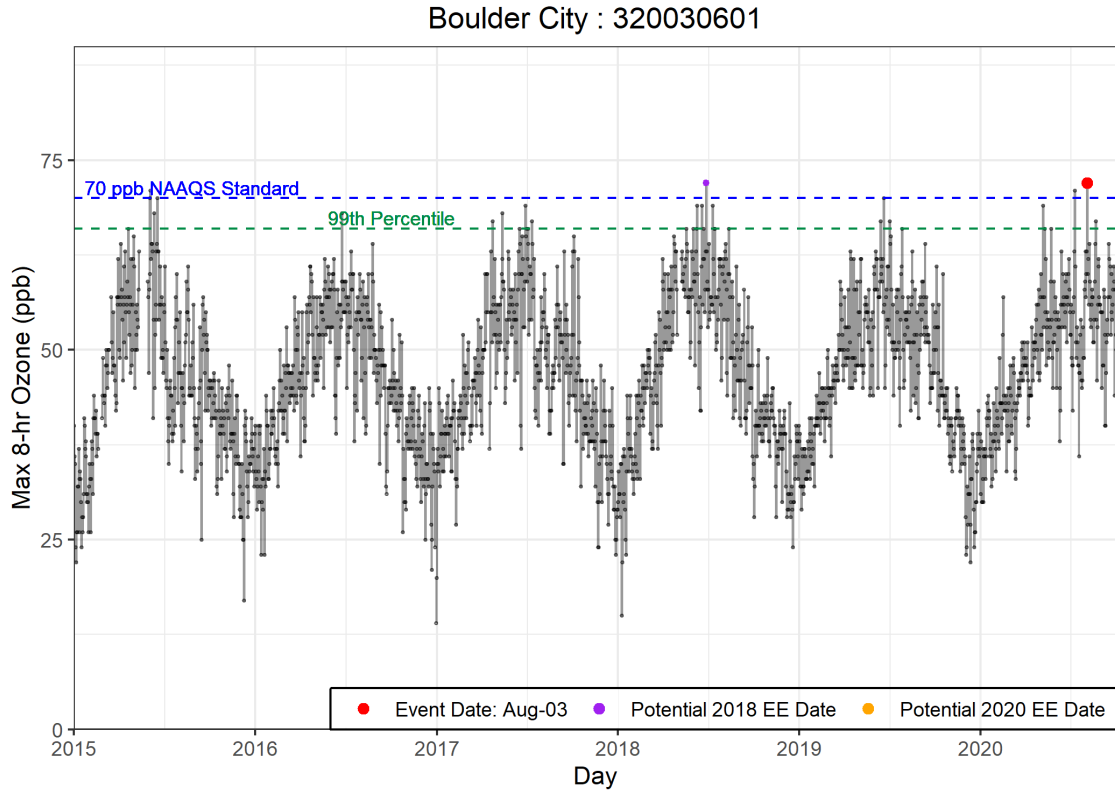
Figure 2-7. Time series of 2015–2020 ozone concentrations at Boulder City.
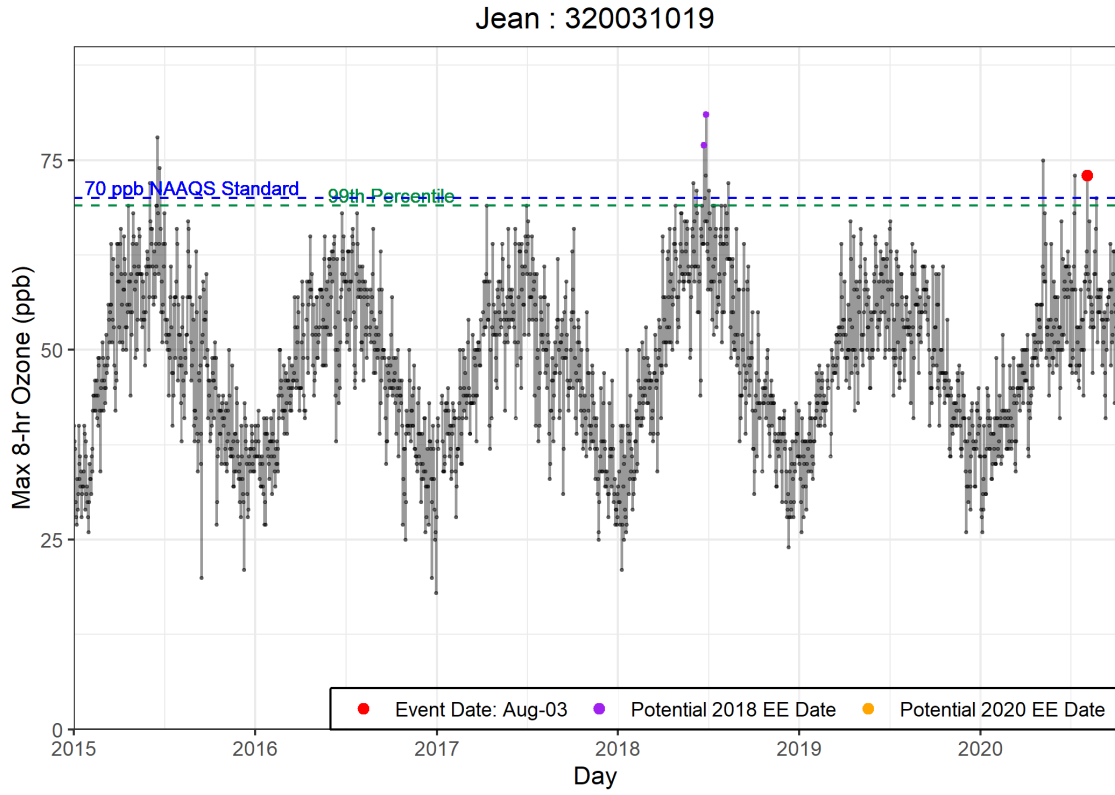
Figure 2-8. Time series of 2015-2020 ozone concentrations at Jean.
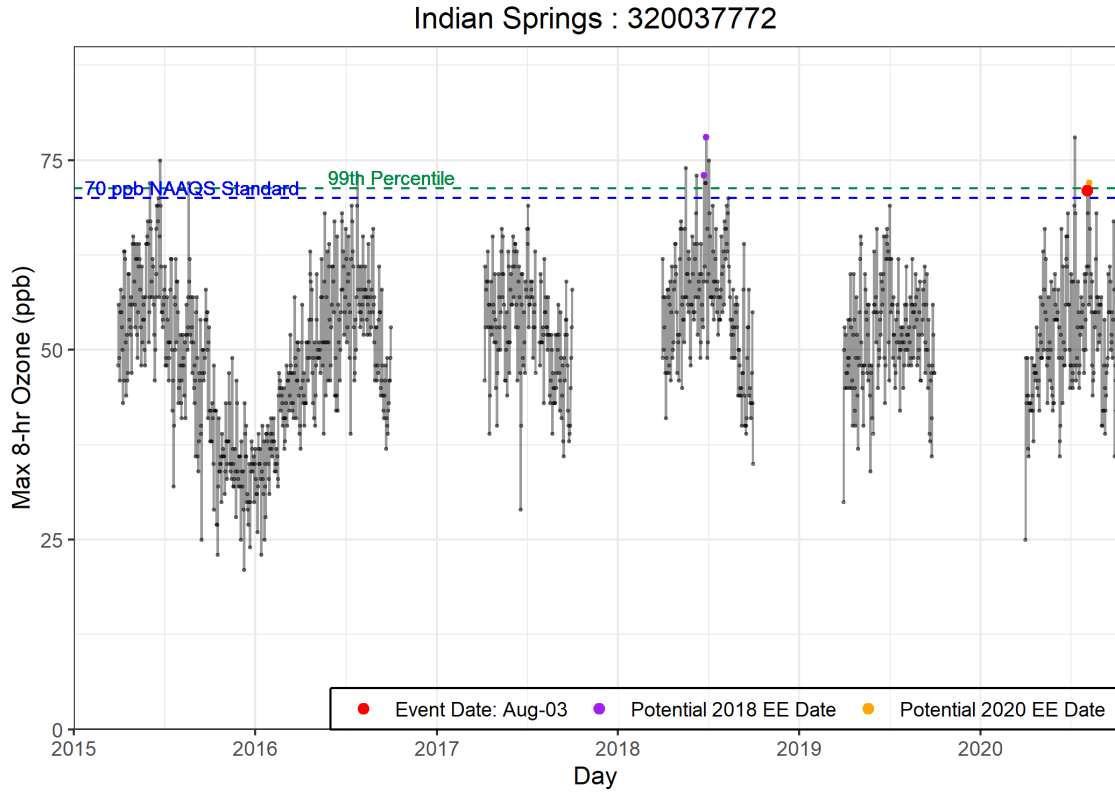
Figure 2-9. Time series of 2015-2020 ozone concentrations at Indian Springs.
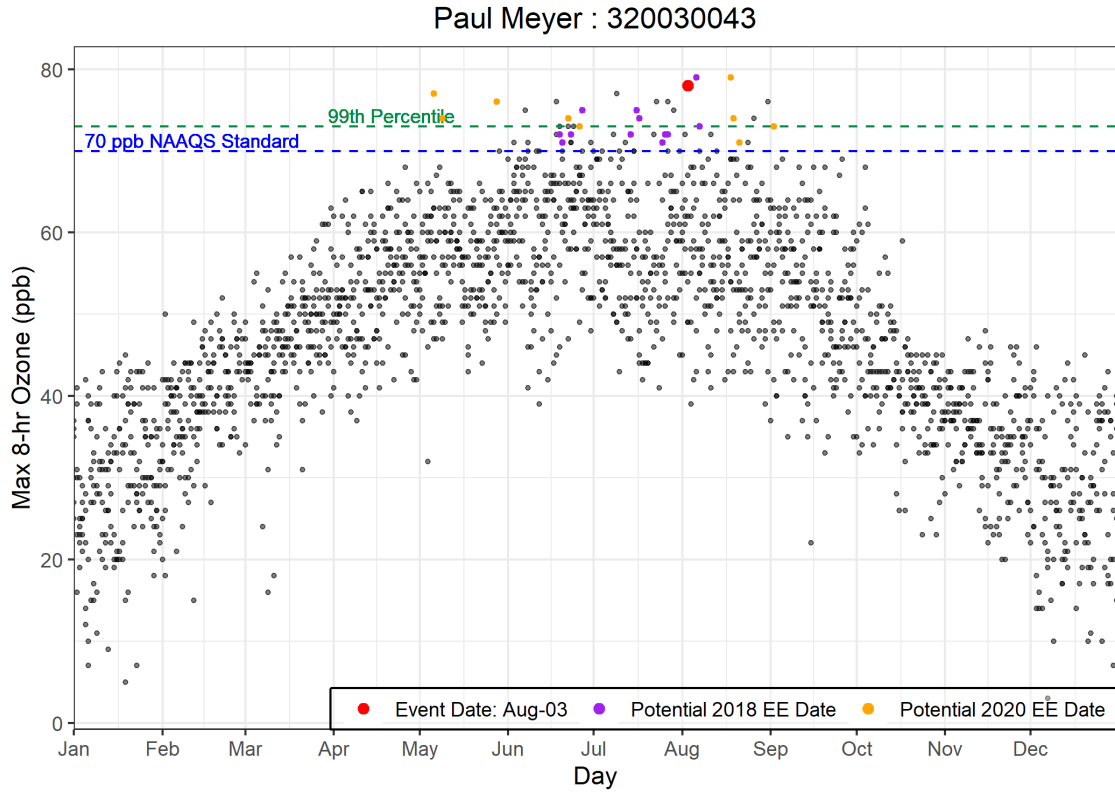
Figure 2-10. Seasonality of 2015-2020 ozone concentrations from Paul Meyer.
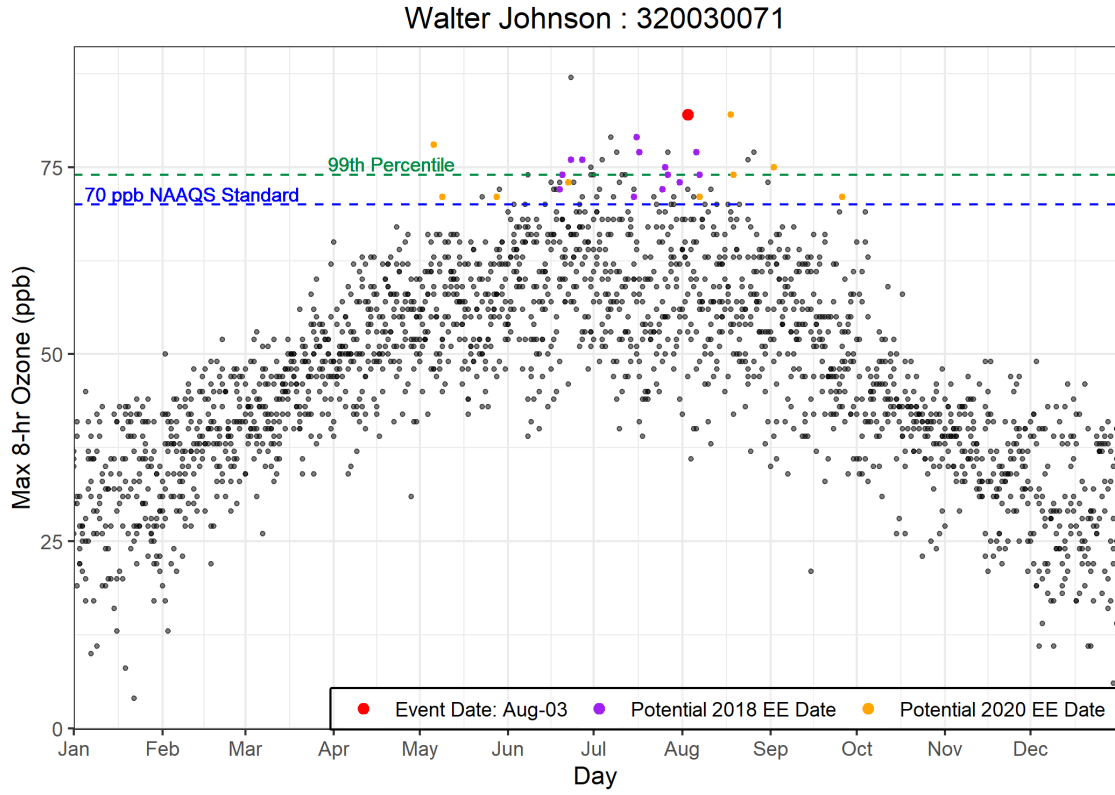
Figure 2-11. Seasonality of 2015-2020 ozone concentrations from Walter Johnson.
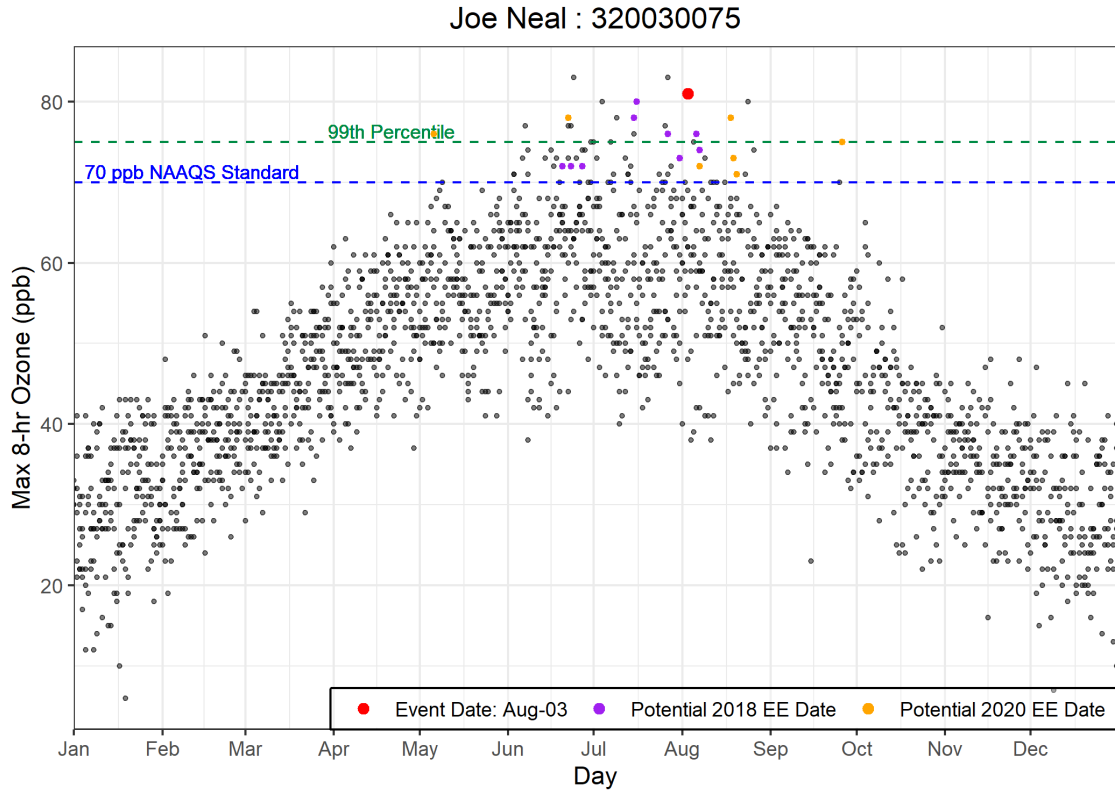
Figure 2-12. Seasonality of 2015-2020 ozone concentrations from Joe Neal.
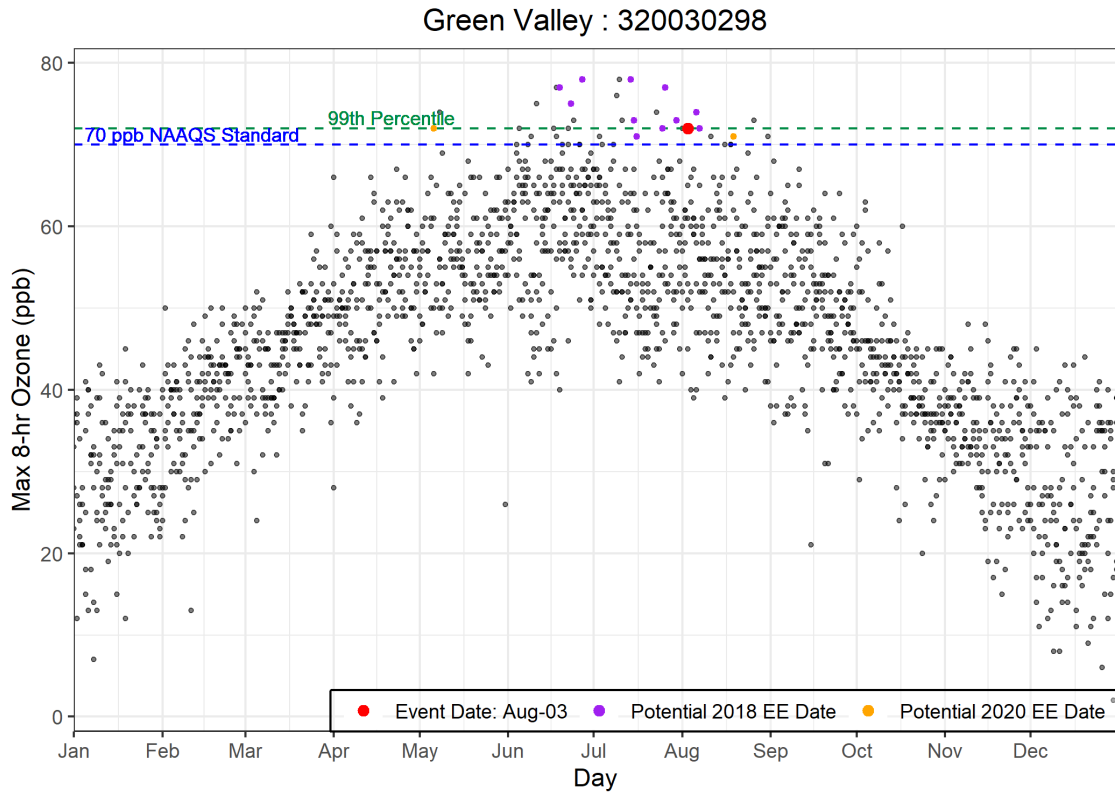
Figure 2-13. Seasonality of 2015-2020 ozone concentrations from Green Valley.
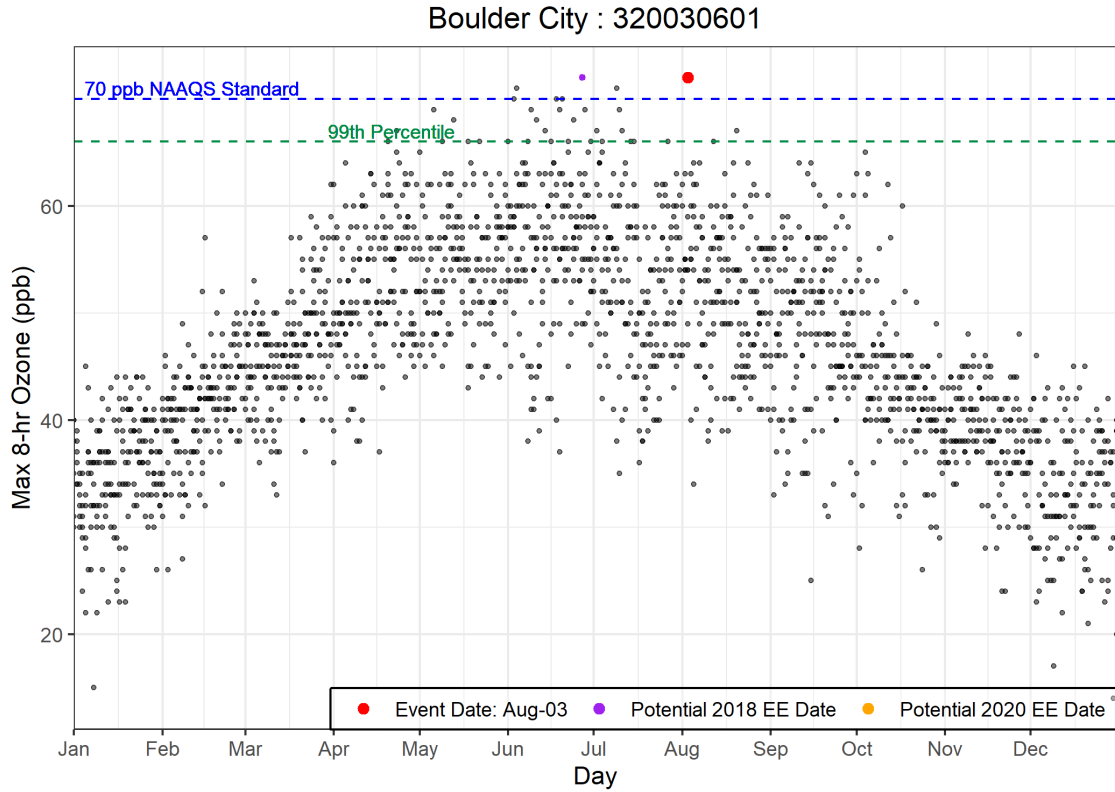
Figure 2-14. Seasonality of 2015-2020 ozone concentrations from Boulder City.
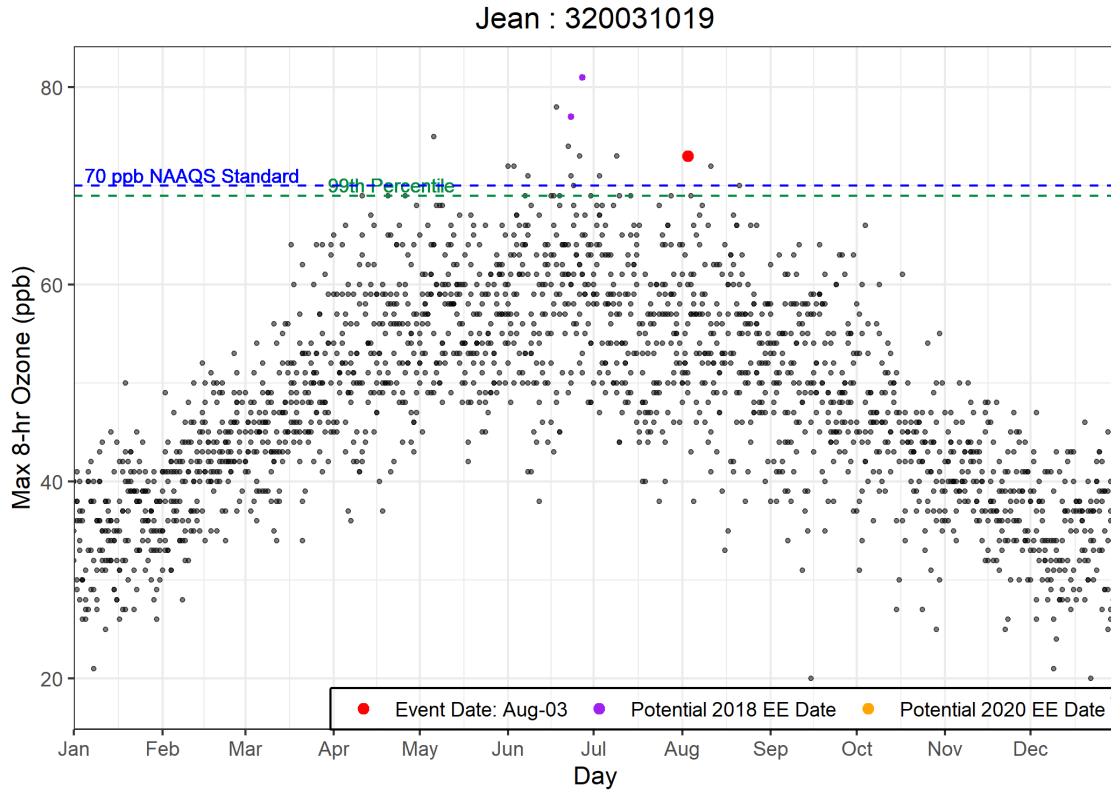
Figure 2-15. Seasonality of 2015-2020 ozone concentrations from Jean.
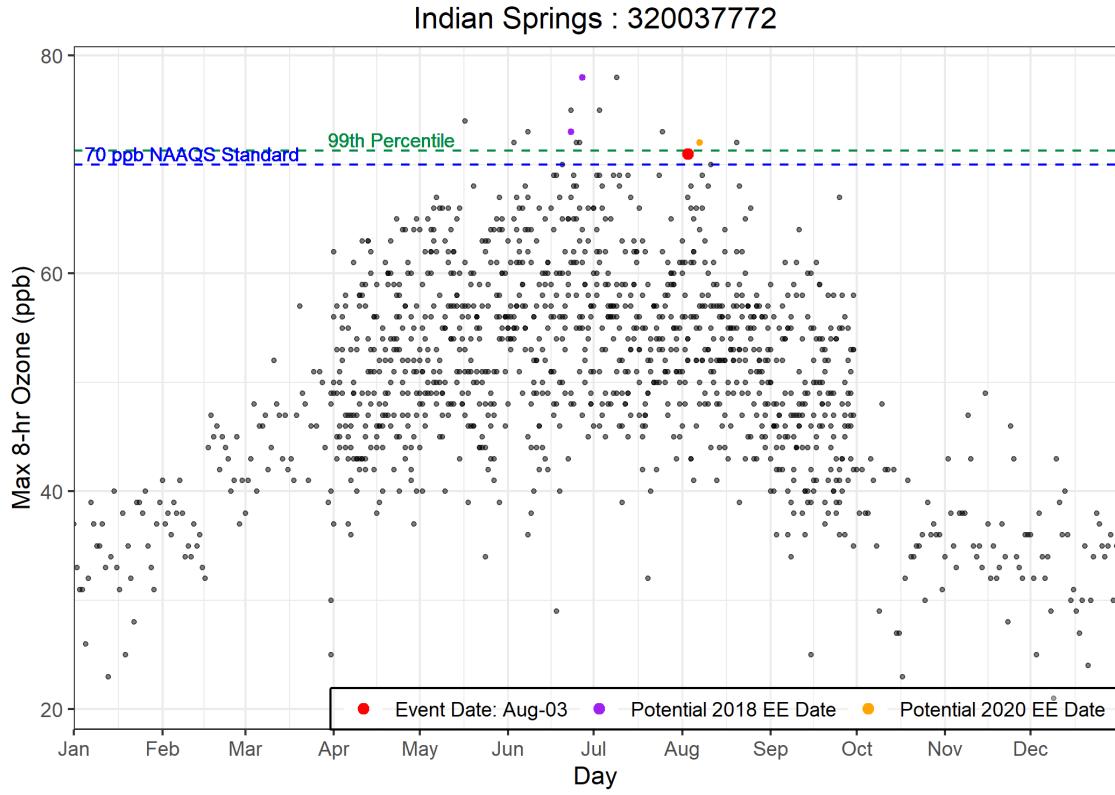
Figure 2-16. Seasonality of 2015-2020 ozone concentrations from Indian Springs.

Hourly O$_3$ Concentration
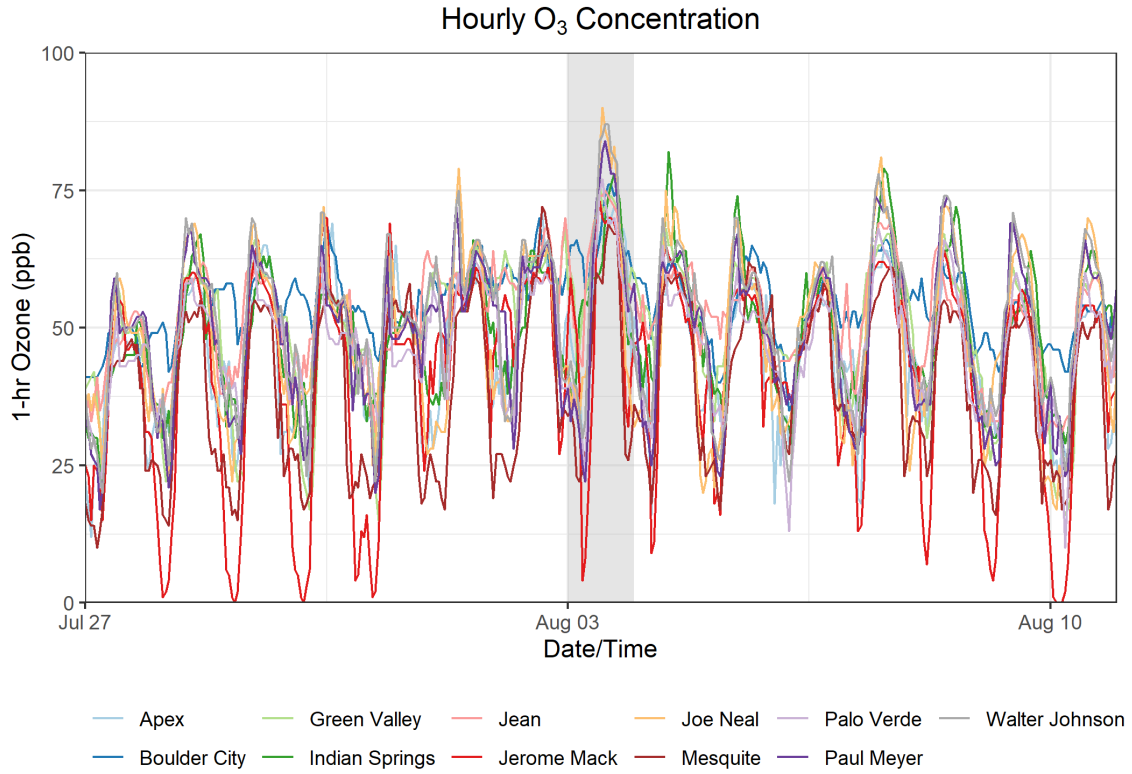
Figure 2-17. Ozone time series at all monitoring sites. Time series of hourly ozone concentrations at monitoring sites in Clark County for one week before and after the August 3 event are shown. August 3, 2020, is shaded for reference.

3. Clear Causal Relationship Analyses

3.1 Tier 1 Analyses

3.1.1 Comparison of Event with Historical Data

To address the Tier 1 exceptional event criterion of comparison with historical ozone, we compared the August 3 exceptional event ozone concentrations at each site with the 2020 ozone record, focusing mainly on the ozone season when highest ozone concentrations occur. **Figures 3-1 through 3-7** depict the 2020 daily maximum ozone record at each monitoring site, along with the 99th percentile of previous 5-year MDA8 ozone and NAAQS criteria ozone concentrations. August 3 ranks in the top 1% for daily maximum ozone concentration during 2020 at six of seven EE-affected monitoring sites. During 2020, August 3 ranks as the highest daily ozone day at the Walter Johnson, Boulder City, and Joe Neal monitoring sites; the second-highest daily ozone day at the Paul Meyer, Green Valley, and Jean monitoring sites; and the third-highest daily ozone day at the Indian Spring monitoring sites (Figures 3-1 through 3-7). When compared with daily ozone rankings on August 3 over the six-year ozone record, the 2020 rankings indicate that August 3, 2020, was an extreme event.
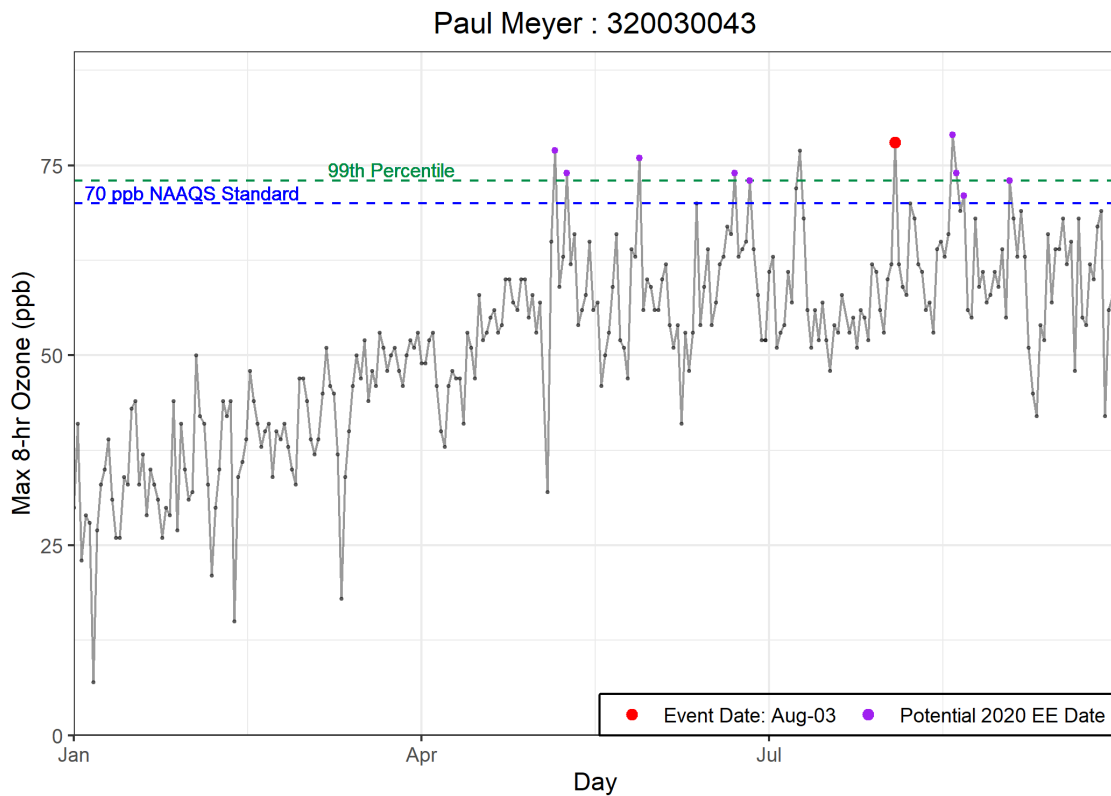
Figure 3-1. Time series of 2020 MDA8 ozone concentrations from Paul Meyer.
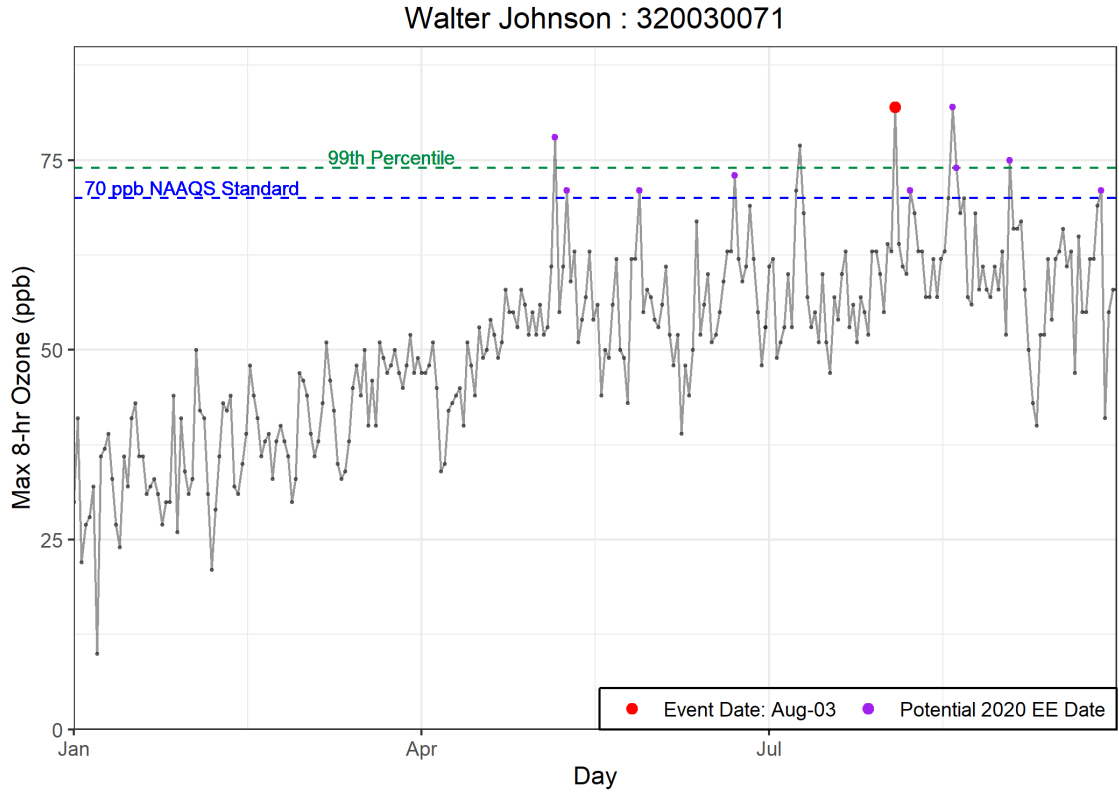
Figure 3-2. Time series of 2020 MDA8 ozone concentrations from Walter Johnson.
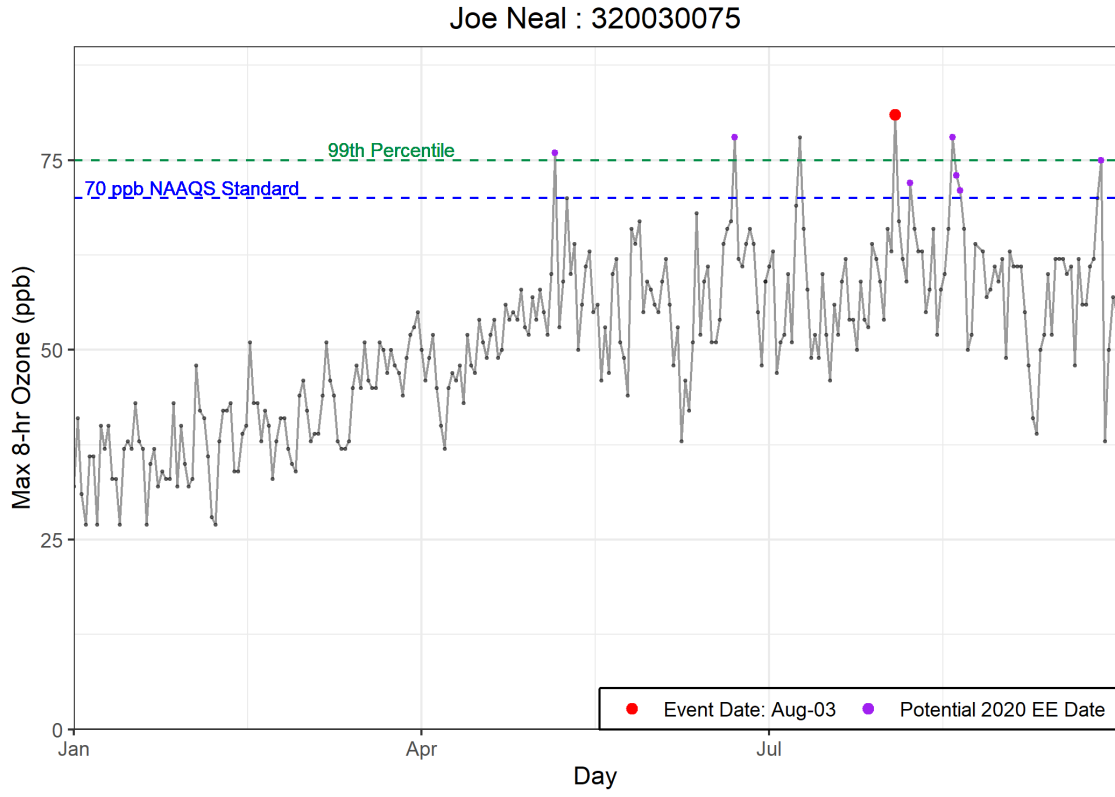
Figure 3-3. Time series of 2020 MDA8 ozone concentrations from Joe Neal.
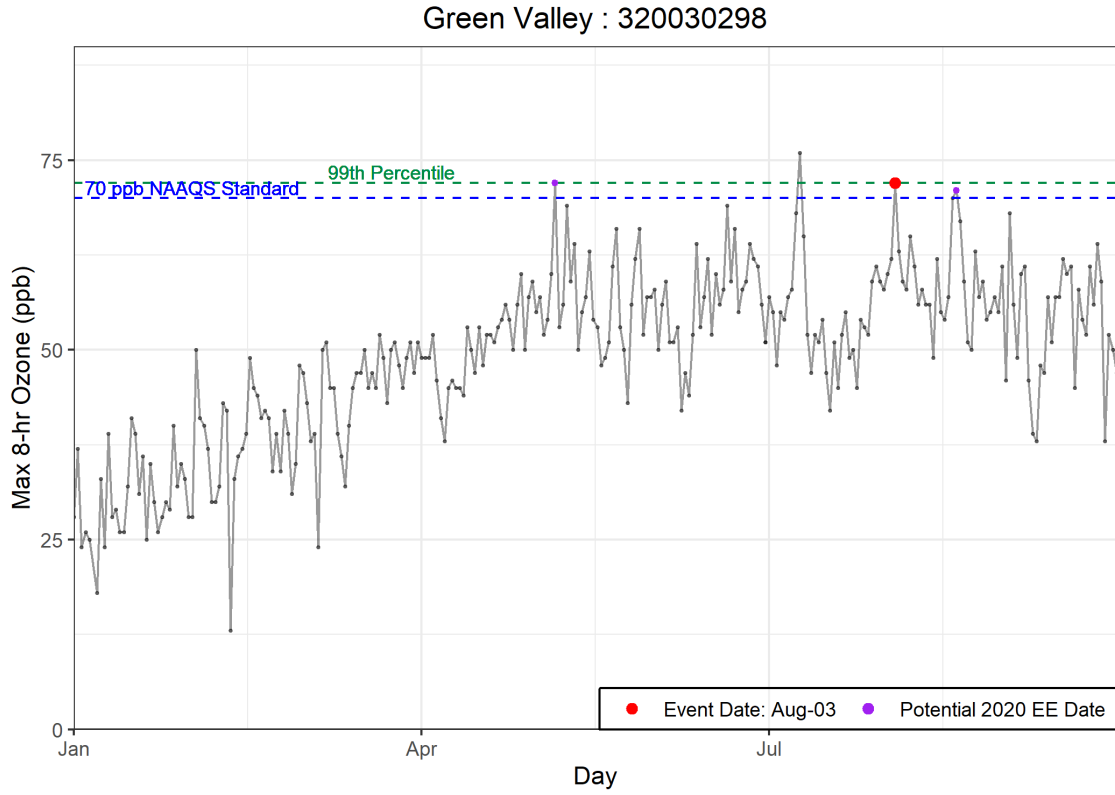
Figure 3-4. Time series of 2020 MDA8 ozone concentrations from Green Valley.
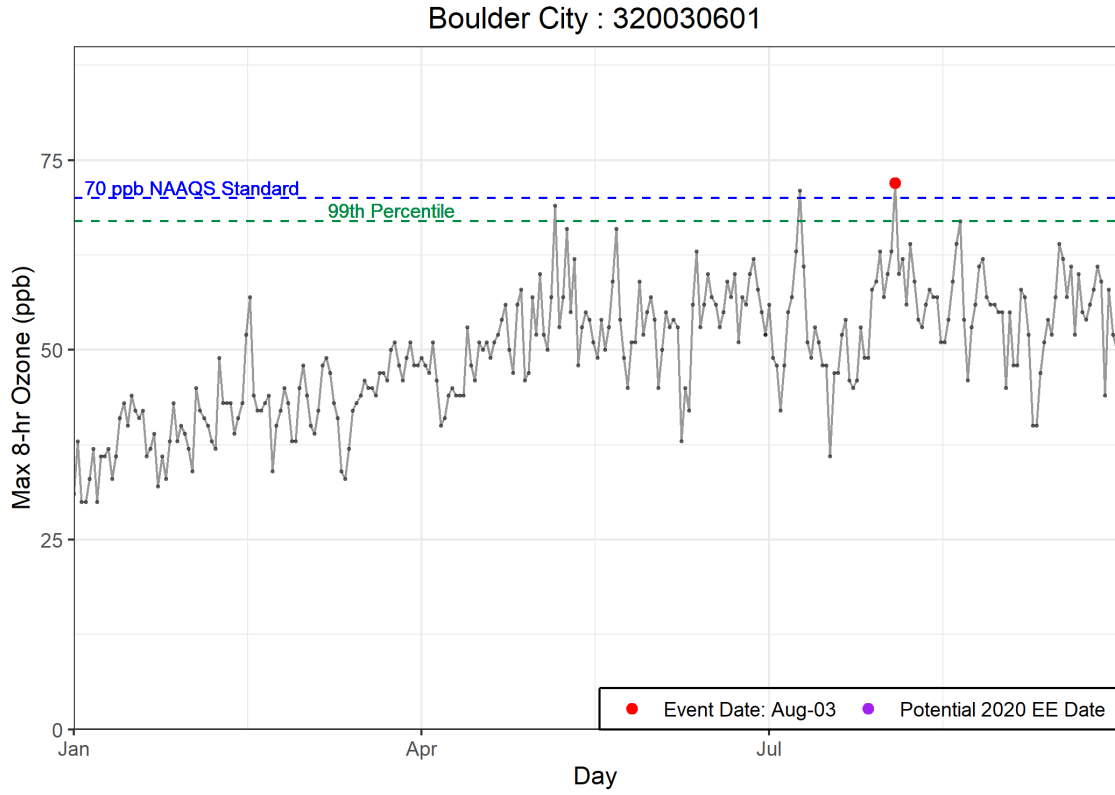
Figure 3-5. Time series of 2020 MDA8 ozone concentrations from Boulder City.
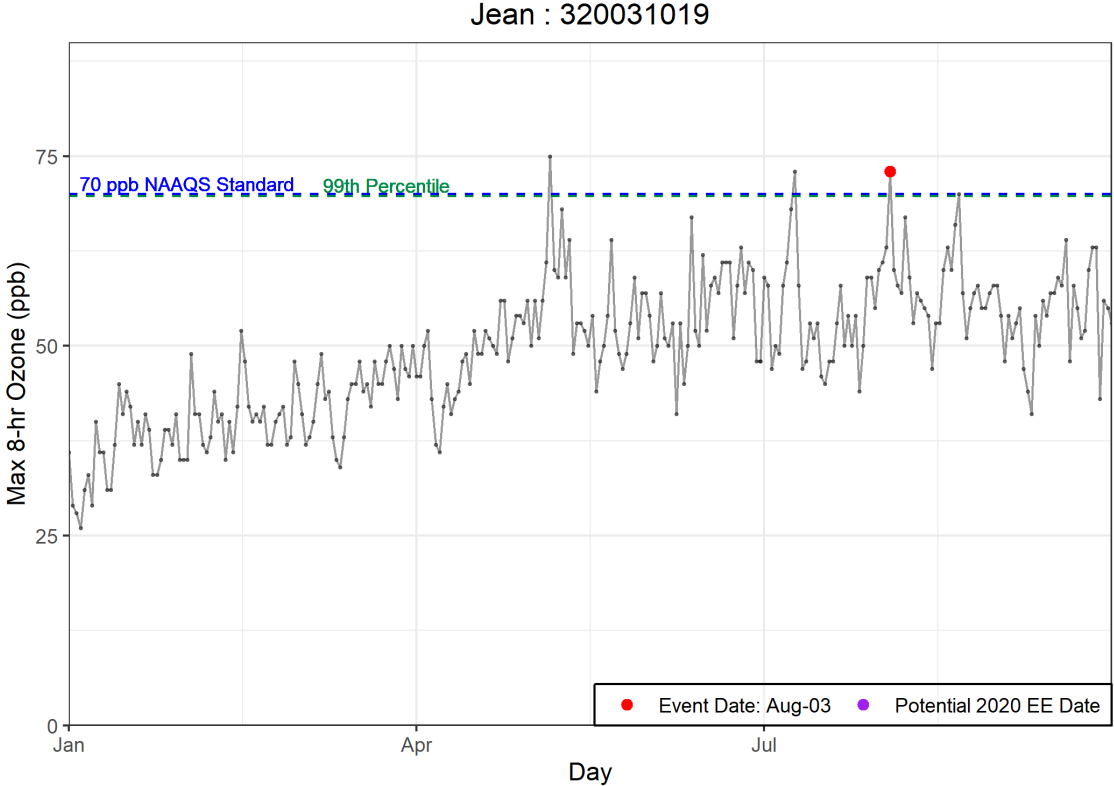
Figure 3-6. Time series of 2020 MDA8 ozone concentrations from Jean.
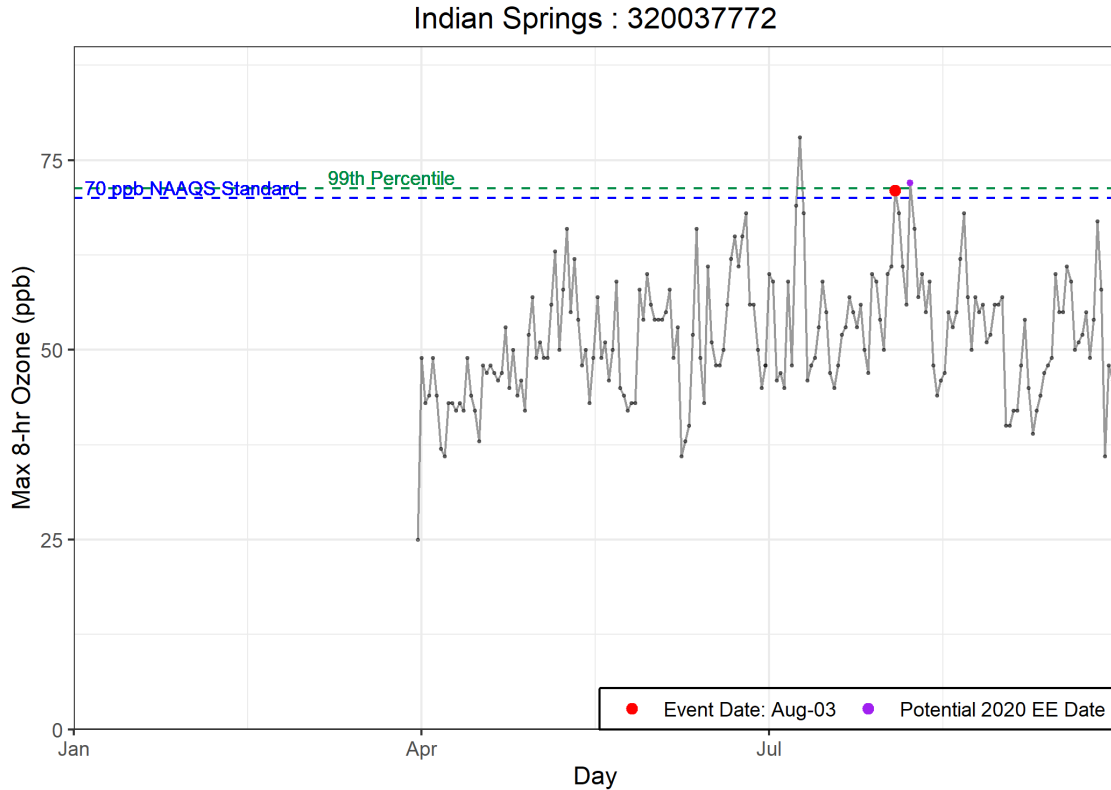
Figure 3-7. Time series of 2020 MDA8 ozone concentrations from Indian Springs.

The August 3, 2020, ozone exceedance occurred during a typical ozone season, but August 3 ozone concentrations were higher than non-event concentrations. **Table 3-1** provides historical monitoring site statistics for each site that was affected on August 3, 2020. The statistics shown are for May through September in 2015-2019; we do not exclude proposed 2018 EE ozone concentrations. The MDA8 ozone concentrations on August 3 were >10 ppb above the mean and median ozone concentrations for the historical ozone season at all seven sites. Six of the seven sites exhibited ozone concentrations at least 5 ppb above the 95th percentile of ozone when compared with historical ozone season non-event days. Because August 3 is during the normal ozone season and MDA8 ozone concentrations could not be clearly distinguished from the 95th percentile ozone concentration at all sites during the non-event historical ozone season, the August 3, 2020, event does not satisfy the key factor for a Tier 1 exceptional event. Tier 2 comparisons of the event-related ozone concentrations with non-event-related high ozone concentrations (>99th percentile over five years or top four highest daily ozone measurements) are described in Section 3.2.2.

Table 3-1. Ozone season non-event comparison. August 3, 2020, MDA8 ozone concentrations for each affected site are shown in the top row. 5-year (2015-2019) average MDA8 ozone statistics for May through September ozone season are shown for each affected site around Clark County to compare with the event ozone concentrations.

	Boulder City 320030601	Green Valley 320030298	Indian Springs 320037772	Jean 320031019	Joe Neal 320030075	Paul Meyer 320030043	Walter Johnson 320030071
Aug. 3	72	72	71	73	81	78	82
Mean	53	56	54	55	57	57	57
Median	54	56	54	55	57	58	57
Mode	57	52	56	57	62	58	57
St. Dev	7	8	8	8	9	8	9
Minimum	25	21	25	20	23	22	21
95 %ile	64	69	66	67	72	70	71
99 %ile	69	74	72	72	78	76	77
Maximum	72	78	78	81	83	79	87
Range	47	57	53	61	60	57	66
Count	894	877	911	914	912	911	917

3.1.2 Ozone, Fire, and Smoke Maps

Ozone and PM$_{2.5}$ Maps

We produced maps of ozone Air Quality Index (AQI), PM$_{2.5}$ AQI, active fire and smoke detections from satellites, and visible satellite imagery that show the transport of smoke to Las Vegas from California on August 3, 2020. These maps also show that high ozone concentrations occurred across multiple states corresponding with the presence of wildfire smoke.

From July 31 through August 3, 2020, moderate and unhealthy ground-level ozone concentrations (indicated by the yellow, orange, and red areas) were detected in the western United States (**Figure 3-8**), especially in California, Utah, and certain parts of Arizona and Nevada. On July 31, high ozone concentrations (i.e., the orange and red areas) are seen in central and southern California. While the ozone over central California seemed to dissipate somewhat in the following two days, the region of enhanced ozone concentrations expanded from the southern California region northeastward to the California/Nevada state border on August 1 and 2. On August 3, the region of high observed ozone expanded further over the northwest corner of Arizona and a large portion of southern Nevada, covering Las Vegas.

A similar spatiotemporal pattern in ozone concentrations was observed in the AQI plots for PM$_{2.5}$ (**Figure 3-9**). According to EPA guidance (U.S. Environmental Protection Agency, 2016), "if plume arrival at a given location coincides with elevation of wildfire plume components (such as PM$_{2.5}$, CO or organic and elemental carbon), those two pieces of evidence combined can show that smoke was

transported from the event location to the monitor with the enhanced ozone concentration." In Sections 3.1.2 through 3.2.4 of this report, we show that the enhanced ozone and PM$_{2.5}$ concentrations observed in the aforementioned regions in the western United States—including Clark County, Nevada—on August 3, 2020, corresponded with the arrival of a smoke plume from the southern California Apple Fire in Riverside County.
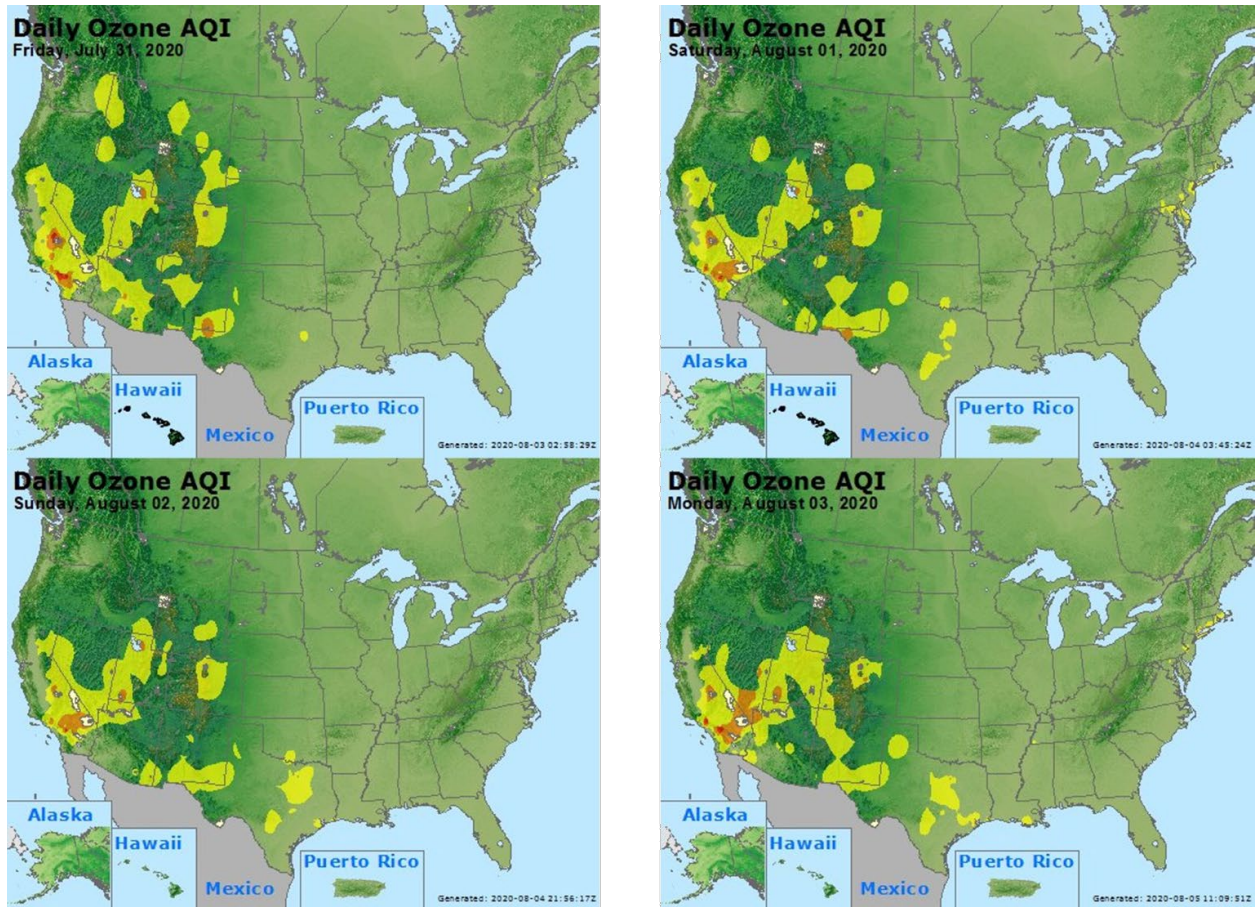
Figure 3-8. Daily ozone AQI for the three days before the August 3 event and the day of the event.
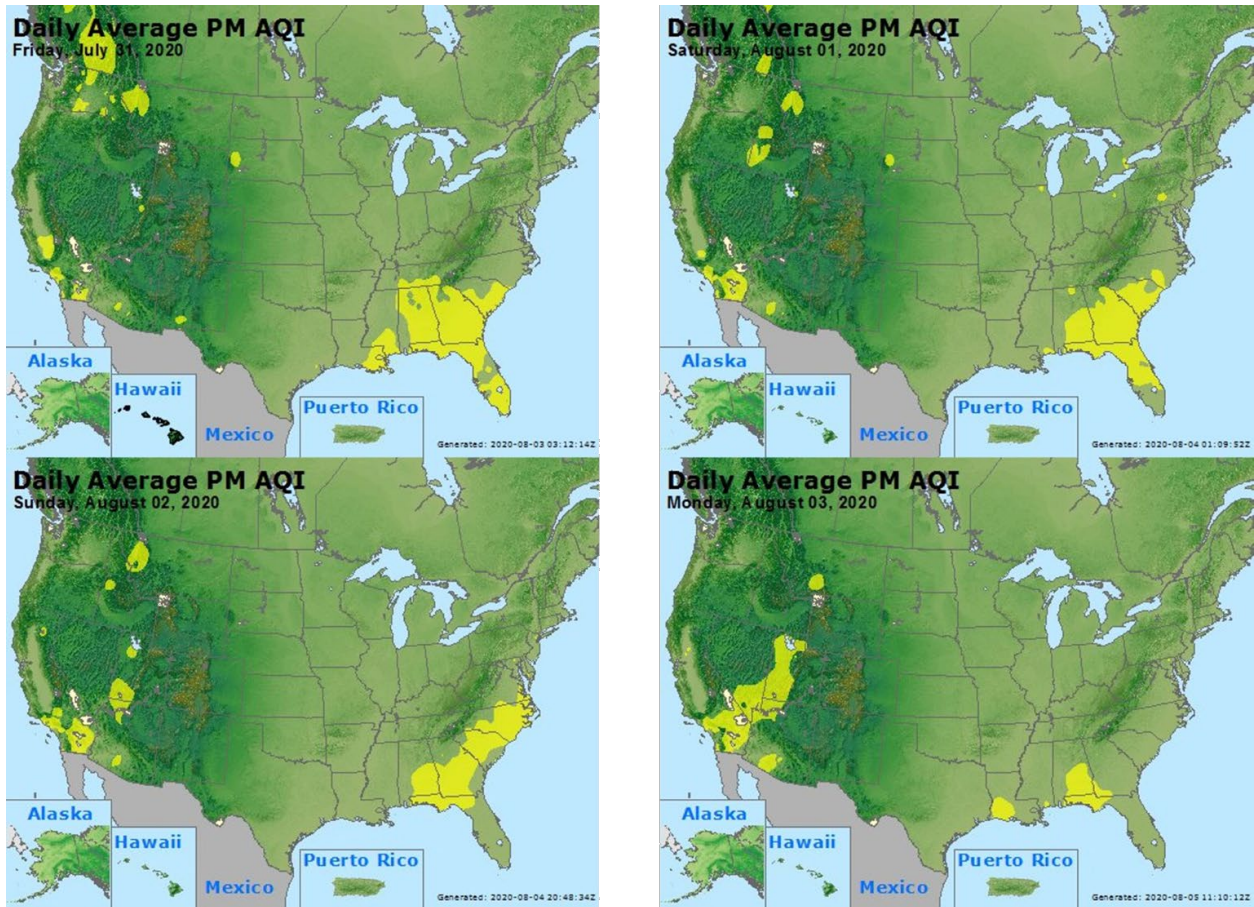
Figure 3-9. Daily PM$_{2.5}$ AQI for the three days before the August 3 event and the day of the event.

HMS Fire Detection Maps

According to EPA's guidance to Tier 1 analysis requirements (U.S. Environmental Protection Agency, 2016), the National Oceanic and Atmospheric Administration (NOAA) HMS Fire and Smoke Product can be used to demonstrate the transport of fire emissions to the impacted monitors. The HMS Fire and Smoke Product consists of

1. A daily fire detection product derived from three satellite data products[1] to spatially and temporally map fire locations at 1 km grid resolution, and

2. A daily smoke product derived from visible satellite imagery[2] that consists of polygons showing regions impacted by smoke.

---

[1] The HMS fire detection product is developed using data from the Moderate Resolution Imaging Spectroradiometer (MODIS), Geostationary Operational Environmental Satellite system (GOES), Advanced Very High Resolution Radiometer (AVHRR) and Visible Infrared Imaging Radiometer Suite (VIIRS) satellite instruments.
[2] The HMS smoke product is derived from GOES-EAST and GOES-WEST visible satellite imagery.

The HMS smoke plume data is based on measurements from several environmental satellites and is reviewed by trained NOAA analysts to identify cases where smoke is dispersed by transport. One can download real-time HMS fire detection and smoke products, and a six-month archive of the products from the NOAA Satellite and Information Service website (ospo.noaa.gov/Products/land/hms.html).

Figure 3-10 shows the HMS smoke plume and fire detection data for July 31 to August 3, 2020. Figure 3-11 shows zoomed-in HMS smoke and fire detections over the southwestern United States, including southern California where the Apple Fire burned, during the same period. As the daily plots indicate, there was concentrated fire activity along the West Coast, in the southeast United States, and in southern Canada along the U.S./Canada border. The daily plots also show substantial smoke plumes forming from California fires and covering the southwest United States on August 3. On August 1, concentrated plumes formed over the southern California fires. Over the following two days, the plumes traveled eastward and expanded over surrounding states, including Clark County in southern Nevada, and across portions of Utah and Arizona. This is consistent with the increased ozone and PM$_{2.5}$ concentrations observed in those regions, as shown above in the AQI plots (Figures 3-10 and 3-11).

The HMS smoke plume data for the days leading up to August 3 were obtained and combined with HYSPLIT back trajectories on high ozone concentration days to identify intersections and assess potential smoke impacts (Section 3.1.3). The following sections provide further evidence of smoke transport, based on HYSPLIT trajectories and satellite data, that traveled from southern California fires (specifically the Apple Fire in Riverside County) to the Clark County area.
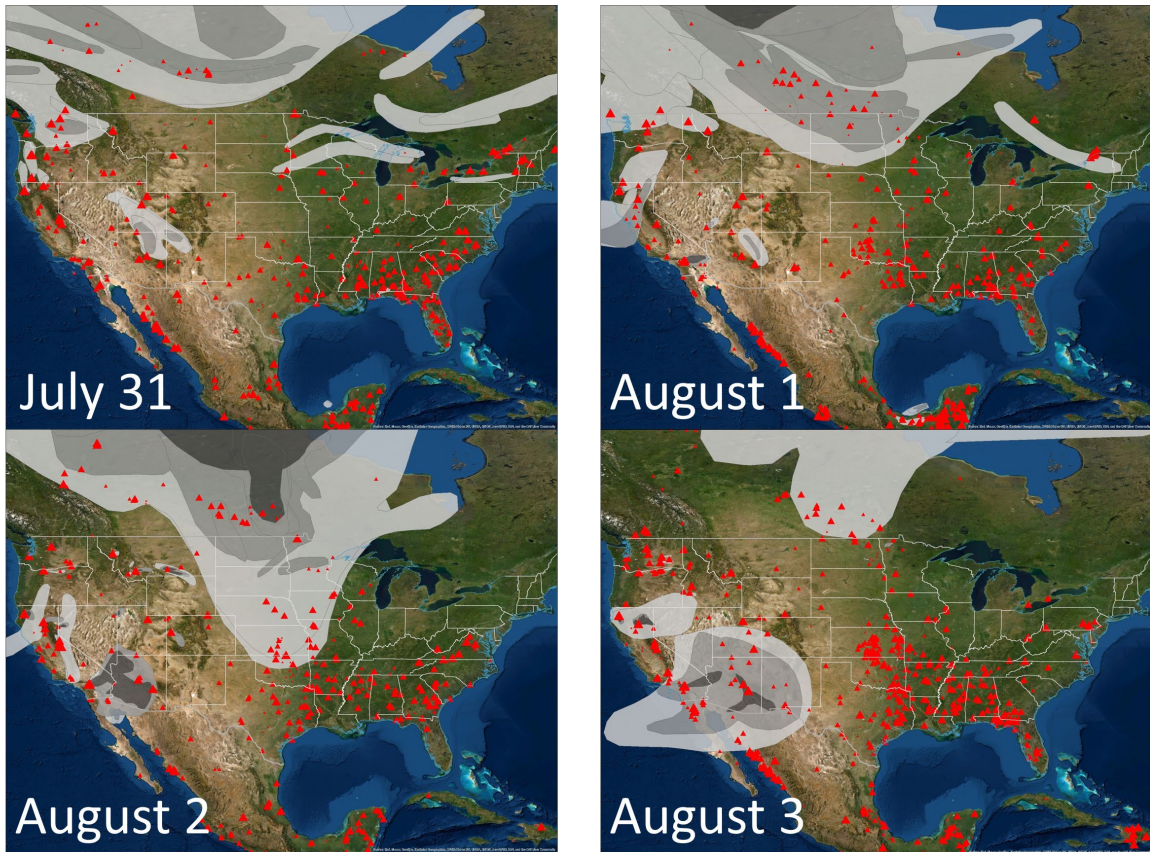
Figure 3-10. Daily HMS smoke over the United States for the three days before the August 3 event and the day of the event. Fire detections are shown as red triangles, and smoke is shown in gray.
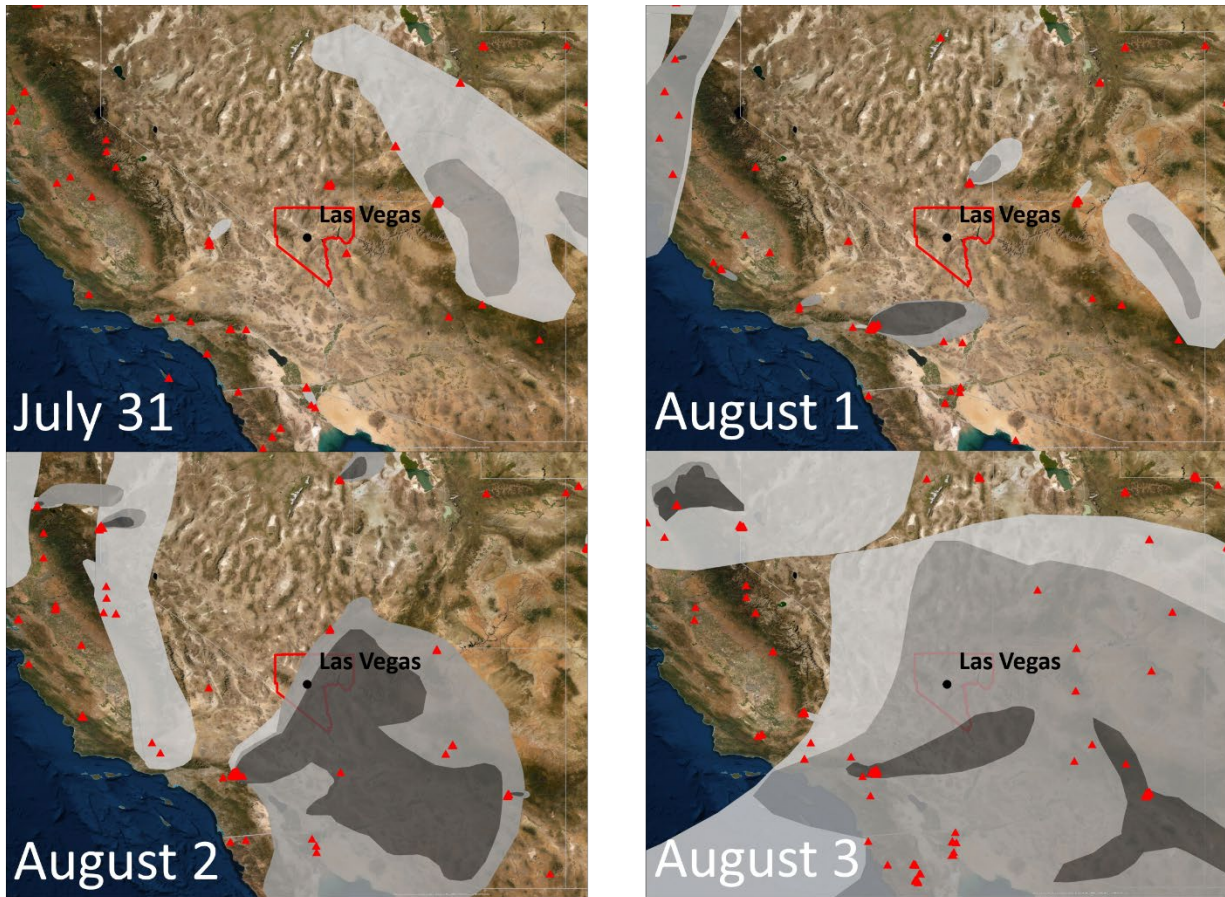
Figure 3-11. Daily HMS smoke over the southwestern United States for the three days before the August 3 event and the day of the event. Fire detections are shown as red triangles, and smoke is shown in gray.

Visible Satellite Imagery

Visible satellite imagery from the MODIS Aqua and Terra satellites shows transport of smoke from the Apple Fire burning in Riverside County in California to the southwestern United States, including Nevada, between July 31 and August 3 (**Figures 3-12 through 3-15**). This is consistent with the evidence of smoke over Las Vegas demonstrated by the HMS maps above. A dense smoke plume started to form on August 1 from the Apple Fire, travelling east. During the following two days (including the day of the event), this plume expanded over southern California, southern Nevada (including Las Vegas) and western Arizona. The movement of this smoke corresponds to the increase in high ozone and PM$_{2.5}$ concentrations in Las Vegas, as shown in the AQI maps above. In addition, the transport of smoke northeastward from southern California is consistent with transport patterns observed in the HYSPLIT trajectory analysis presented in Section 3.1.3, as well as the satellite and ground-based measurements of smoke-associated species presented in Sections 3.2.3 and 3.2.4.
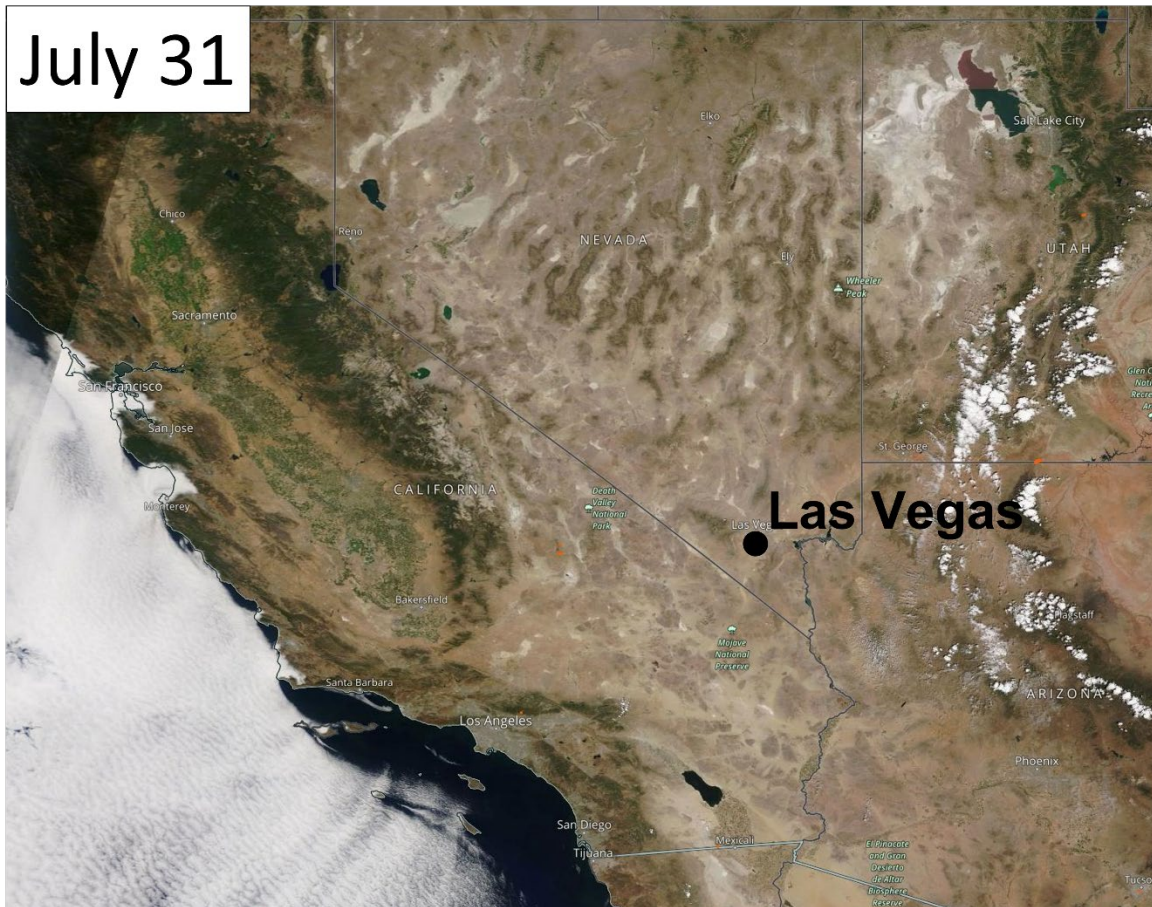
Figure 3-12. Visible satellite imagery from over southern California, Nevada, and Arizona on July 31, 2020. Source: NASA Worldview.
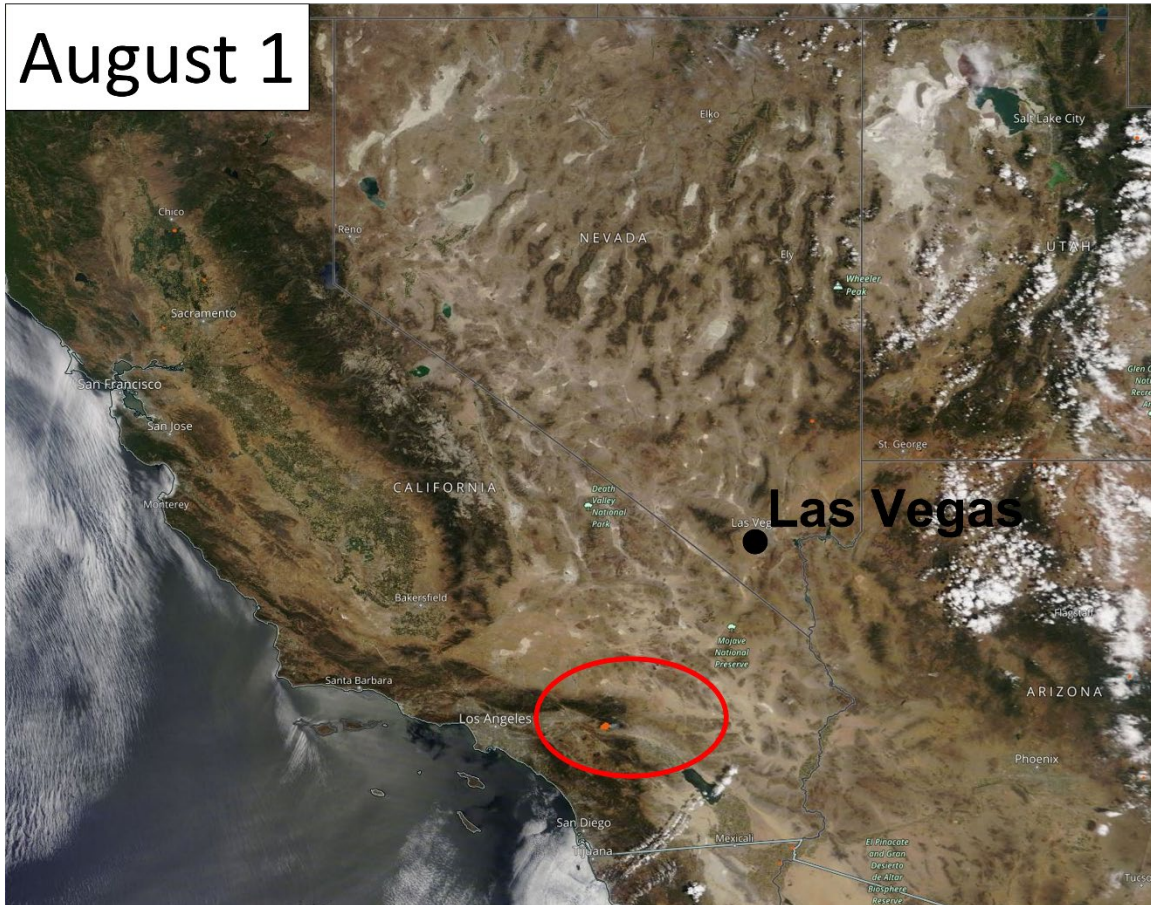
Figure 3-13. Visible satellite imagery from over southern California, Nevada, and Arizona on August 1, 2020. Source: NASA Worldview.
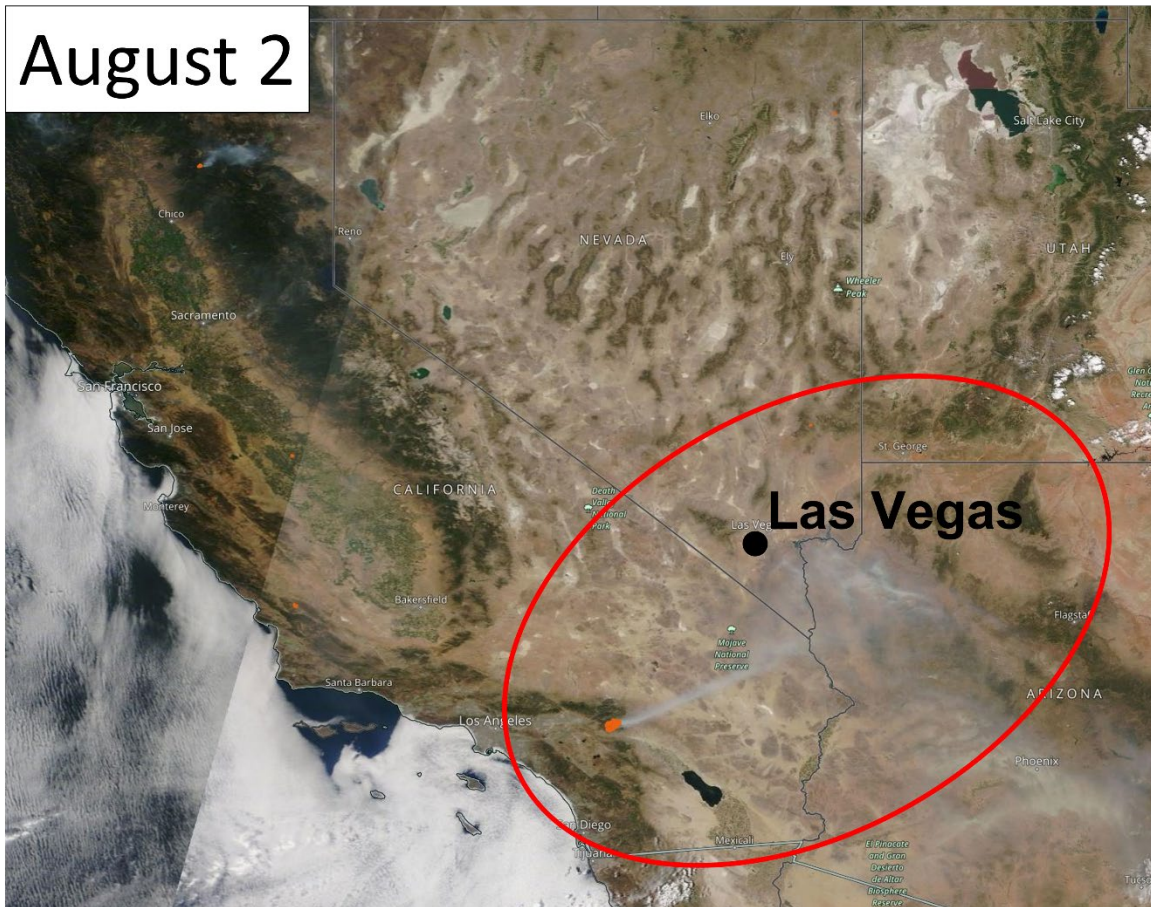
Figure 3-14. Visible satellite imagery from over southern California, Nevada, and Arizona on August 2, 2020. Source: NASA Worldview.

Figure 3-15. Visible satellite imagery from over southern California, Nevada, and Arizona on August 3, 2020. Source: NASA Worldview.

3.1.3   HYSPLIT Trajectories

HYSPLIT trajectories were run to demonstrate the transport of air parcels to Las Vegas from upwind areas, and to show transport of smoke-containing air parcels from wildfires toward the affected monitors. These trajectories show that air was transported from the Apple Fire in southern California, specifically in Riverside County, to the Clark County area in the days prior to the event and on August 3, 2020. Combined with satellite observations described in Sections 3.1.2 and 3.2.3, the trajectories demonstrate that smoke was transported from southern California to Las Vegas, Nevada.

NOAA's online HYSPLIT model tool was used for the trajectory modeling (http://ready.arl.noaa.gov/HYSPLIT.php). HYSPLIT is a commonly used model that calculates the path of a single air parcel from a specific location and height above the ground over a period of time; this path is the modeled trajectory. HYSPLIT trajectories can be used as evidence that fire emissions were transported to an air quality monitor. This type of analysis is important for meeting Tier 1 requirements and is required under Tier 3.

The model options used for this study are summarized in Table 3-2. The meteorological data from the North American Mesoscale Forecast System (NAM, 12-km resolution) and High-Resolution Rapid Refresh (HRRR, 3-km resolution) model were used (ready.noaa.gov/archives.php). These data are high in spatial resolution, are readily available for HYSPLIT modeling over the desired lengths of time and are expected to capture fine-scale meteorological variability. All backward trajectory start times were selected to align with peak ozone concentrations at a site where an exceedance occurred. The average hour of peak ozone concentration was chosen as the starting time for monitoring sites within the greater Las Vegas area (e.g., average hour of peak ozone concentrations of Paul Meyer, Walter Johnson, Joe Neal, and Green Valley). Additionally, the back trajectory matrix analysis was initiated in the late morning and early afternoon (19:00 UTC or 11:00 a.m. local standard time [LST], and 21:00 UTC or 1 p.m. LST) to better understand the full event-day transport of ozone and its precursors. As suggested in the EPA's exceptional event guidance (U.S. Environmental Protection Agency, 2016), a backward trajectory length of 72 hours was selected to assess whether smoke from the current day or from the previous two days may have been transported over a long distance to the monitoring sites. Further investigation showed that smoke from the Apple Fire was transported to Clark County within 24 to 48 hours. Therefore, 48-hour backward trajectory durations were used in this analysis. Trajectories were initiated at 50 m, 500 m, and 1,000 m above ground level to capture transport throughout the mixed boundary layer, as ozone precursors may be transported aloft and influence concentrations at the surface through vertical mixing. Three backward trajectory approaches available in the HYSPLIT model were used in this analysis, including site-specific trajectories, trajectory matrix, and trajectory frequency. Site-specific back trajectories were run to show direct transport from the wildfire smoke to the affected site(s). This analysis is useful in linking smoke impacts at a single location (i.e., an air quality monitor) to wildfire smoke. Matrix back trajectories were run to show the general air parcel transport patterns from the Las Vegas area to the wildfire smoke plumes. Similarly, matrix forward trajectories were run to show air parcel transport patterns from the fires to the Las Vegas area. Matrix trajectories are useful in analyzing air transport over areas larger than a single air quality site. Trajectory frequency analysis shows the frequency with which multiple trajectories initiated over multiple hours pass over a grid cell on a map. Trajectory frequencies are useful in estimating the temporal and spatial patterns of air transport from a source region to a specific air quality monitor. Additionally, a forward trajectory matrix was run for the southern California Apple Fire location to evaluate transport patterns in the direction of Clark County. Together, these trajectory analyses indicate the transport patterns into Clark County on August 3, 2020.

Table 3-2. HYSPLIT run configurations for each analysis type, including meteorology data set, time period of run, starting location(s), trajectory time length, starting height(s), starting time(s), vertical motion methodology, and top of model height.

	Backward Trajectory Analysis – Site-Specific	Back Trajectory Analysis – Matrix	Backward Trajectory Analysis – Frequency	Forward Trajectory Analysis – Matrix	Backward Trajectory Analysis – High Resolution
Meteorology	12-km NAM	12-km NAM	12-km NAM	12-km NAM	3-km HRRR
Time Period	July 31 – August 3, 2020	August 3, 2020	July 31 – August 3, 2020	August 2 – August 3, 2020	July 31 – August 3, 2020
Starting Location	36.1489 N, 115.2019 W, Boulder City, Indian Springs, Jean	Evenly spaced grid covering Las Vegas, Nevada	36.1489 N, 115.2019 W	Evenly spaced grid covering the Apple Fire	36.1489 N, 115.2019 W
Trajectory Time Length	48 hours	48 hours	48 hours	32 hours	48 hours
Starting Heights (AGL)	50 m, 500 m, 1,000 m	500 m, 1,000 m, 1,500 m	500 m	100 m, 250 m, 500 m	50 m, 500 m, 1,000 m
Starting Times	19:00 UTC, 20:00 UTC, 21:00 UTC, 23:00 UTC	19:00 UTC	19:00 UTC	19:00 UTC	19:00 UTC
Vertical Motion Method	Model Vertical Velocity	Model Vertical Velocity	Model Vertical Velocity	Model Vertical Velocity	Model Vertical Velocity
Top of Model	10,000 m	10,000 m	10,000 m	10,000 m	10,000 m

Site-specific backward trajectories were calculated from the Las Vegas Valley (36.1489 N, 115.2019 W), Indian Spring, Jean, and Boulder City monitoring sites on August 3, 2020. We chose to model all trajectories for sites within the Las Vegas metropolitan area using the Las Vegas Valley location. The Indian Springs, Jean, and Boulder City monitoring sites were far enough outside of the Las Vegas Valley to warrant initiating separate back trajectories. The hours of peak ozone concentrations at the Boulder City, Indian Springs, and Jean sites were chosen as the model starting times to align with smoke impacts at the surface. The average hour of peak ozone concentrations was chosen as the

starting time for the Las Vegas Valley backward trajectories The backward trajectories from the Las Vegas Valley, together with measured ozone (8-hour begin time average) and HMS smoke for August 3 are shown in Figure 3-16. All three trajectories, each at a different height, follow a similar backward path from the Las Vegas Valley, passing near or directly over the active fires in southern California (specifically the Apple Fire). HMS smoke plume data are also displayed in Figure 3-17 through 3-19 with trajectories from Boulder City, Indian Springs, and Jean. Each figure shows the back trajectory intersecting with the smoke plume from the Apple Fire in southern California. Additionally, enhanced ozone concentrations were observed at all Clark County sites along with the presence of smoke. Figure 3-20 shows back trajectories from the Las Vegas Valley location and HMS smoke from the day of the exceptional event (August 3) and the day before the exceptional event (August 2). Back trajectories initiated at all three heights intersect the smoke plume from the Apple Fire over southern California and Nevada on August 2 or 3. Previous-day trajectory plots (Figure 3-21) show the formation of the smoke plume and its transport over the three days prior to the exceedance event. On July 31, southern California and southern Nevada were free of smoke plumes, and ozone concentration over the Las Vegas region stayed low. On August 1, the Apple Fire in Riverside County, together with other southern California fires, had become active, creating a dense concentrated plume over southern California. On August 2, the plume from the southern California fires was transported northeastward, covering the Las Vegas region, providing smoke plumes in Clark County on the day prior to the August 3 exceptional event. Figure 3-22 shows the high-resolution (3 km) backward trajectories from the Las Vegas Valley on August 3. The results are consistent in that all three trajectories pass over southern California on August 2.
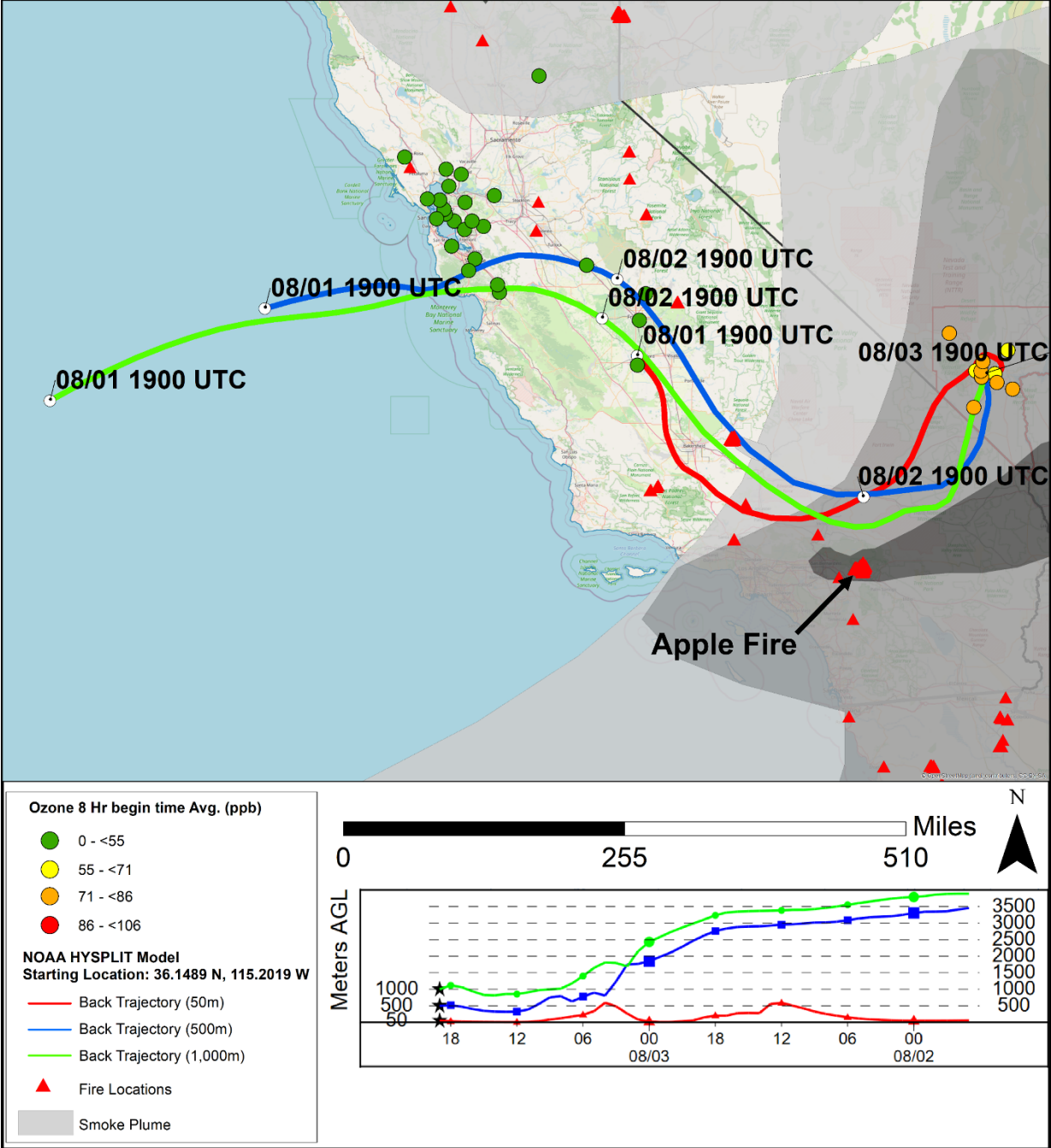
Figure 3-16. HYSPLIT back trajectories from downtown Las Vegas (Las Vegas Valley location), ending at 19:00 UTC on August 3, 2020. 48-hour, NAM back trajectories are shown for 50 m (red), 500 m (blue), and 1,000 m (green) above ground level. HMS smoke from August 3, 2020, is shown using shades of gray. Eight-hour ozone averages are shown as circles (green to red), and HMS fires are shown as red triangles.
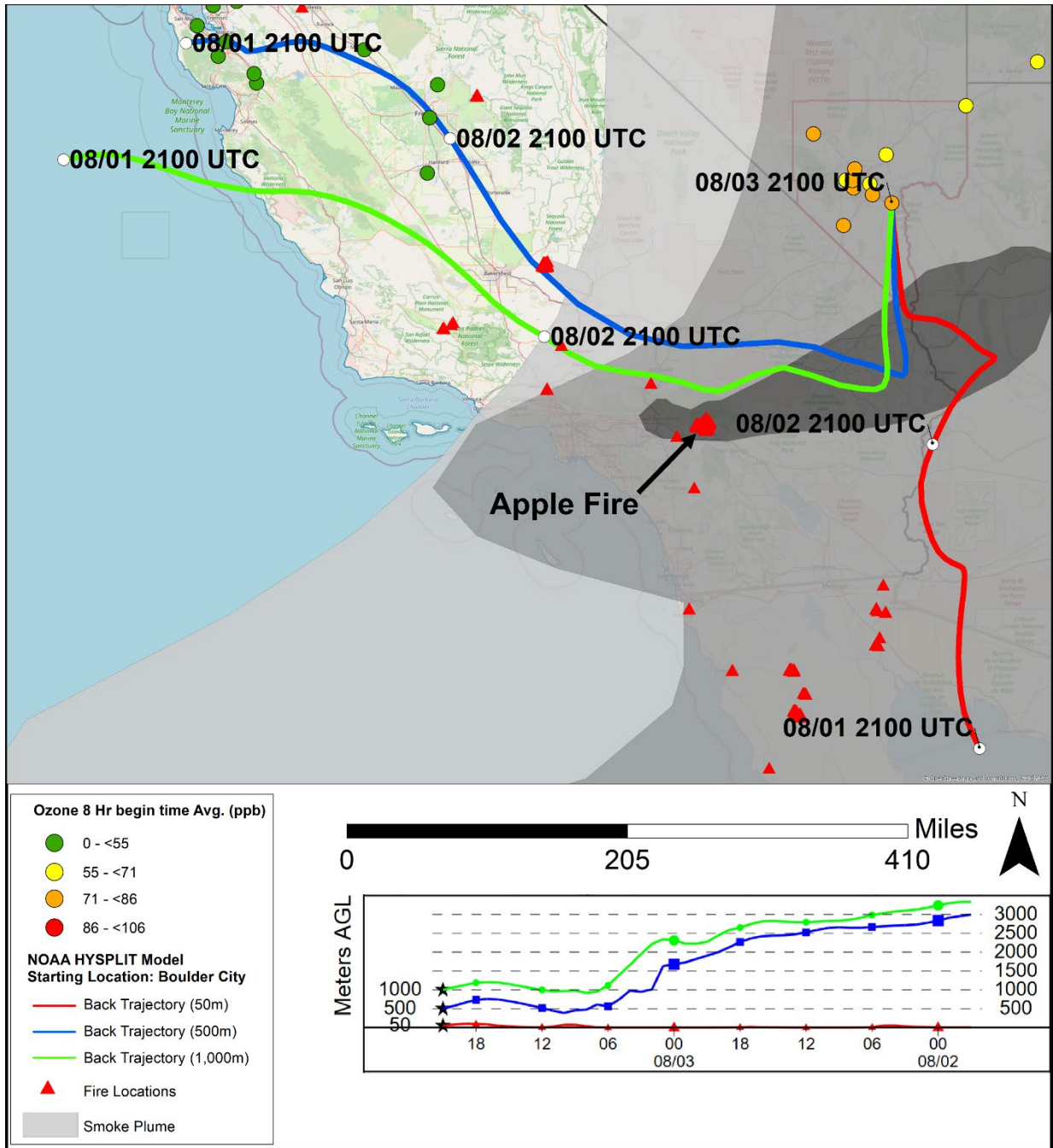
Figure 3-17. HYSPLIT back trajectories with smoke from Boulder City, ending at 21:00 UTC on August 3, 2020. 48-hour, NAM back trajectories are shown for 50 m (red), 500 m (blue), and 1,000 m (green) above ground level. HMS smoke from August 3, 2020, is shown using shades of gray. Eight-hour ozone averages are shown as circles (green to red), and HMS fires are shown as red triangles.
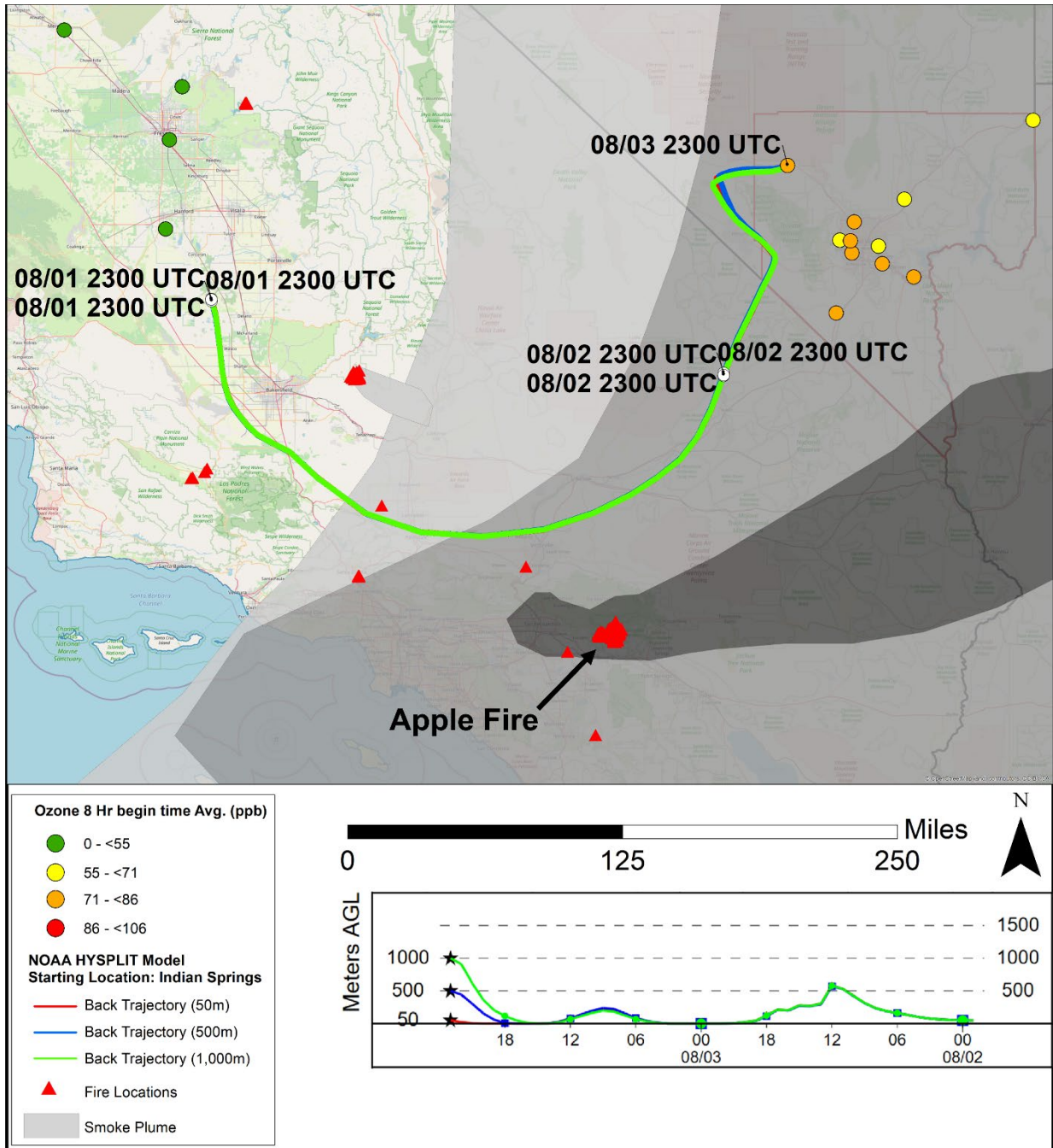
Figure 3-18. HYSPLIT back trajectories with smoke from the Indian Springs site, ending at 23:00 UTC on August 3, 2020. 48-hour, NAM back trajectories initiated from Indian Springs are shown for 50 m (red), 500 m (blue), and 1,000 m (green) above ground level. HMS smoke from August 3, 2020, is shown using shades of gray. Eight-hour ozone averages are shown as circles (green to red), and HMS fires are shown as red triangles.
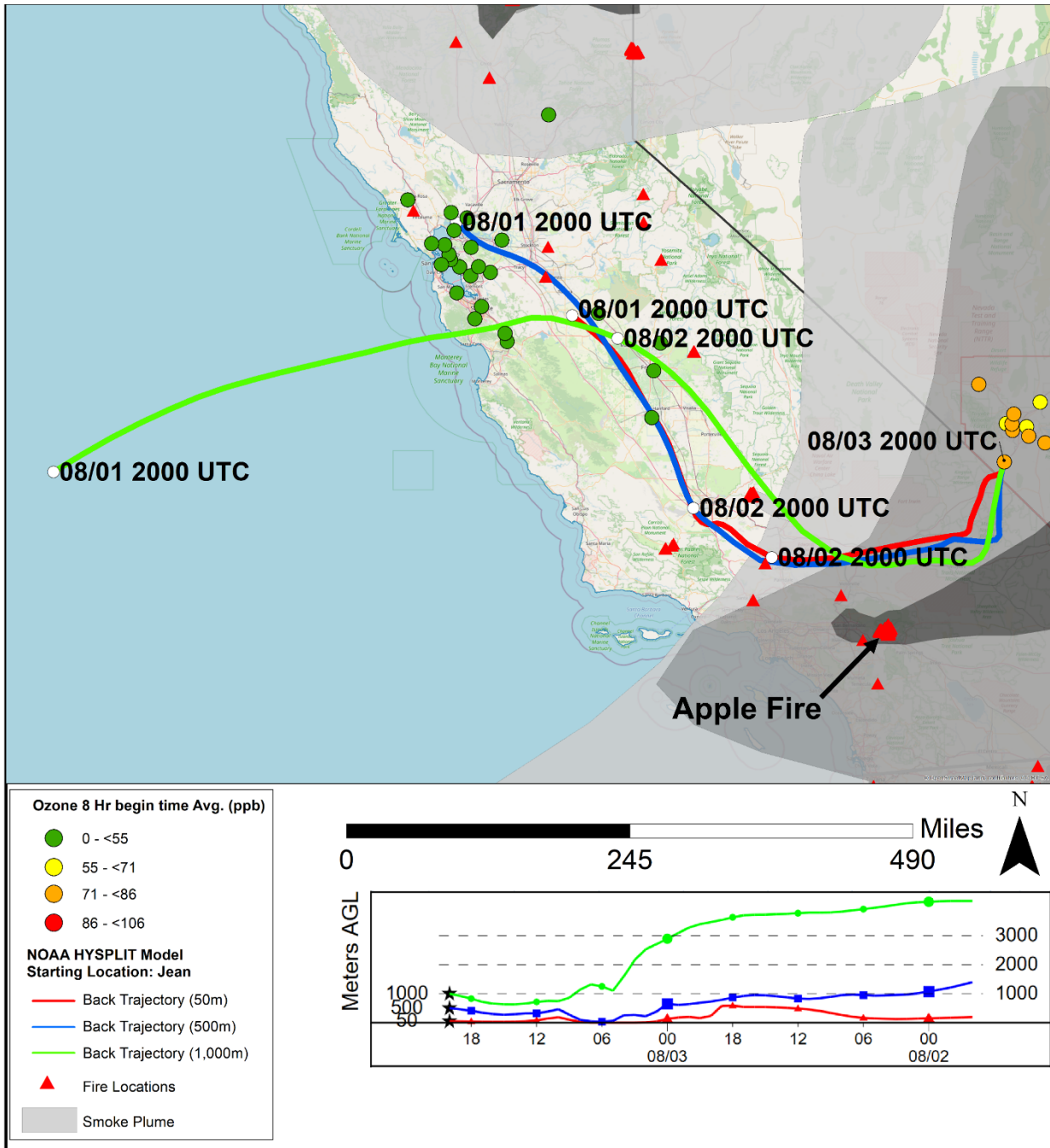
Figure 3-19. HYSPLIT back trajectories with smoke from the Jean site, ending at 20:00 UTC on August 3, 2020. 48-hour, NAM back trajectories initiated from Jean are shown for 50 m (red), 500 m (blue), and 1,000 m (green) above ground level. HMS smoke from August 3, 2020, is shown using shades of gray. Eight-hour ozone averages are shown as circles (green to red), and HMS fires are shown as red triangles.
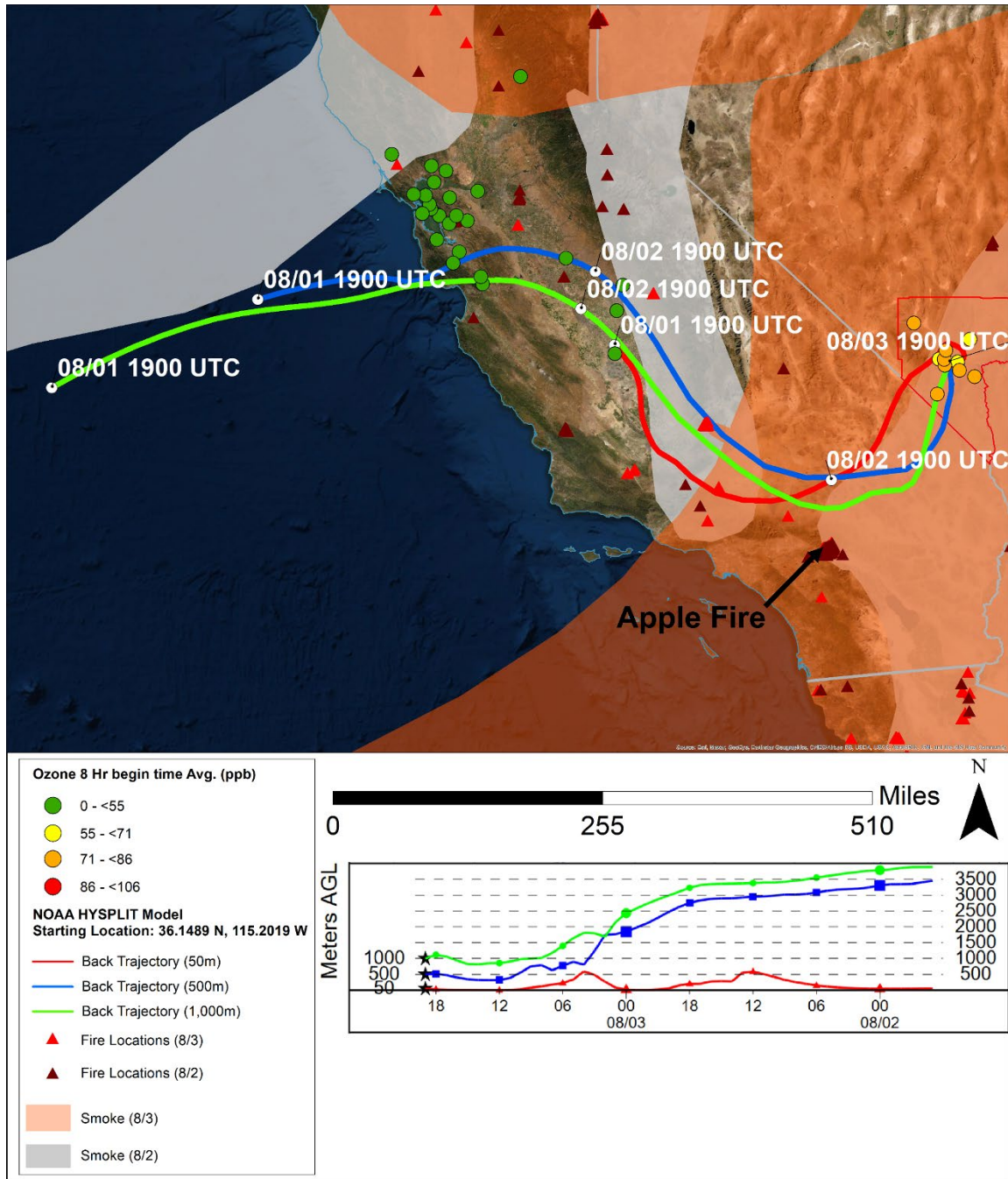
Figure 3-20. 48-hour NAM back trajectories initiated at the Las Vegas Valley location, ending at 19:00 UTC on August 3, 2020, are shown for 50 m (red), 500 m (blue), and 1,000 m (green) above ground level, along with HMS smoke on August 3 (orange) and August 2 (grey). The shading indicates the presence of HMS smoke, intensity is not shown). Eight-hour ozone averages are shown as circles (green to red), and HMS fires on August 2 and August 3 are shown as red triangles.
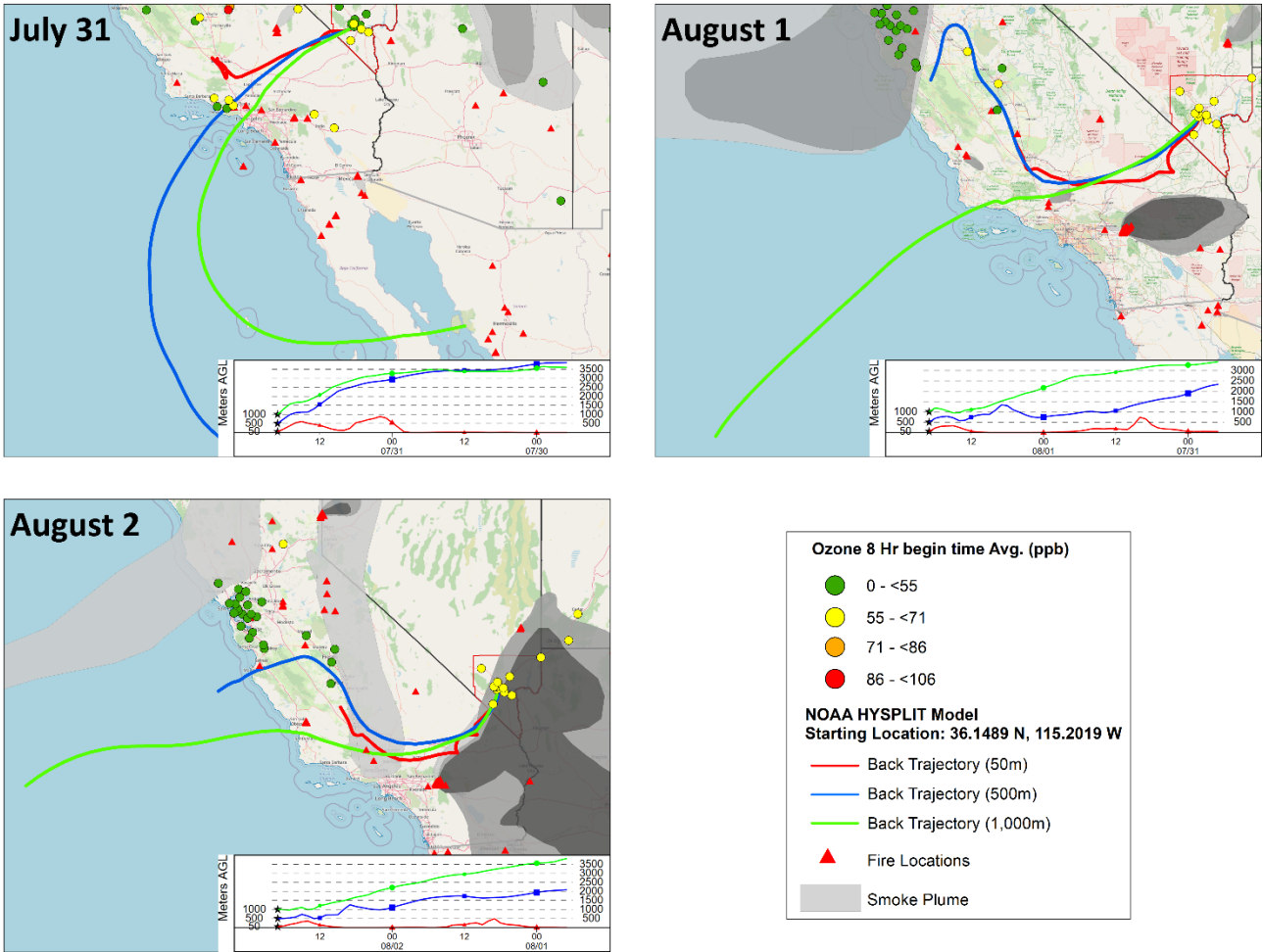
Figure 3-21. 48-hour, NAM back trajectories initiated from downtown Las Vegas for the three days prior to the exceptional event on August 3, are shown for 50 m (red), 500 m (blue), and 1,000 m (green) above ground level. HMS smoke is shown in each panel corresponds to the respective day between July 31 and August 2.
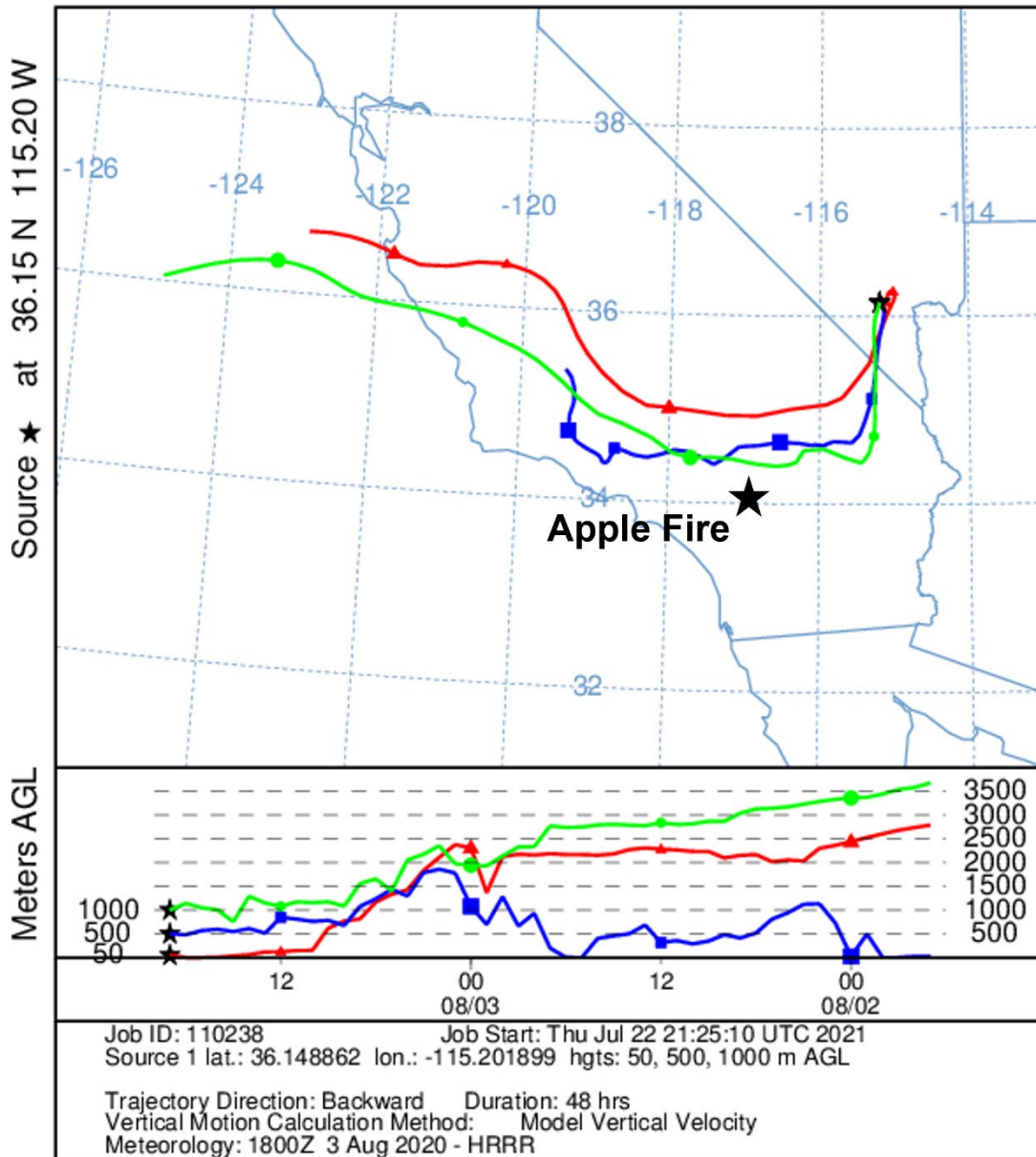
Figure 3-22. 48-hour, HRRR HYSPLIT back trajectories initiated on August 3 at 18:00 UTC from downtown Las Vegas are shown for 50 m (red), 500 m (blue), and 1,000 m (green) above ground level. The location of the Apple Fire in southern California is marked with a black star.

To identify variations in meteorological patterns of transported air to Las Vegas, we generated a HYSPLIT trajectory matrix. For this approach, trajectories are run in an evenly spaced grid of source locations. **Figure 3-23** shows 48-hour backward trajectory matrices with source locations encompassing Las Vegas. The matrix backward trajectories were initiated in the late morning (19:00

UTC or 11:00 a.m. LST) of August 3, 2020, at a starting height of 500 m, 1,000 m, and 1,500 m above ground level (AGL) to capture transport to the lower troposphere of the Las Vegas area. As shown in both plots, the transported air intersecting Las Vegas on August 3, 2020, follows a similar pattern. Consistent with the trajectories depicted in Figure 3-16, transported air from the West Coast traveled across central California and down to southern California, where the smoke plume from the Apple Fire was spread across a large area, and progressed northeast to intersect Las Vegas at 500 m, 1,000 m, and 1,500 m AGL.

The third trajectory approach used in this analysis was HYSPLIT trajectory frequency. In this option, a trajectory from a single location and height starts every three hours. Using a continuous 0.25-degree grid, the frequency of trajectories passing through each grid cell is totaled and then normalized by the total number of trajectories. Figure 3-24 shows a 48-hour backward trajectory frequency plot starting from the Las Vegas Valley and 500 m AGL on August 3, 2020. The trajectory frequency plot yields similar results as those from the previous two approaches; transported air impacting the Las Vegas Valley on August 3, 2020, predominately came from central and southern California, near the Apple Fire.
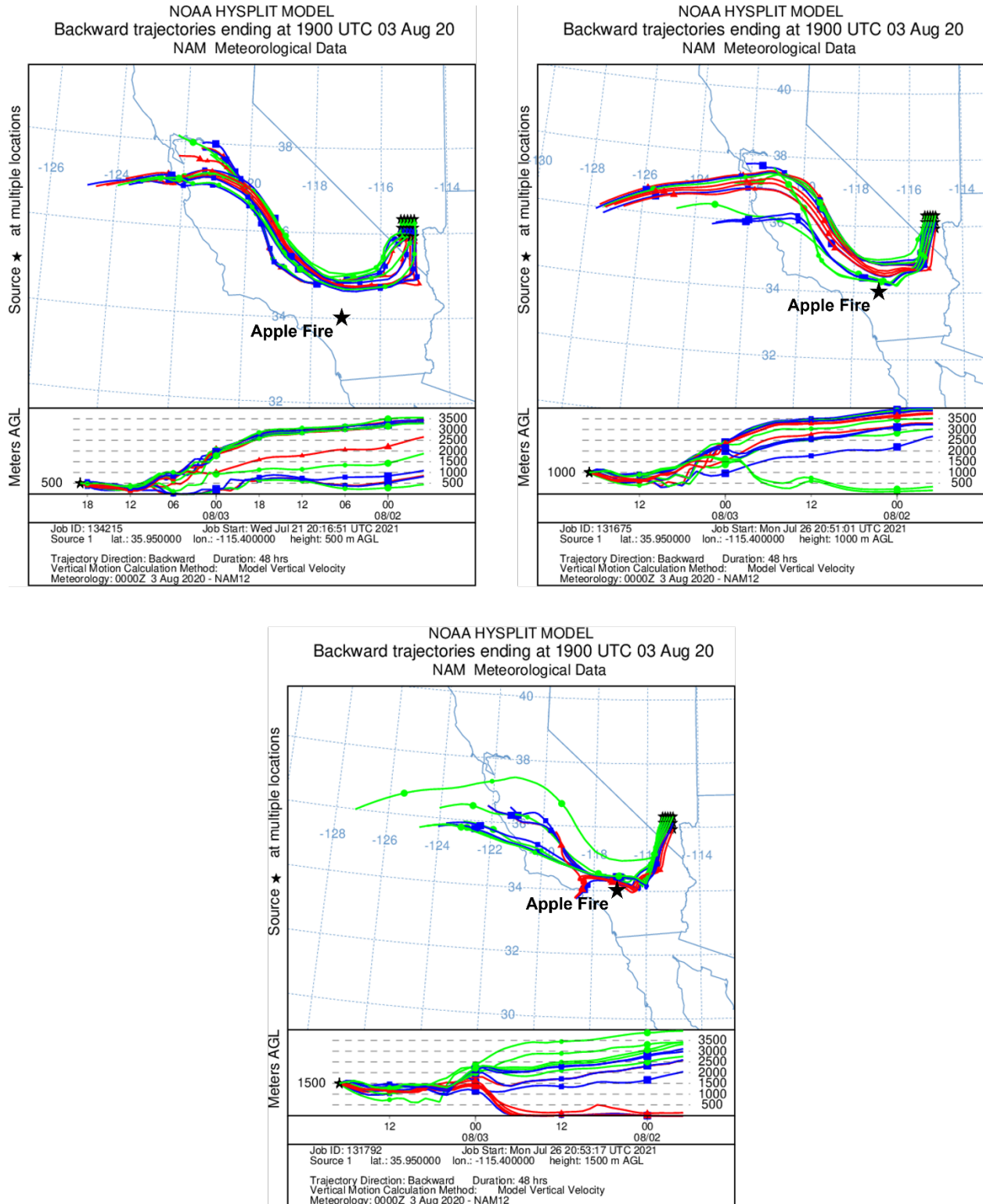
Figure 3-23. HYSPLIT back trajectory matrix. A 48-hour, NAM back trajectory matrix was initiated on August 3 at 19:00 UTC (11:00 a.m. LST) from downtown Las Vegas at 500 m, 1,000 m, and 1,500 m above ground level. The location of the Apple Fire in southern California is marked with a black star.
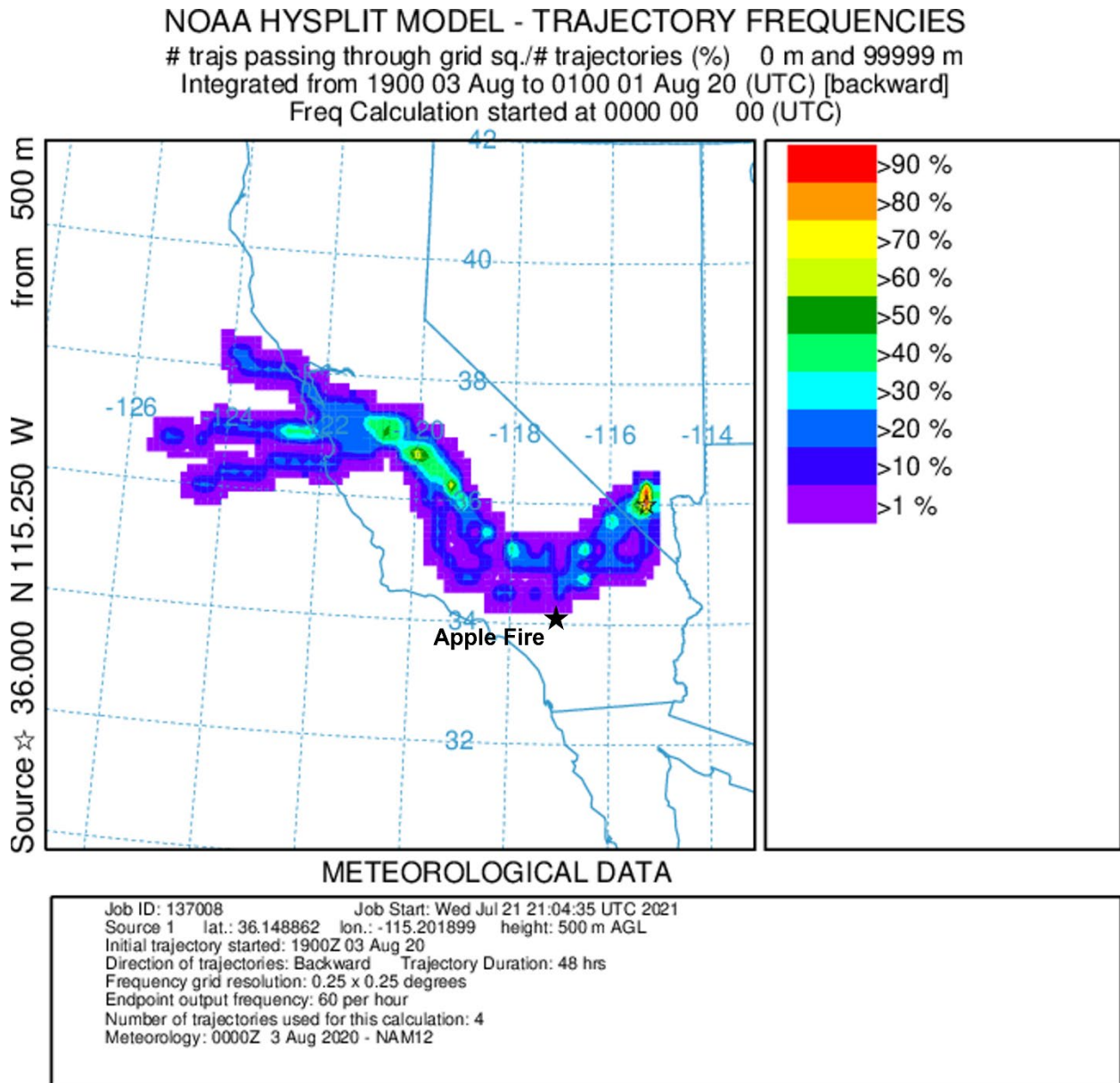
Figure 3-24. HYSPLIT back trajectory frequency. A 48-hour, NAM frequency of back trajectories was initiated on August 3 at 19:00 UTC (11:00 a.m. LST) from downtown Las Vegas at 500 m above ground level. The colors within the frequency plot indicate the percent of trajectories that pass through a grid square. The location of the Apple Fire in southern California is marked with a black star.

Forward trajectories were run from fire locations in southern California starting at 20:00 UTC on August 2 (**Figure 3-25**), which corresponds with the time when the back trajectories intersect the smoke plume from the Apple Fire. 100 m, 250 m, and 500 m were chosen as the starting heights to

capture transport at multiple heights within the lower troposphere and due to uncertainty about the height of the smoke plumes from the Apple Fire. A subset of forward trajectories from the Apple Fire pass over the Las Vegas area on the evening of August 2 and the morning of August 3 at altitudes of ≤ 2. 5 km within the planetary boundary layer (PBL), consistent with PBL heights from ceilometer data (Section 3.3.1). These forward trajectories, combined with the back trajectories shown above, further support the transport of smoke from the southern California Apple Fire to Clark County, Nevada.
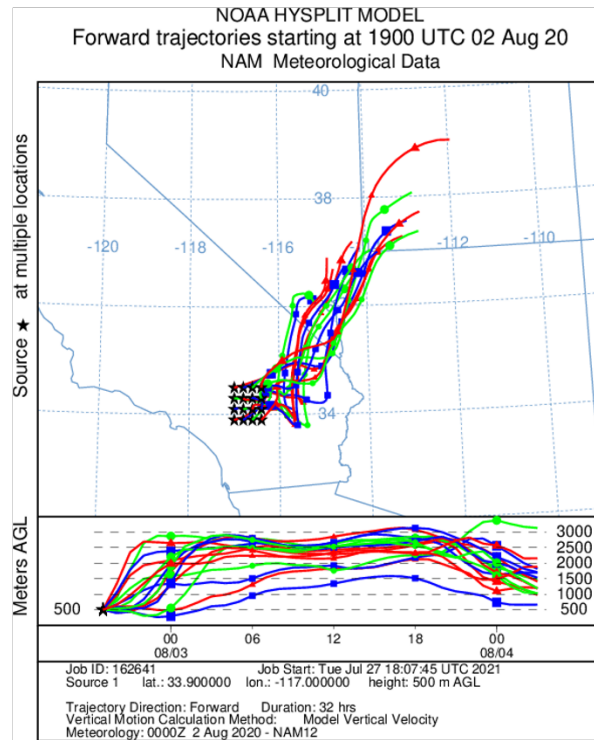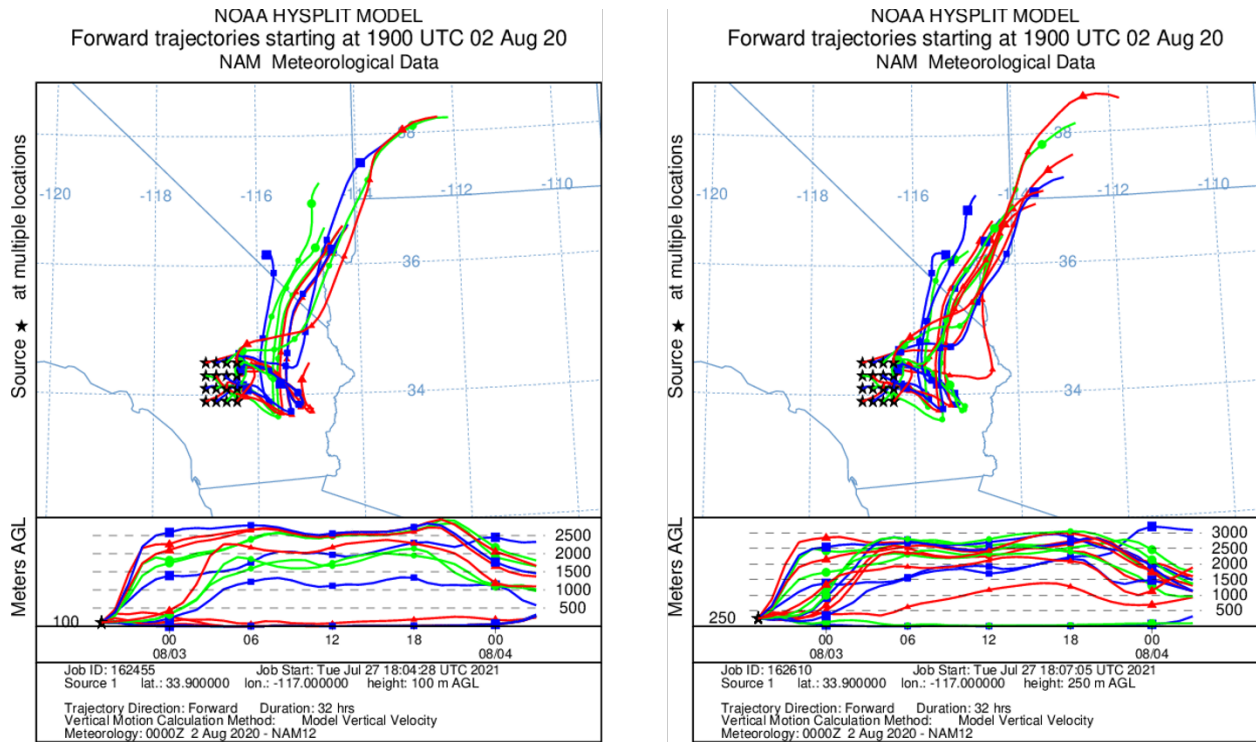
Figure 3-25. HYSPLIT forward trajectory matrix. A 32-hour, NAM forward trajectory matrix was initiated on August 2 at 19:00 UTC (11:00 a.m. LST) from the Apple Fire at 100 m, 250 m, and 500 m above ground level.

3.1.4 Media Coverage and Ground Images

News, weather, and environmental organizations provided widespread coverage of the effects of smoky conditions on air quality in Clark County. The Apple Fire in California was widely cited as the source of the wildfire smoke. On August 3, National Weather service (NWS) Las Vegas posted a tweet, shown in **Figure 3-26,** in anticipation of expected poor air quality in Clark County resulting from wildfire smoke (https://twitter.com/NWSVegas/status/1290260081792045056?s=20). The smoke advisory issued by Clark County DAQ appears in **Appendix A**. Additionally, 40 CFR 50.14(c)(1)(i) requires that air agencies must "notify the public promptly whenever an event occurs or is reasonably anticipated to occur which may result in the exceedance of an applicable air quality standard" in accordance with the mitigation requirement at 40 CFR 51.930(a)(1). Appendix A provides further details on Clark County Department of Environment and Sustainability's public notification for the potential exceptional event on August 3, 2020.

Figure 3-26. Tweet posted by the National Weather Service, Las Vegas, on August 3 cautioning residents of Southern Nevada to expect smoky conditions for the afternoon.

The *Las Vegas Review Journal* reported the headline "Smoke from Apple Fire Prompts 2-day Air-Quality Advisory for Clark County" on August 3, citing a direct quote from NWS meteorologist Barry Pierce, warning citizens to expect smoky conditions to persist through the night.

Similarly, the Las Vegas Review-Journal in Las Vegas reported that "smoke from the `Apple Fire` in Southern California has resulted in Clark County issuing a smoke and ozone advisory for Monday and Tuesday" in an article entitled "Smoke advisory issued in Clark County due to California 'Apple Fire`" (**https://www.reviewjournal.com/local/weather/smoke-from-apple-fire-prompts-2-day-air-quality-advisory-for-clark-county-2086924/**). KLAS-TV and KTNV, Las Vegas-based news organization, both referenced an advisory put out by Clark County Department of Environment and Sustainability (see Appendix A) that cautioned citizens in Clark County about enhanced smoke and ozone conditions resulting from the Apple Fire near Los Angeles (**https://www.ktnv.com/news/smoke-ozone-advisory-issued-due-to-wildfire-smoke**; **https://www.8newsnow.com/news/local-news/california-apple-fire-spreads-to-20k-acres-smoke-impacts-southern-nevada/**).

Ground images from the Clark County Department of Environment and Sustainability, Division of Air Quality's visibility cameras, located on the roof of the M Hotel in Las Vegas, clearly show the smoky conditions that persisted on August 3 (**Figure 3-27**). When compared to images taken on a clear day (May 21, 2020) (**Figure 3-28**), the August 3 images show drastically reduced visibility and an opaque gray haze in every direction due to wildfire smoke.
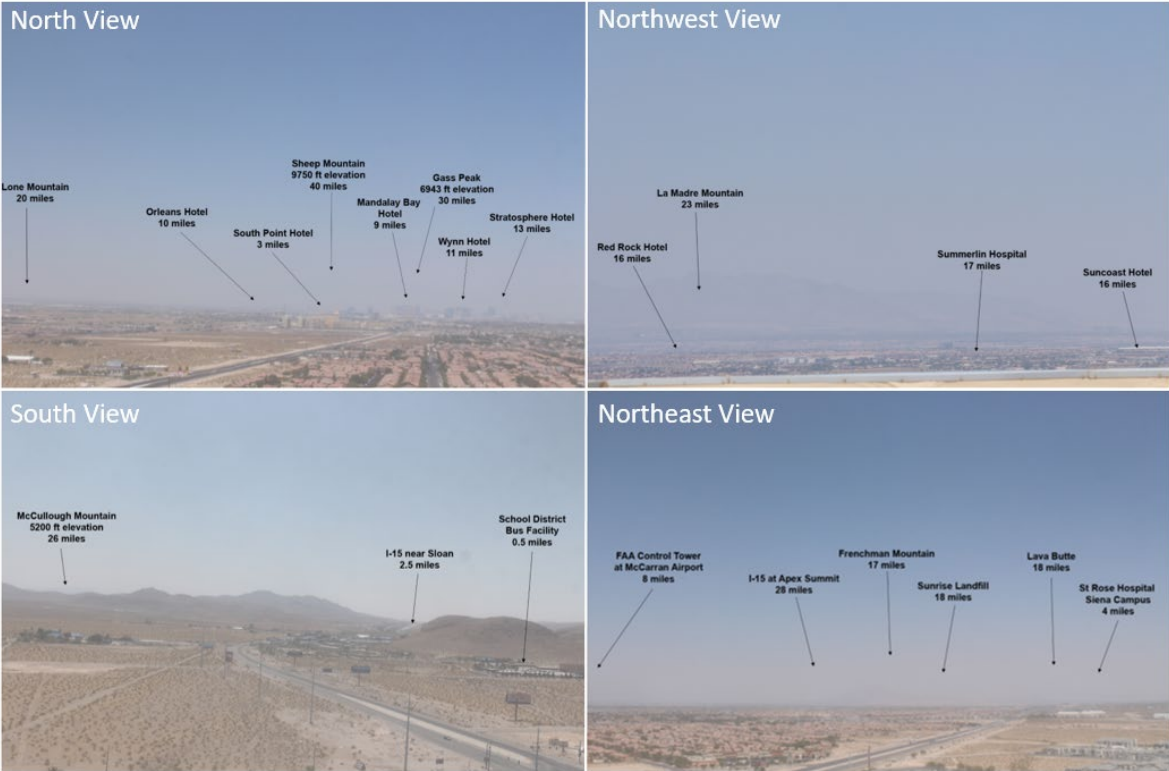
Figure 3-27. Clark County visibility images from August 3, 2020. Images taken from webcams set up in Clark County are shown for the exceptional event on August 3. Each image is labeled with the viewing direction and landmarks.
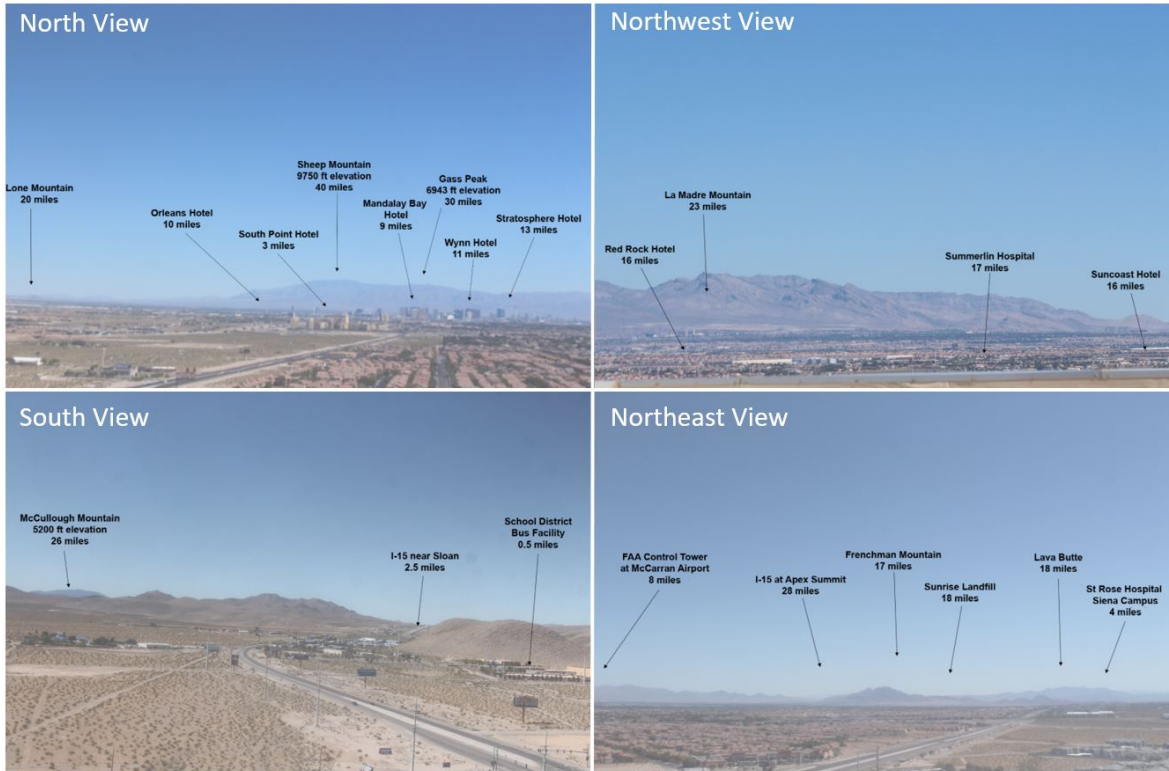
Figure 3-28. Visibility images taken from webcams set up in Clark County are shown for a clear day (May 21, 2020). Each image is labeled with the viewing direction and landmarks.

3.2   Tier 2 Analyses

3.2.1   Key Factor #1: Q/d Analysis

The exceptional event guidance (U.S. Environmental Protection Agency, 2016) describes a method used to relate the quantity of smoke emissions and distance of the fire to an exceeding monitor. The resulting quantity, called Q/d, may be used to screen fires that meet a conservative threshold of air quality impacts.[3] This section provides the results of the Q/d analyses for fires that were likely to have contributed to the August 3 ozone event in Clark County. Based on media coverage, transport analysis, and ground/satellite-based analyses in Section 3.1, the Apple Fire in southern California

---

[3] Specifically, fires with a Q/d value meeting the 100 tons/km threshold may qualify for a Tier 2 demonstration of a clear causal relationship. However, this threshold is insufficient to identify all cases where ozone impacts from smoke may have occurred. Pages 16-17 of the guidance state: "To determine an appropriate and conservative value for the Q/d threshold (below which the EPA recommends Tier 3 analyses for the clear causal relationship), the EPA conducted a review. The reviews and analyses did not conclude that particular ozone impacts will always occur above a particular value for Q/d. For this reason, a Q/d screening step alone is not sufficient to delineate conditions where sizable ozone impacts are likely to occur." (U.S. Environmental Protection Agency, 2016).

contributed to smoky conditions and high ozone concentrations in Clark County, Nevada on that date.

Figure 3-29 shows large fires burning in the vicinity of Clark County on August 3, 2020, including the Apple Fire in southern California. Table 3-3 shows agency data available for the Apple Fire (as of December 2020). The Apple Fire started on July 31, 2020, as a result of a malfunctioning diesel engine and quickly turned into a large fire. It then ran uphill into steep, rugged, wildland terrain that was inaccessible to most firefighting methods (https://inciweb.nwcg.gov/incident/article/6902/53409). By August 3, 2020, the Apple Fire had burned approximately 27,000 acres according to InciWeb estimates (https://inciweb.nwcg.gov/incident/6902). The total size of the fire amounted to 33,424 acres with an official containment date of November 16, 2020.
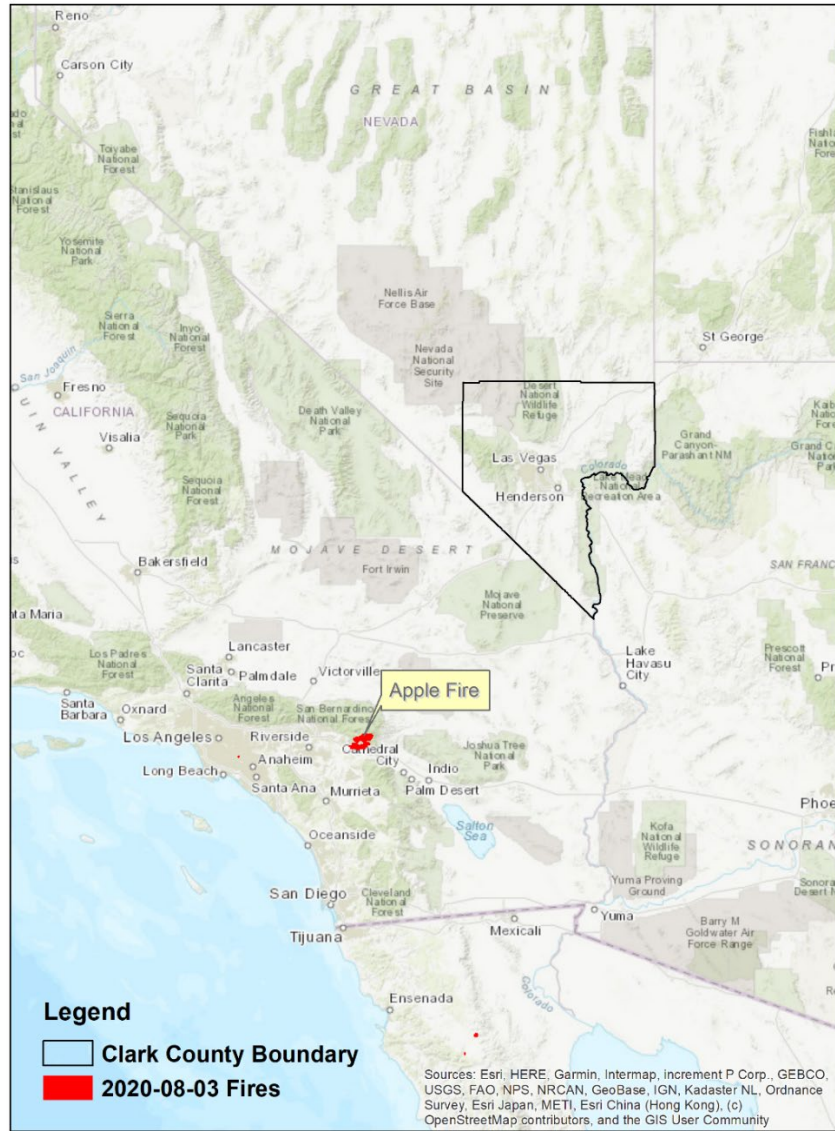
Figure 3-29. Large fires burning on August 3, 2020, in the vicinity of Clark County are shown in red. The Clark County boundary is shown in black.

Key factor #1 for a Tier 2 demonstration requires an analysis of wildfire smoke emissions from a qualifying fire and the distance of the fire to the affected monitor(s). To identify qualifying fires, the guidance "recommends generating 24-hour back trajectories from the affected ozone monitoring site(s) beginning at each hour of these two or three dates" (U.S. Environmental Protection Agency, 2016). Three dates would be used only if the 8-hour averaging period for the daily maximum 8-hour ozone data include hours falling on two dates (i.e., the 8-hour average includes at least 11 p.m. and midnight on two distinct calendar days). For this demonstration, 24-hour HYSPLIT back trajectories were generated from the monitor location starting on each hour of the day of the exceedance.

The guidance states that "...fires that are close to any of these back trajectories" may be used to calculate Q/d (U.S. Environmental Protection Agency, 2016). To identify fires that fall near the

HYSPLIT trajectories, trajectories were buffered by a distance of 25% of the distance traveled by the trajectory, which is consistent with uncertainty reported for HYSPLIT trajectory modeling (Draxler, 1991). **Figure 3-30** shows the back trajectories and buffer of uncertainty from Clark County, Nevada. All fires falling within the uncertainty buffer of one or more trajectories were considered candidates for calculating Q/d.

Table 3-3. Fire data for the Apple Fire associated with the August 3 exceptional event. Information includes start/containment date, cause of the fire, the agency's estimate of the area burned by the exceptional event date (August 3, 2020) and the total reported acres burned.

Fire Name	Start Date	Contained Date	Cause	Area Burned by EE Date (acres)	Total Area Burned (acres)
Apple Fire	7/31/2020	11/16/2020	Human	26,850	33,424

To calculate Q/d for a qualifying fire, the total daily emissions of NO_x and reactive VOCs (rVOCs) in tons is divided by the distance from the fire to impacted monitors. BlueSky Playground Version 3.0.1 (**https://tools.airfire.org/playground/v3/**) was used to estimate emissions of NO_x and VOCs for the qualifying fire on a daily basis. Daily fire growth was identified using agency reports directly or news reports citing official sources. The fire's location—as reported in InciWeb or by CAL FIRE—was used to identify the distance to the impacted monitors and fuelbed type. Emissions calculations were based on very dry conditions.

EPA guidance recommends that an event may qualify for a Tier 2 demonstration if the Q/d value for a single fire, or the aggregate Q/d across multiple fires, exceeds a conservative value of 100 tons/km. Daily Q/d results indicate that significant emissions of NO_x and rVOCs occurred from the Apple Fire during the days leading up to and including the day of the exceedance (**Table 3-4**). However, due to the significant distance between the fire and the monitor location, the emissions were not large enough to reach the Q/d threshold of 100 tons/km for a Tier 2 demonstration, and it was determined that Tier 3 analyses were needed to demonstrate a clear causal relationship.
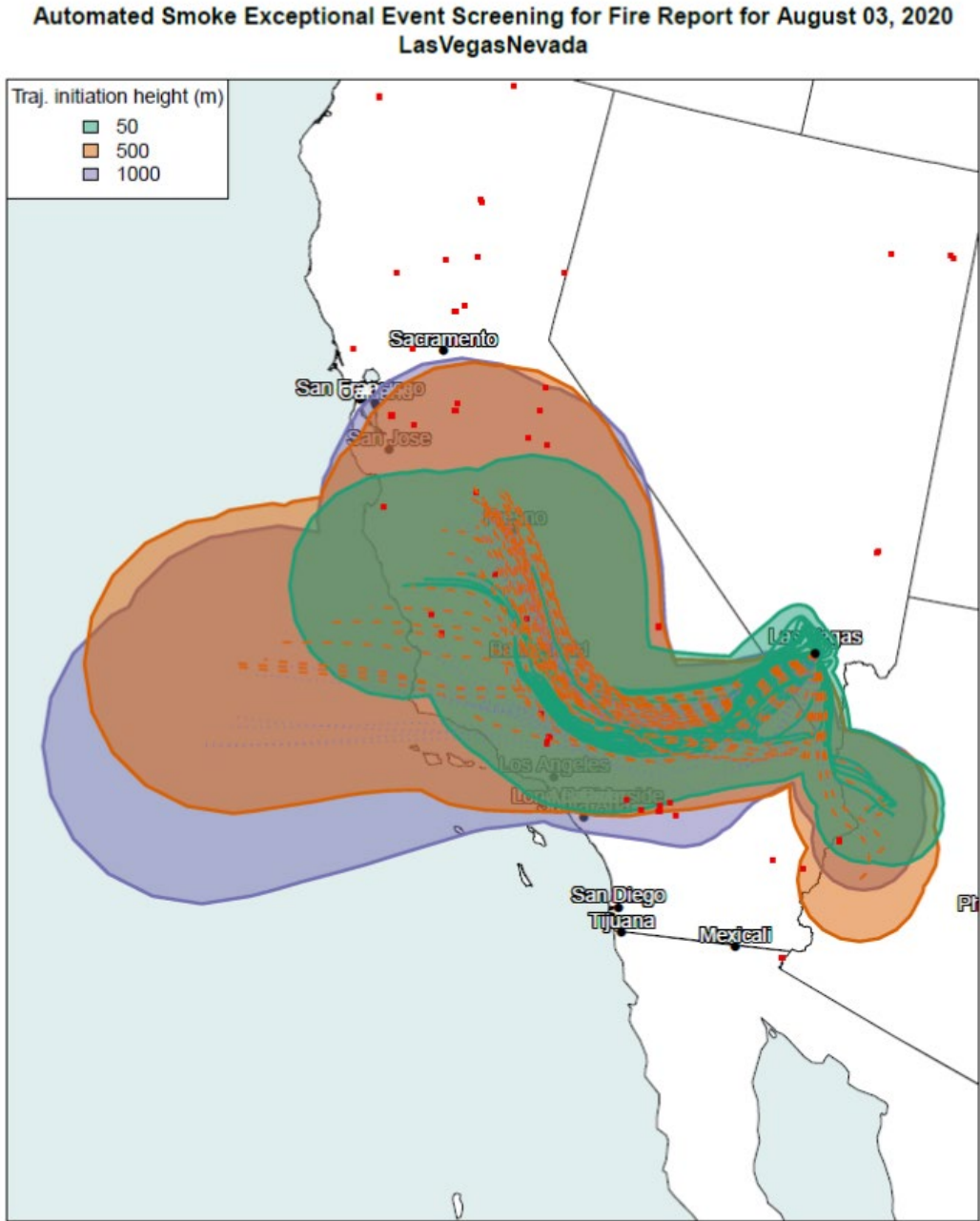
Figure 3-30. Q/d analysis. 24-hour back trajectories are shown as solid or dotted lines. The starting height of the back trajectory is indicated by the color. Uncertainty buffers, calculated as 25% of the distance traveled by the trajectory, are shown in colored polygons. Active fires on August 3 are shown as red squares. Fires falling within one or more uncertainty buffer(s) were used to calculate individual and aggregate Q/d values.

Table 3-4. Daily growth, emissions, and Q/d for the Apple Fire. Daily growth for July 31 and August 1 were identified based on agency reports obtained from the Riverside County Fire Department reports at **rvcfire.org/_Layouts/Incident%20Information/IncidentInfoDetail.aspx?4558**, and growth for August 2 and 3 were obtained from the Incident Information System (InciWeb) at **inciweb.nwcg.gov/incident/6902**.

Date	Area (Acres)	Daily Growth (Acres)	NOx (Tons)	VOCs (Tons)	Reactive VOCs (Tons)	Distance (Km)	Q/d (Tons/km)
8/3/2020	26,850	400	13	68	41	290	0.2
8/2/2020	26,450	11,450	370	1,941	1,165	290	5.3
8/1/2020	15,000	13,280	429	2,251	1,351	290	6.1
7/31/2020	1720	1720	56	292	175	290	0.8

The results of the Q/d analysis presented in this section agree with and further strengthen the conceptual model and Tier 3 weight of evidence of a clear causal relationship between the identified wildfires smoke emissions and the monitored ozone exceedance identified in this demonstration.

3.2.2 Key Factor #2: Comparison of Event Concentrations with Non-Event Concentrations

Another key factor in determining whether the August 3, 2020, exceedance event is exceptional is to compare event ozone concentrations with non-event concentrations via percentile and rank-order analysis. Table 3-5 shows August 3, 2020, concentrations as a percentile in comparison with the last six years of data (with and without the other proposed 2018 and 2020 EE days included) at each site in Clark County. For the seven monitoring sites (i.e., Paul Meyer, Walter Johnson, Joe Neal, Green Valley, Boulder City, Jean, and Indian Springs) that show a NAAQS exceedance on August 3, all of the exceedances are greater than or equal to the 99th percentile when compared to the last six years of data, even with all other proposed 2018 and 2020 exceptional event days included. Without the other exceptional event days included, the percentiles are slightly higher (>99th percentile). Additionally, other non-event sites show very high percentiles as well (>97th percentile), suggesting a widespread ozone event across Clark County. To confirm that the calculated percentiles are not biased by non-ozone season data, Table 3-6 shows the August 3 percentile ranks for all monitoring sites around Clark County in comparison with the last six years of ozone season (May to September) data. For five of the seven monitoring sites (Walter Johnson, Paul Meyer, Joe Neal, Boulder City, and Jean), the August 3 percentile ranks above the 99th percentile (with all proposed 2018 and 2020 exceptional event days included). Green Valley and Indian Springs show percentile ranks of 98.1 and 98.6, respectively. When the other possible exceptional event days are excluded, the percentile ranks for Green Valley and Indian Springs increase to 99.0 and 98.9, respectively. Although not all of the sites showed a >99th percentile rank for August 3 compared with the last six ozone seasons, this

analysis confirms that the August 3 exceptional event included unusually high concentrations of ozone when compared with the last six years of data and the last six ozone seasons.

Table 3-5. Six-year percentile ozone. The August 3 exceptional event ozone concentration at each site is calculated as a percentile of the last six years with and without other 2018 and 2020 exceptional events included in the historical record.

AQS Site Code	Site Name	6-Year Percentile	6-Year Percentile w/o EE Dates
320030071	Walter Johnson	100.	*100.*
320030043	Paul Meyer	99.9	*100.*
320030075	Joe Neal	99.9	*99.9*
320030298	Green Valley	99.1	*99.5*
320030022	Apex	97.9	*98.2*
320030023	Mesquite	99.1	*99.1*
320030073	Palo Verde	98.9	*99.1*
320030540	Jerome Mack	98.6	*99.1*
320030601	Boulder City	100.	*100.*
320031019	Jean	99.8	*99.9*
320037772	Indian Springs	99.0	*99.2*

Table 3-6. Six-year, ozone-season percentile ozone. The August 3 exceptional event ozone concentration at each site is calculated as a percentile of the last six years' ozone season (May–September) with and without other 2018 and 2020 exceptional events included in the historical record.

AQS Site Code	Site Name	6-Year Percentile	6-Year Percentile w/o EE Dates
320030071	Walter Johnson	99.9	*99.9*
320030043	Paul Meyer	99.8	*100.*
320030075	Joe Neal	99.8	*99.8*
320030298	Green Valley	98.1	*99.0*
320030022	Apex	97.1	*97.5*
320030023	Mesquite	98.7	*98.7*
320030073	Palo Verde	97.4	*98.0*
320030540	Jerome Mack	96.7	*97.9*
320030601	Boulder City	100.	*100.*
320031019	Jean	99.5	*99.7*
320037772	Indian Springs	98.6	*98.9*

We also compared the rank-ordered concentrations at each site for 2020. As shown in Figures 2-3 through 2-9, 2020 ozone concentrations were not atypically low, which might bias our rank-ordered analysis for August 3, 2020. Tables 3-7 through 3-13 show the rank-ordered ozone concentrations for 2018 through 2020 and the design values for 2020, with the proposed 2018 and 2020 exceptional events included. For all seven monitoring sites that showed an exceedance of the NAAQS, August 3 was in the top four highest ozone concentrations for 2020.

Table 3-7. Site-specific ozone design values for the Paul Meyer monitoring site. The top five highest ozone concentrations for 2018-2020 at Paul Meyer are shown, and proposed exceptional event days in 2018 and 2020 are included.

Paul Meyer Rank	2018	2019	2020
Highest	79	74	79
Second Highest	76	72	78
Third Highest	75	70	77
Fourth Highest	75	69	77
Fifth Highest	74	69	76
Design Value		73	

Table 3-8. Site-specific ozone design values for the Walter Johnson monitoring site. The top five highest ozone concentrations for 2018-2020 at Walter Johnson are shown, and proposed exceptional event days in 2018 and 2020 are included.

Walter Johnson Rank	2018	2019	2020
Highest	79	77	82
Second Highest	77	69	82
Third Highest	77	69	78
Fourth Highest	76	68	77
Fifth Highest	76	68	75
Design Value		73	

Table 3-9. Site-specific ozone design values for the Joe Neal monitoring site. The top five highest ozone concentrations for 2018-2020 at Joe Neal are shown, and proposed exceptional event days in 2018 and 2020 are included.

Joe Neal Rank	2018	2019	2020
Highest	80	74	81
Second Highest	78	70	78
Third Highest	76	69	78
Fourth Highest	76	68	78
Fifth Highest	74	67	76
Design Value		74	

Table 3-10. Site-specific ozone design values for the Green Valley monitoring site. The top five highest ozone concentrations for 2018-2020 at Green Valley are shown, and proposed exceptional event days in 2018 and 2020 are included.

Green Valley Rank	2018	2019	2020
Highest	78	73	76
Second Highest	78	72	72
Third Highest	78	71	72
Fourth Highest	77	70	71
Fifth Highest	77	70	70
Design Value		72	

Table 3-11. Site-specific ozone design values for the Boulder City monitoring site. The top five highest ozone concentrations for 2018-2020 at Boulder City are shown, and proposed exceptional event days in 2018 and 2020 are included.

Boulder City Rank	2018	2019	2020
Highest	72	70	72
Second Highest	69	67	71
Third Highest	69	67	69
Fourth Highest	69	66	67
Fifth Highest	66	65	66
Design Value		67	

Table 3-12. Site-specific ozone design values for the Jean monitoring site. The top five highest ozone concentrations for 2018-2020 at Jean are shown, and proposed exceptional event days in 2018 and 2020 are included.

Jean Rank	2018	2019	2020
Highest	81	67	75
Second Highest	77	67	73
Third Highest	73	66	73
Fourth Highest	72	66	70
Fifth Highest	72	65	68
Design Value		69	

Table 3-13. Site-specific ozone design values for the Indian Springs monitoring site. The top five highest ozone concentrations for 2018-2020 at Indian Springs are shown, and proposed exceptional event days in 2018 and 2020 are included.

Indian Springs Rank	2018	2019	2020
Highest	78	69	78
Second Highest	75	66	72
Third Highest	74	66	71
Fourth Highest	73	65	69
Fifth Highest	73	65	68
Design Value		69	

For further comparison with non-event ozone concentrations, Table 3-14 shows 5-year (2015-2019) MDA8 ozone statistics for the week before and after August 3. This two-week window analysis shows that each affected monitoring site shows MDA8 ozone concentrations on August 3, 2020, to be well above the average and at or above the 95th percentile of the last five years of data.

The percentile, rank-ordered analyses, and the two-week window analysis, indicate that all affected monitoring sites on August 3, 2020, showed unusually high ozone concentrations compared with non-event concentrations. This conclusion supports a key factor, suggesting that August 3 was an exceptional event in Clark County, Nevada.

Table 3-14. Two-week non-event comparison. August 3, 2020, MDA8 ozone concentrations for each affected site are shown in the top row. 5-year (2015-2019) average MDA8 ozone statistics for July 27 through August 11 are shown for each affected site around Clark County to compare with the event ozone concentrations.

	Boulder City 320030601	Green Valley 320030298	Indian Springs 320037772	Jean 320031019	Joe Neal 320030075	Paul Meyer 320030043	Walter Johnson 320030071
Aug. 3	72	72	71	73	81	78	82
Mean	53	56	56	56	60	59	59
Median	54	56	55	56	60	59	60
Mode	54	52	52	57	59	59	68
St. Dev	7	8	7	7	10	9	9
Minimum	34	39	41	38	38	39	36
95 %ile	63	71	68	67	74	72	73
99 %ile	66	73	71	72	81	78	77
Maximum	72	74	72	73	83	79	82
Range	38	35	31	35	45	40	46
Count	96	96	96	96	96	96	96

3.2.3 Satellite Retrievals of Pollutant Concentrations

Satellite retrievals of pollutants associated with wildfire smoke, such as AOD, CO, and NO_x, can provide evidence that smoke was present at a monitoring site. We examined maps of Multi-Angle Implementation of Atmospheric Correction (MAIAC) AOD from the Moderate Resolution Imaging Spectroradiometer (MODIS) instrument onboard the Aqua and Terra satellites, CO retrievals from the Atmospheric Infrared Sounder (AIRS) instrument onboard the Aqua satellite, and NO_2 retrievals from the Ozone Monitoring Instrument (OMI). NO_2 satellite retrievals from OMI were inconclusive for this event and moved to **Appendix B**. These maps provide evidence to support the transport of smoke from the Apple Fire in southern California to Clark County, Nevada, as already demonstrated with visual imagery and trajectories in Sections 3.1 and 3.2. MODIS AOD measurements indicate the concentration of light-absorbing aerosols, including those emitted by wildfires, in the total atmospheric column. Between July 31 and August 3, AOD measurements show the movement of a dense plume of aerosols originating from the Apple Fire (**Figure 3-31**). This plume spread from southern California to southeastern Nevada and western Arizona between July 31 and August 2. A surface area of low pressure centered over the border between California, Nevada, and Arizona transported the smoke plume eastward (see Section 3.3.1 for more details). MODIS AOD retrievals indicate enhanced AOD in the Clark County area on August 3 (**Figure 3-32**).
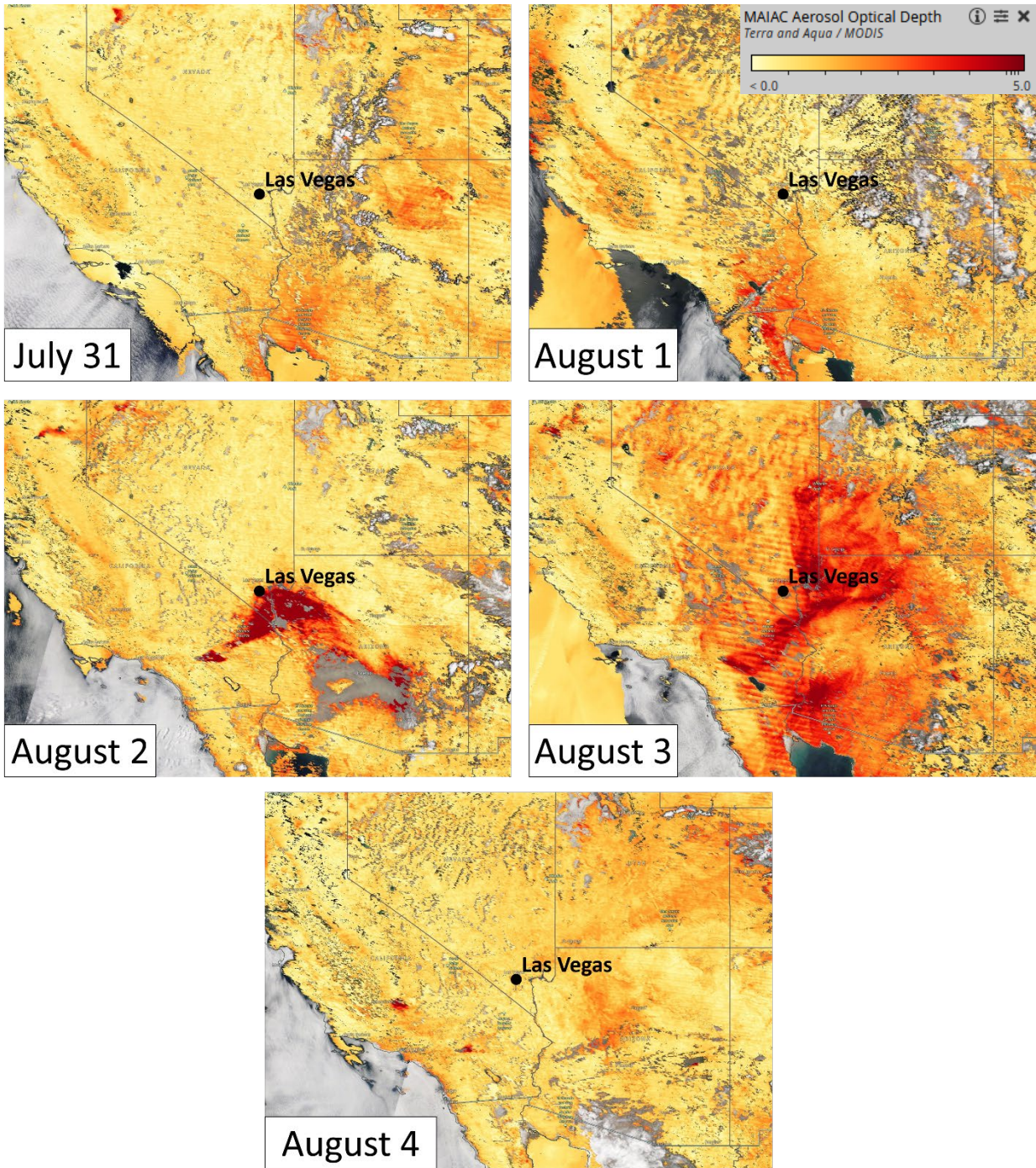
Figure 3-31. MAIAC MODIS Aqua/Terra combined AOD retrievals for the three days before the exceptional event, during the exceptional event, and one day after the exception event are shown. On August 3, impacts from the Apple Fire are circled in red.
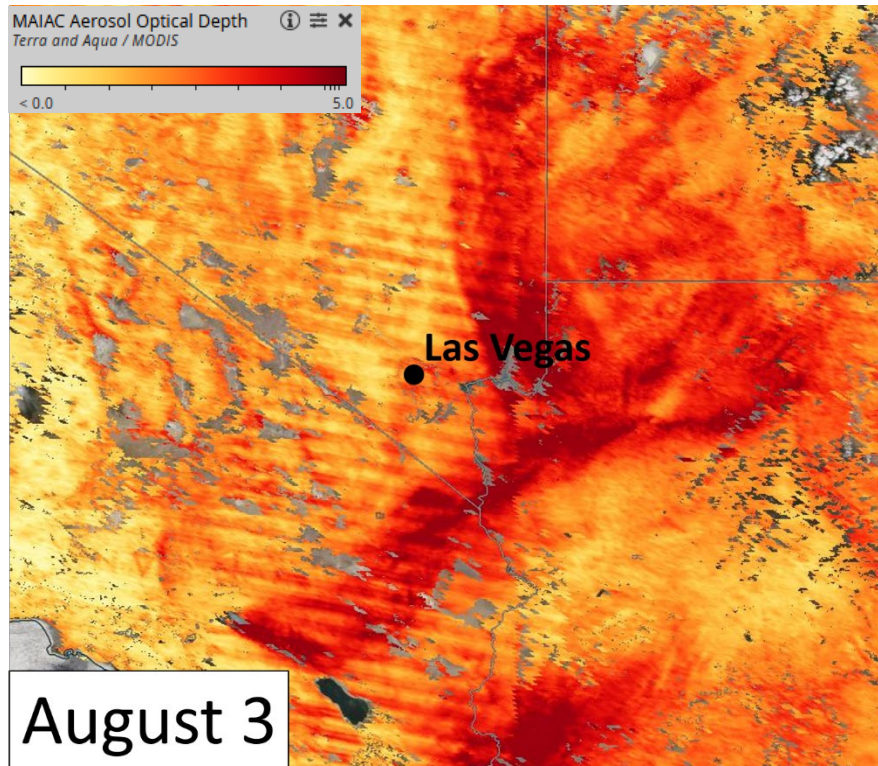
Figure 3-32. A zoomed-in view (over Clark County and the Apple Fire) of the MAIAC MODIS Aqua/Terra combined AOD retrieval during the exceptional event on August 3, 2020.

CO measurements at 500 hPa from AIRS show a similar pattern of smoke plume transport seen in the MODIS AOD data noted above. Excluding areas outside of the swath width from the AIRS instrument, the maps show smoke transport from the Apple Fire to the Clark County area between July 31 and August 4 (**Figure 3-33**). Areas of enhanced CO originating from the Apple Fire that spread throughout southern California, southeastern Nevada, and western Arizona can be clearly distinguished by August 2. By August 3, CO concentrations in areas of Clark County were up to approximately 115 ppbv at 500 hPa (**Figure 3-34**).
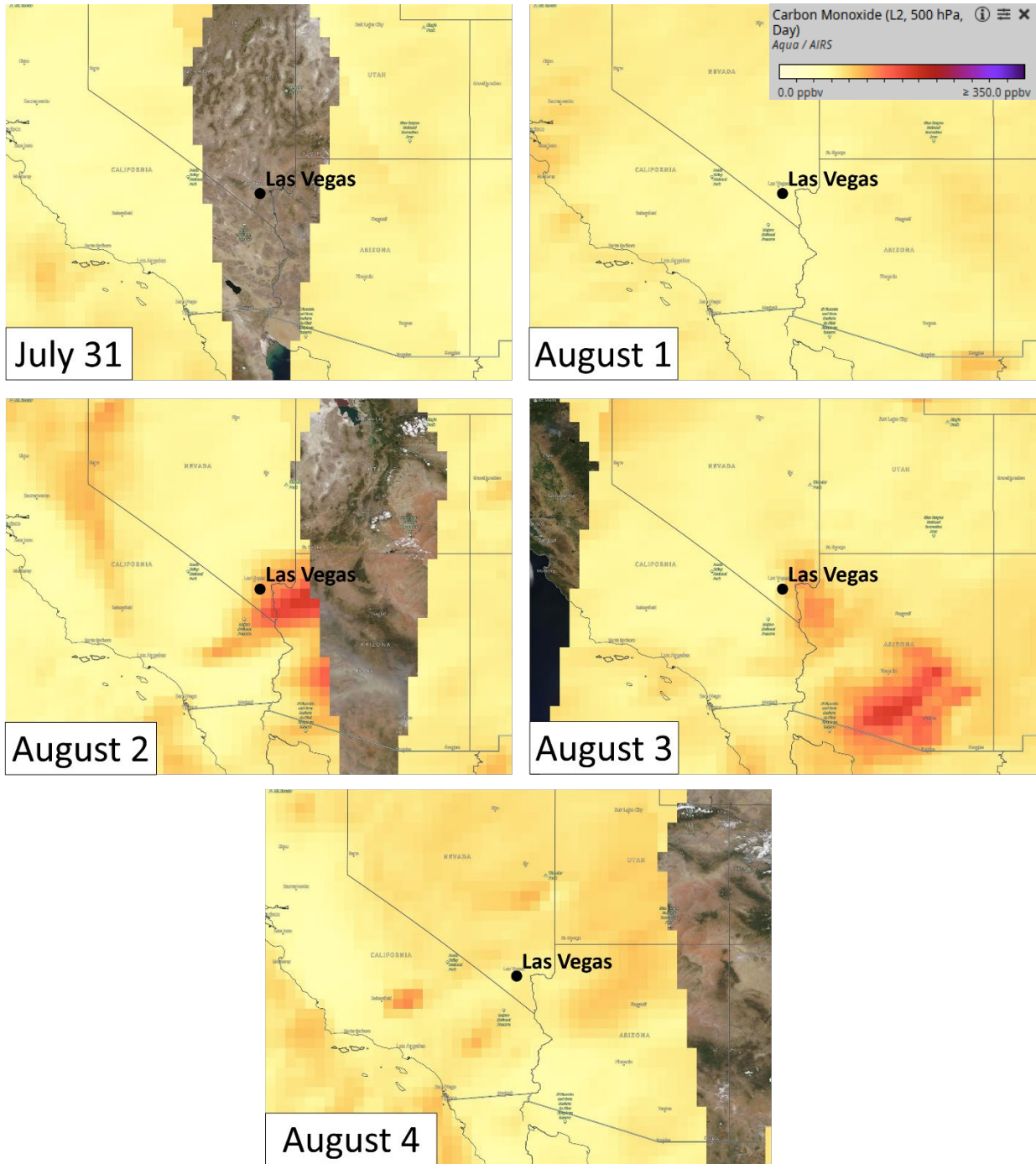
Figure 3-33. MODIS Aqua AIRS CO retrievals for the three days before, during the exceptional event on August 3, 2020, and one day after the exceptional event.
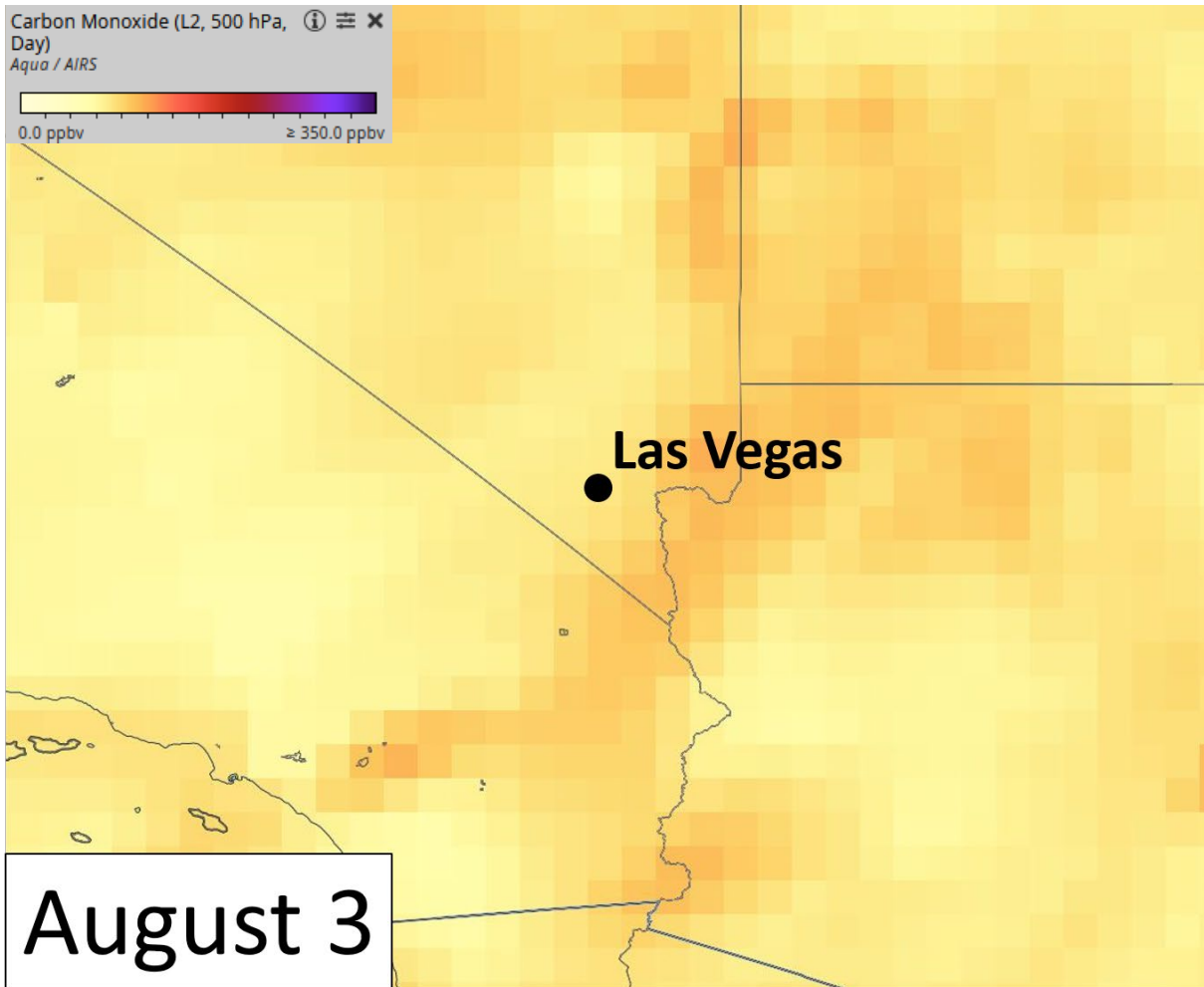
Figure 3-34. A zoomed-in view (over Clark County and the Apple Fire) of the Aqua AIRS CO retrieval during the exceptional event on August 3, 2020.

3.2.4 Supporting Pollutant Trends and Diurnal Patterns

Ground measurements of wildfire plume components (e.g., PM$_{2.5}$, CO, NO$_x$, and VOCs) can be used to further demonstrate that smoke impacted ground-level air quality if enhanced concentrations or unusual diurnal patterns are observed. We examined concentrations of PM$_{2.5}$, CO, NO, NO$_2$, and TNMOC measured at all exceedance sites as well as other nearby sites in Clark County. If PM$_{2.5}$, CO, NO$_x$, and VOCs were enhanced at the time the smoke plume arrived in Clark County, these measurements would provide additional supporting evidence of smoke impacts in the area.

Figure 3-35 shows an overall view of the magnitude of pollutant concentrations measured around Clark County in the week before and after the August 3 event. The peak daily concentration of PM$_{2.5}$ at exceedance-affected monitoring sites and nearby sites shows a marked increase on August 3 compared to the weeks surrounding August 3. This initial rise on August 3 coincides with the rise in

ozone on that day. The high PM$_{2.5}$ levels sustained through August 4, and then returned to typical concentrations. Although spikes in NO, NO$_2$, and TNMOC also occurred on August 3, these increases are similar in magnitude to increases observed on nearby dates. The rest of this section examines temporal abnormalities and site-specific trends for each supporting pollutant. Because less than one season's worth of data is available for TNMOC, this pollutant is excluded from detailed examination below.
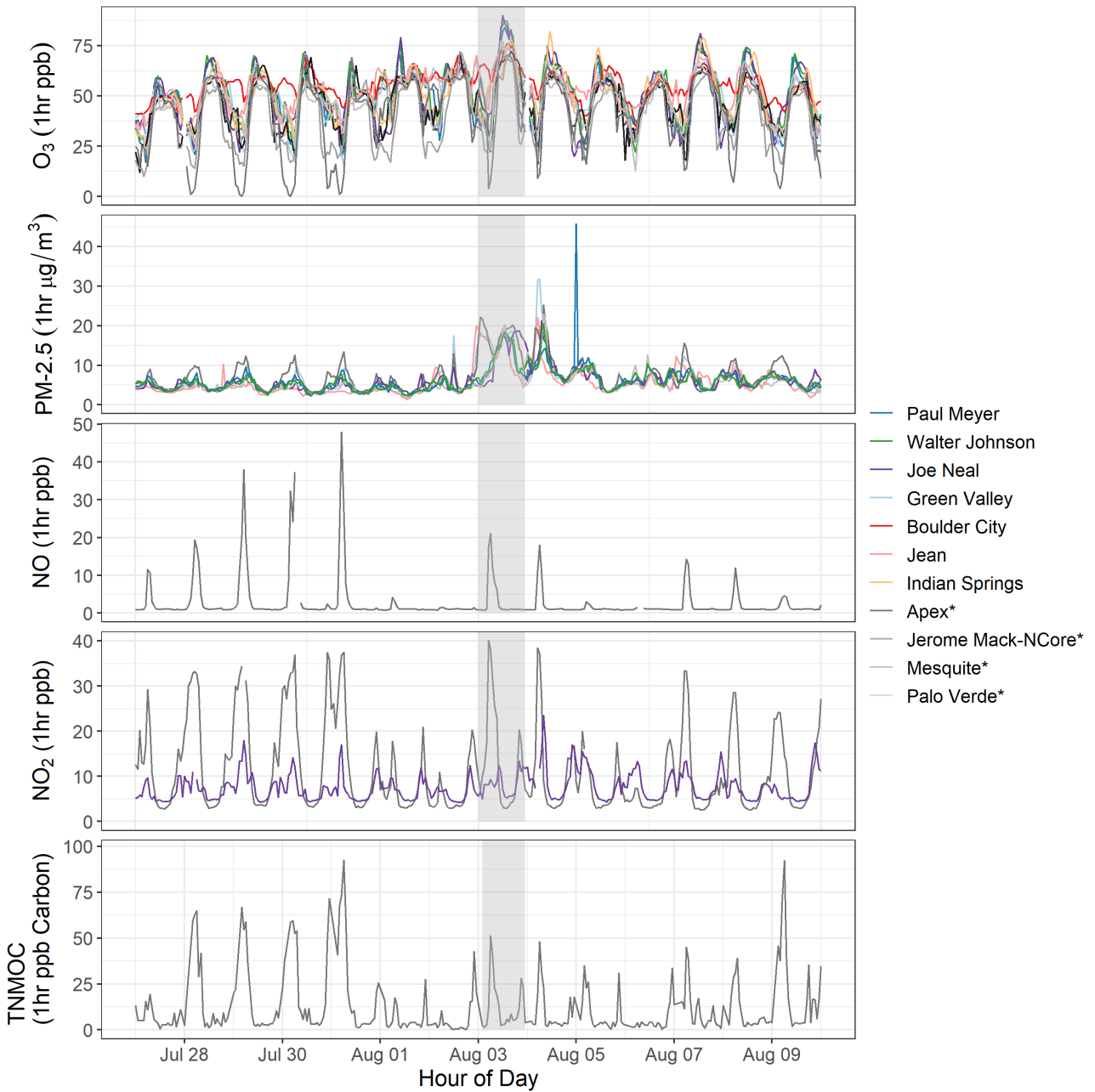
Figure 3-35. Hourly concentrations of ozone, PM$_{2.5}$, NO$_x$, and TNMOC. Colored lines represent sites in exceedance for ozone on August 3. Gray lines represent supporting sites in Clark County (marked with a star in the legend). The gray shaded area represents August 3.

Unusual diurnal patterns of supporting surface pollutant measurements can provide evidence that smoke impacted Clark County air quality. **Figure 3-36** shows the diurnal profile for ozone and PM$_{2.5}$ at multiple sites in Clark County alongside the 5-year seasonal (May to September) average ozone,

where data are available. On a typical day, the diurnal profile of ozone shows a peak around midday and an overnight trough, while the diurnal profile of $PM_{2.5}$ remains fairly constant with a slight dip during daylight hours. The $PM_{2.5}$ diurnal profile during the August 3 exceedance event exhibits a distinct deviation from the seasonal mean diurnal profile. Upwind sites Jean and Green Valley showed a factor of more than two increase in $PM_{2.5}$ concentrations overnight on August 2 into the morning of August 3 that demonstrates an abnormal $PM_{2.5}$ source in the Clark County area. These elevated concentrations sustained throughout the event date at these two sites. Three other sites on August 3 showed factors of 2 to 3 increase during the day relative to typically low seasonal mean $PM_{2.5}$ concentrations. Diurnal profiles of $PM_{10}/PM_{2.5}$ (**Appendix C**) show the relative contribution of PM_{10} was at or below average relative to $PM_{2.5}$ during the midday $PM_{2.5}$ enhancement, indicating that the contribution of dust to abnormalities in $PM_{2.5}$ concentration are minimal. The magnitudes of both ozone and $PM_{2.5}$ concentrations were well above average at their peak at all sites on August 3.
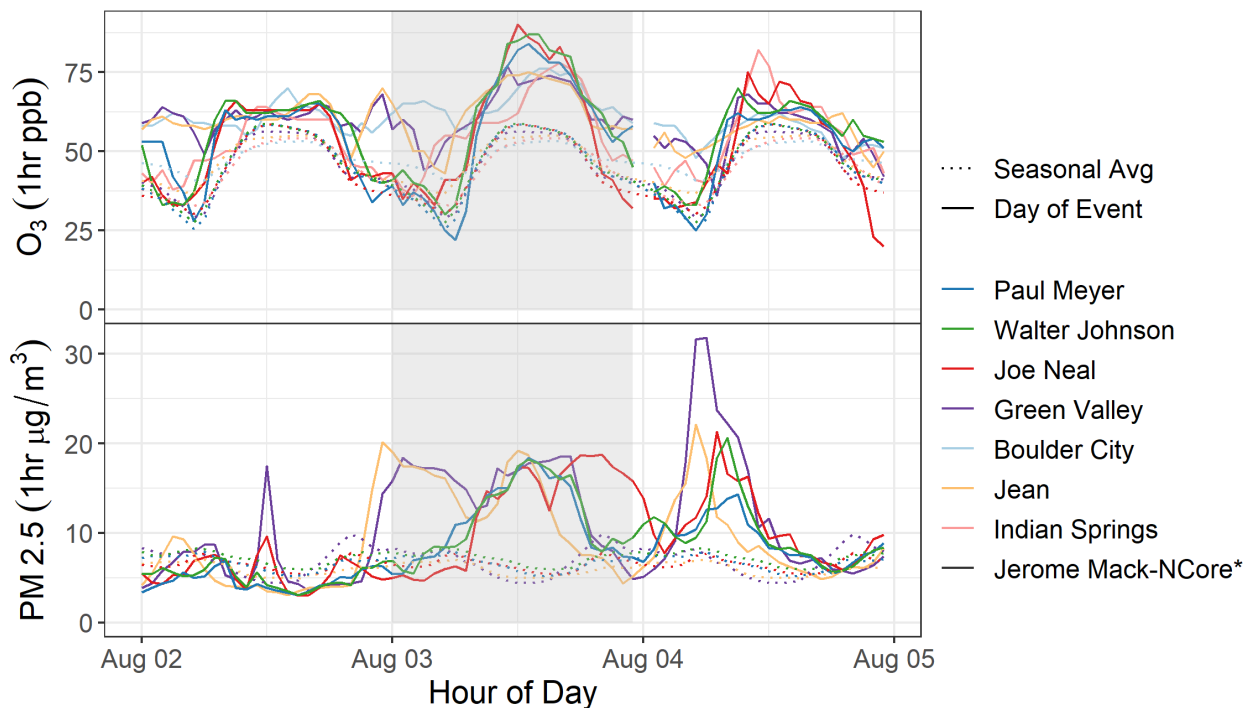
Figure 3-36. August 3 diurnal profiles of ozone and $PM_{2.5}$ (solid line), and the 5-year seasonal (May-September) average (dotted line) at sites in exceedance during the August 3, 2020, event period. August 3 is shaded in gray.

Figures 3-37 through 3-41 further display the diurnal profile and average seasonal diurnal profile of ozone and $PM_{2.5}$ concentrations broken out by event-affected monitoring site where data are available. The 5-year 5th to 95th percentile range is shown for reference. Five years of $PM_{2.5}$ data are available from Green Valley and Jean, four years from Paul Meyer, and one year from Walter Johnson

and Joe Neal. On August 3, concentrations of both ozone and PM$_{2.5}$ at every site rose above the 5-year 95th percentile at their peak value for the day.
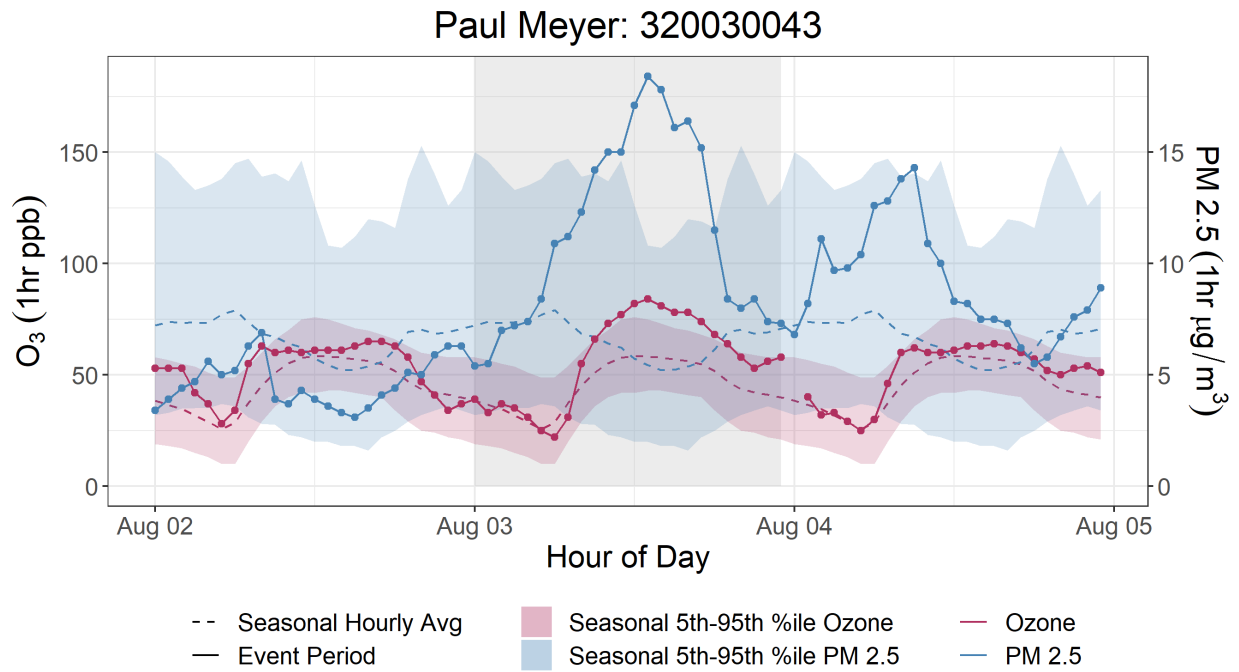
Figure 3-37. Diurnal profile of ozone (red) and PM$_{2.5}$ (blue) concentrations at Paul Meyer, including concentrations on August 3 (solid line) and the 5-year seasonal (May-September) average (dotted line). Data from Jerome Mack are plotted for 5-year seasonal average PM$_{2.5}$. Shaded ribbons represent the 5-year 5th-95th percentile range.
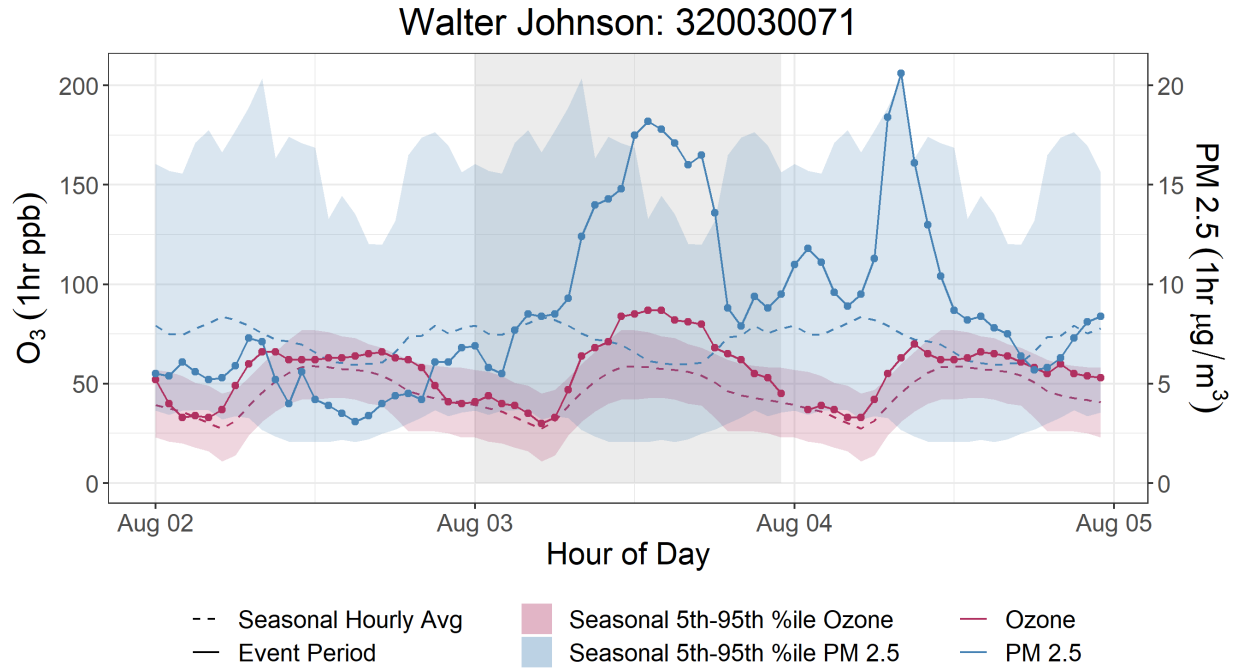
Figure 3-38. Diurnal profile of ozone (red) and PM$_{2.5}$ (blue) at Walter Johnson, including concentrations on August 3 (solid line) and the 5-year seasonal (May-September) average (dotted line). Data from Jerome Mack are plotted for 5-year seasonal average PM$_{2.5}$. Shaded ribbons represent the 5-year 5th-95th percentile range.
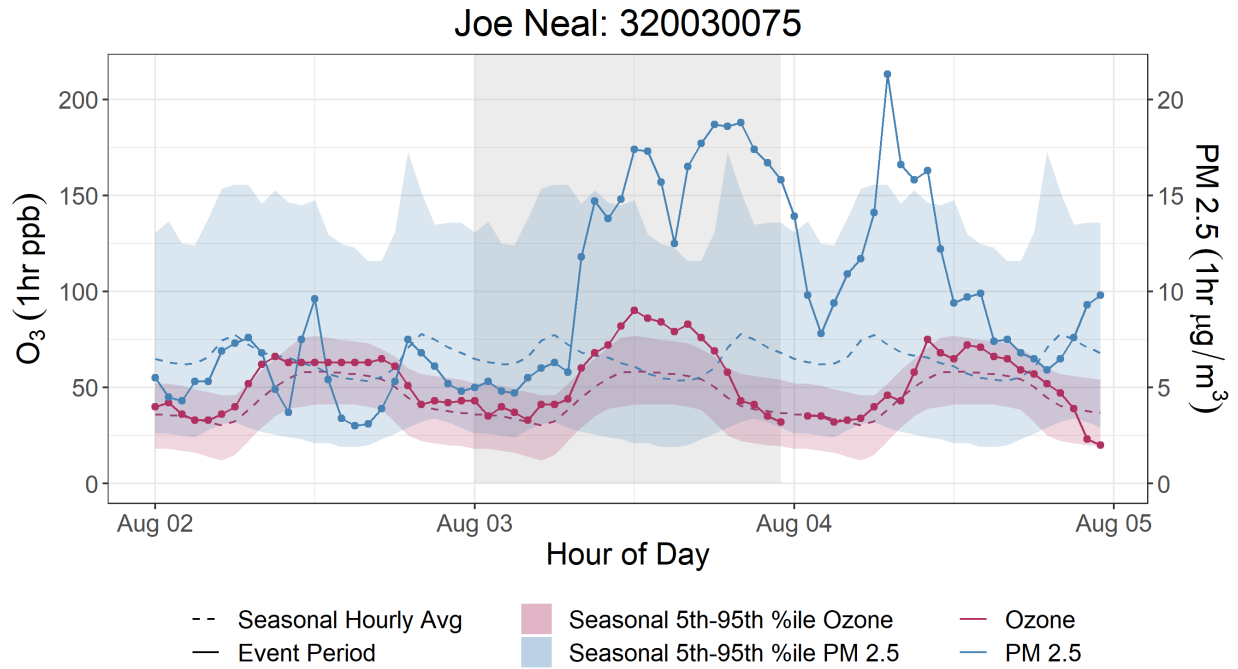
Figure 3-39. Diurnal profile of ozone (red) and PM$_{2.5}$ (blue) at Joe Neal, including concentrations on August 3 (solid line) and the 5-year seasonal (May-September) average (dotted line). Data from Jerome Mack are plotted for 5-year seasonal average PM$_{2.5}$. Shaded ribbons represent the 5-year 5th-95th percentile range.
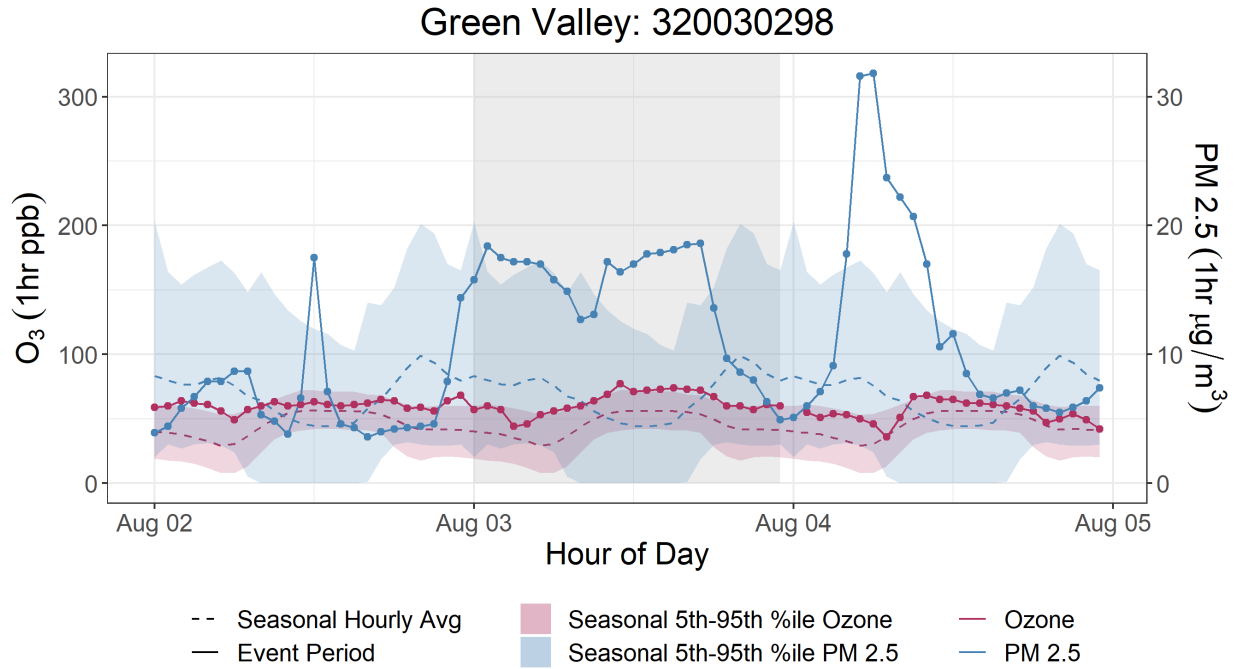
Figure 3-40. Diurnal profile of ozone (red) and PM$_{2.5}$ (blue) at Green Valley, including concentrations on August 3 (solid line) and the 5-year seasonal (May-September) average (dotted line). Data from Jerome Mack are plotted for 5-year seasonal average PM$_{2.5}$. Shaded ribbons represent the 5-year 5th-95th percentile range.
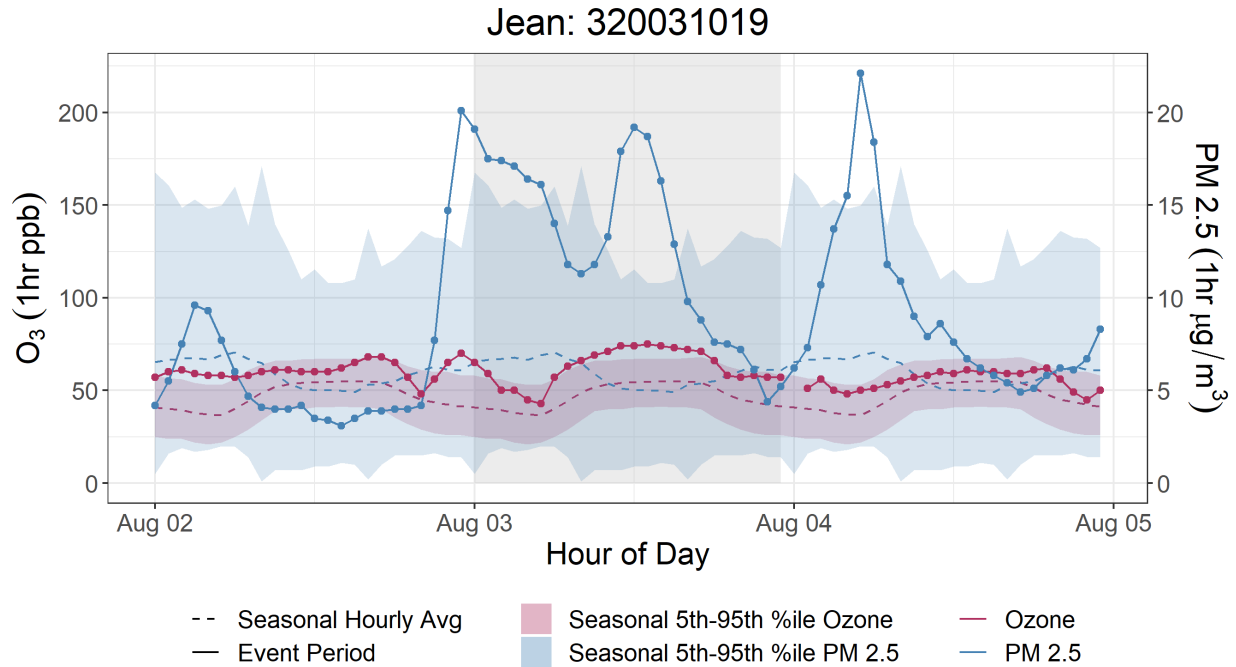
Figure 3-41. Diurnal profile of ozone (red) and PM$_{2.5}$ (blue) at Jean, including concentrations on August 3 (solid line) and the 5-year seasonal (May-September) average (dotted line). Data from Jerome Mack are plotted for 5-year seasonal average PM$_{2.5}$. Shaded ribbons represent the 5-year 5th-95th percentile range.

Two years of measurements of CO are available from the Joe Neal site. The diurnal profile of CO during the August 3 event period and the 5th-95th percentile range of the seasonal diurnal profile are displayed in **Figure 3-42**. CO at the Joe Neal site deviated from the expected diurnal pattern during the event period and increased concurrently with ozone. CO reached a peak midday concentration comparable to the 95th percentile of seasonal midday CO concentrations and remained elevated above average throughout the afternoon. One year of CO data is also available from Green Valley. Though this upwind site did not show elevated concentrations during the event period (see Appendix C), a peak in midday CO concentrations at Green Valley corresponds with the similar feature observed at Joe Neal. The consistent, abnormal midday maximum in CO concentrations at these two monitoring sites relative to seasonal mean diurnal trends provides evidence for wildfire emission plume impacts in Clark County on August 3.
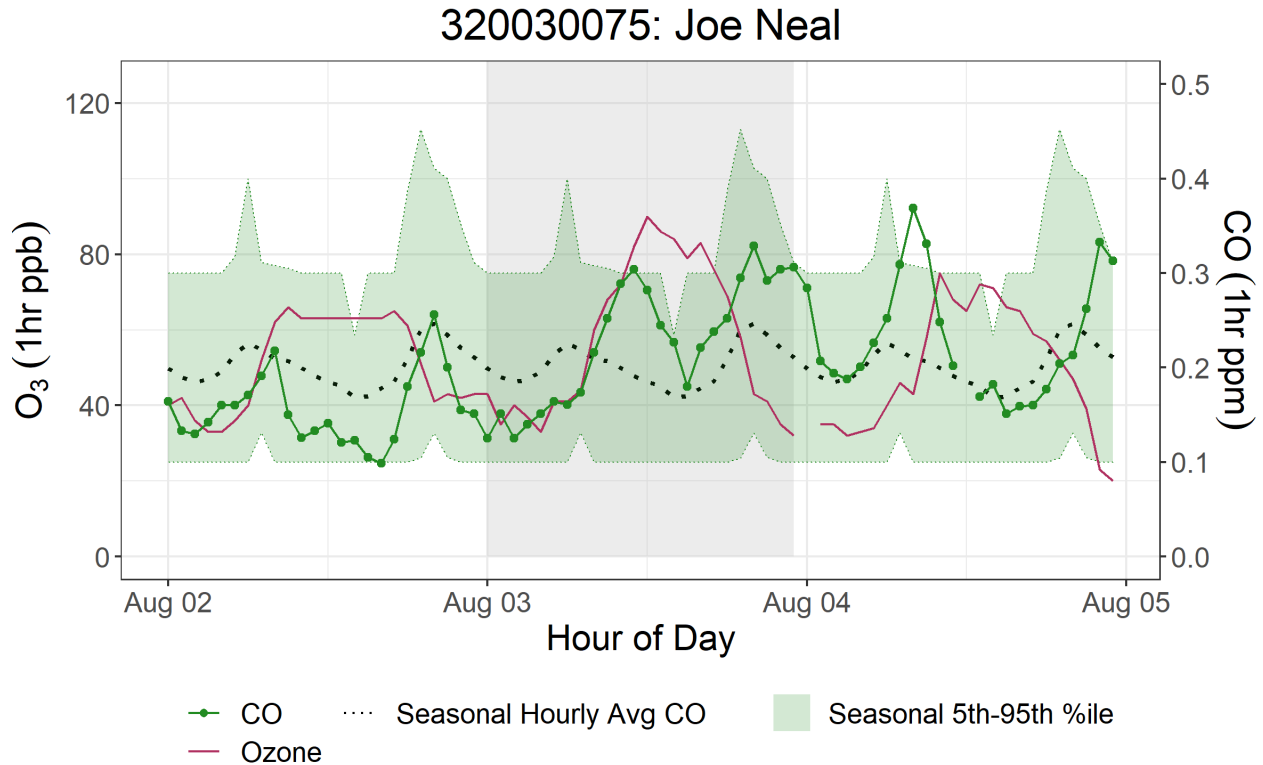
Figure 3-42. Ozone (red) and CO (green) concentrations at Joe Neal during the August 3 event period. The dashed line shows the seasonal (May–September) average CO diurnal profile. The green shaded area indicates the seasonal 5th to 95th percentile values for statistical reference. The gray box highlights August 3.

Concentrations of NO_x (NO and NO_2) were examined for the August 3 event in Clark County. NO_2 data are available at one event site, Joe Neal, as well as the NCore reference site, Jerome Mack (five years and four years of data, respectively). NO data is only available at Jerome Mack (five years of data). NO_2 concentrations at the event site were not elevated beyond the diurnal average, though the daily peak occurred later in the morning than usual. This pattern is mirrored at Jerome Mack for both NO and NO_2. Available NO_x profiles from Joe Neal and Jerome Mack are included in Appendix C.

The supporting pollutant trends and diurnal patterns, showing $PM_{2.5}$, CO, NO_x, and ozone concentrations outside of their normal seasonal or yearly historical averages provide additional proof of smoke impacts on the Clark County area on August 3, 2020. Wildfires can generate the precursors needed to create ozone, NO_x, and VOCs. While ozone concentrations can be suppressed very near a fire due to NO_x titration, downwind areas are likely to see an increase in ozone concentrations due to the presence of both precursor gases and sufficient UV radiation (i.e., when an air mass leaves an area of very thick smoke that inhibited solar radiation) (Finlayson-Pitts and Pitts Jr, 1997; Jaffe et al., 2008; Bytnerowicz et al., 2010). Ozone precursors from wildfire smoke can also be transported a significant distance downwind, and if these compounds are mixed into an urban area (such as Las

Vegas), the ozone concentrations produced can be significantly higher than they would be from either the smoke plume or the urban area alone (Jaffe et al., 2013; Wigder et al., 2013; Lu et al., 2016; Brey and Fischer, 2016). Since we find evidence of smoke impacts on August 3 in Clark County via supporting pollutant measurements and other analyses in Sections 3.1 and 3.2, we suggest that both the direct transport of ozone and the transport of ozone precursor gases from the Apple Fire in southern California likely caused the ozone exceedance.

Filter samples were also taken at the Jerome Mack monitoring site (including a collocated sample) in Clark County every three days during 2020. From these filter samples, concentrations of levoglucosan (a wildfire smoke tracer) were analyzed by the Desert Research Institute (DRI) via gas chromatography-mass spectroscopy (GC-MS). Levoglucosan is produced by the combustion of cellulose and is emitted during large wildfire events, which can then be transported downwind (Simoneit et al., 1999; Simoneit, 2002; Bhattarai et al., 2019). Levoglucosan has an atmospheric lifetime of one to four days before it is lost due to atmospheric oxidation, and can therefore be used as a tracer of biomass burning (wildfires) far downwind from its source (Hoffmann et al., 2009; Hennigan et al., 2010; Bhattarai et al., 2019; Lai et al., 2014). In the Las Vegas region, residential wood combustion has historically not been a significant contributor to levoglucosan concentrations during the late summer time frame (Kimbrough et al., 2016). Table 3-15 shows levoglucosan concentration, uncertainty, and positive/negative detection certainty on the days before and after the August 3 event. Because filter samples are only taken every three days, August 4 data are analyzed because no data were collected on August 3. Table 3-15 also shows the average levoglucosan concentration from 19 2018-2019 background days together with its standard deviation, and propagated uncertainty at the Jerome Mack site for comparison. On these background days, no ozone exceedance was observed, and fire/smoke influence was minimal according to HMS. Before the August 3 EE event, zero levoglucosan concentrations and negative detections are seen at the Jerome Mack monitoring sites. However, after smoke from the Apple Fire reached Clark County on August 3, non-zero levoglucosan concentrations and a positive detection are seen. The 53 ng/m^3 detection of levoglucosan in Clark County at the Jerome Mack monitoring site is significantly higher than the background average of 2±3 ng/m^3, providing evidence that wildfire smoke affected the Clark County area during the time period immediately following the August 3 ozone exceedance.

Table 3-15. Levoglucosan concentrations at monitoring sites around Clark County, Nevada, before and after the August 3 ozone event. Positive or negative detection is also shown.

Sample Date	Sampling Site	Levoglucosan (ng/m^3)	Levoglucosan Uncertainty (ng/m^3)	Levoglucosan Detected?
Background days (2018-2019)	Jerome Mack	2±3	1	N/A
8/1/2020	Jerome Mack	0.0	1	Negative
	Collocated-Jerome Mack	0.0	1	Negative
8/4/2020	Jerome Mack	53	5	Positive

3.3   Tier 3 Analyses

3.3.1 Total Column and Meteorological Conditions

Satellite analyses and HYSPLIT trajectories shown in Section 3.1 provide strong evidence that smoke was present over Clark County at the time of the exceptional event on August 3, 2020. However, the visible true color, AOD, and CO satellite data do not provide information about the vertical distribution of visible or measured smoke components. We examined satellite-retrieved aerosol vertical profiles and ceilometer mixing height measurements to determine whether the smoke plume was present at or near the surface on August 3.

The Cloud-Aerosol Light Detection and Ranging (LIDAR) and Infrared Pathfinder Satellite Observation (CALIPSO) system is a remote sensing instrument mounted on the CloudSat satellite that provides vertical profile measurements of atmospheric aerosols and clouds. Detected aerosols are classified into marine, marine mixture, dust, dust mixture, clean/background, polluted continental, smoke, and volcanic aerosol types. Unfortunately, CALIPSO did not pass over either the Apple Fire or Clark County immediately before, during, or immediately following the August 3 event, and is not included in this report.

The mesoscale and local meteorological conditions from July 31 to August 3 provide evidence for transport of smoke from the Apple Fire in southern California to Clark County, Nevada, and subsequent vertical mixing of smoke from aloft to the surface. Upper-level wind barbs at 500 hPa indicate that the southwest winds from an upper-level high pressure system south of Clark County

could transport any lofted smoke from the Apple Fire northeastward to the Clark County area (**Figure 3-43**).
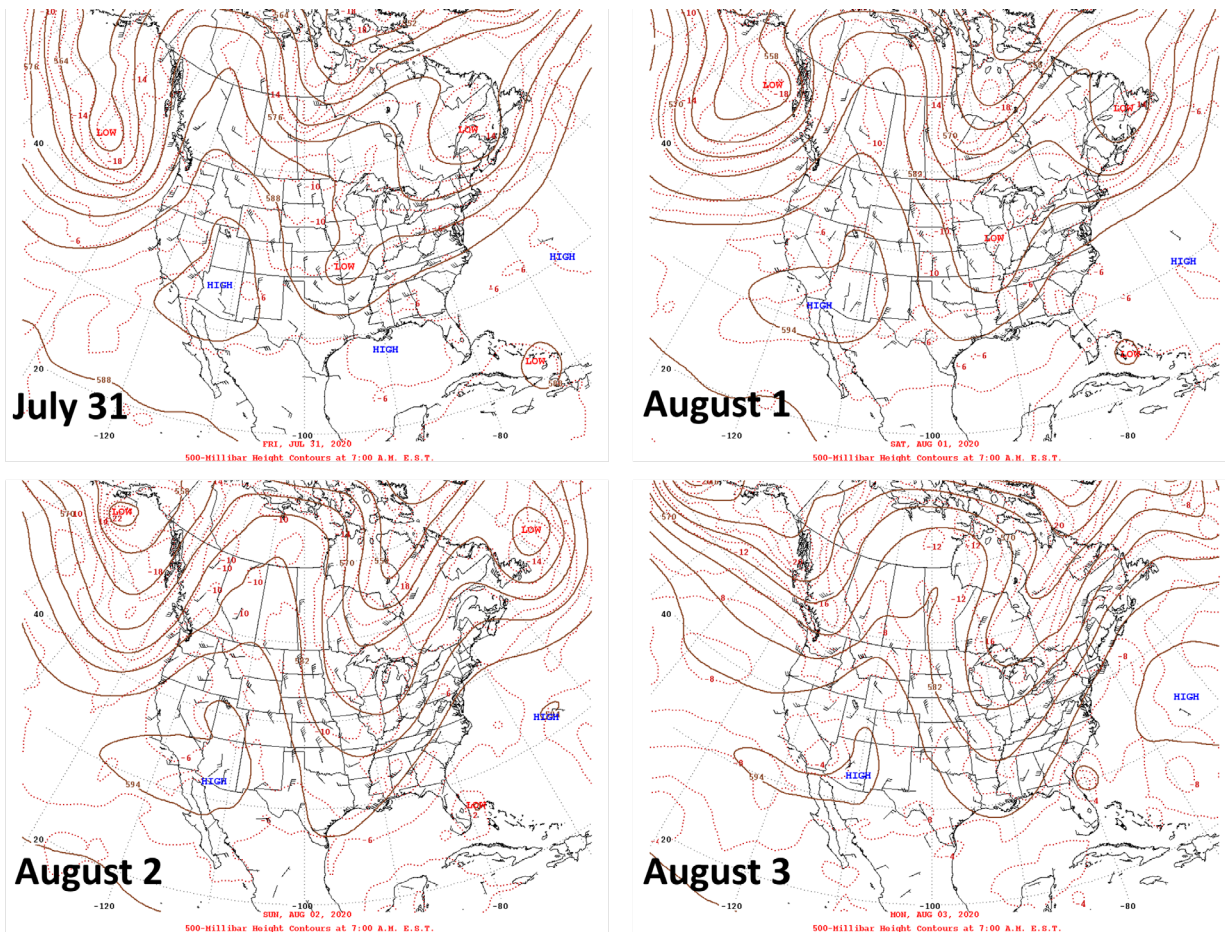
Figure 3-43. Daily upper-level meteorological maps for the three days leading up to the exceptional event and during the August 3 exceptional event.

Local observations of mixing heights in the Las Vegas area on August 2 and August 3 suggest that smoke was likely mixed into the lower levels of the atmosphere. Ceilometer data from the Jerome Mack site indicate mixing heights on August 2 and August 3 between approximately 2,000 m and 2,700 m for several hours during the day (**Figure 3-44**). Furthermore, a surface low-pressure system was centered over the border of Nevada and California between July 31 and August 3. Low pressure at the surface is often associated with enhanced vertical mixing in the lower troposphere (**Figure 3-45**). Mixing height data from the ceilometer and the surface weather maps provide evidence of enhanced vertical mixing in the lower troposphere when smoke was present over Clark County.
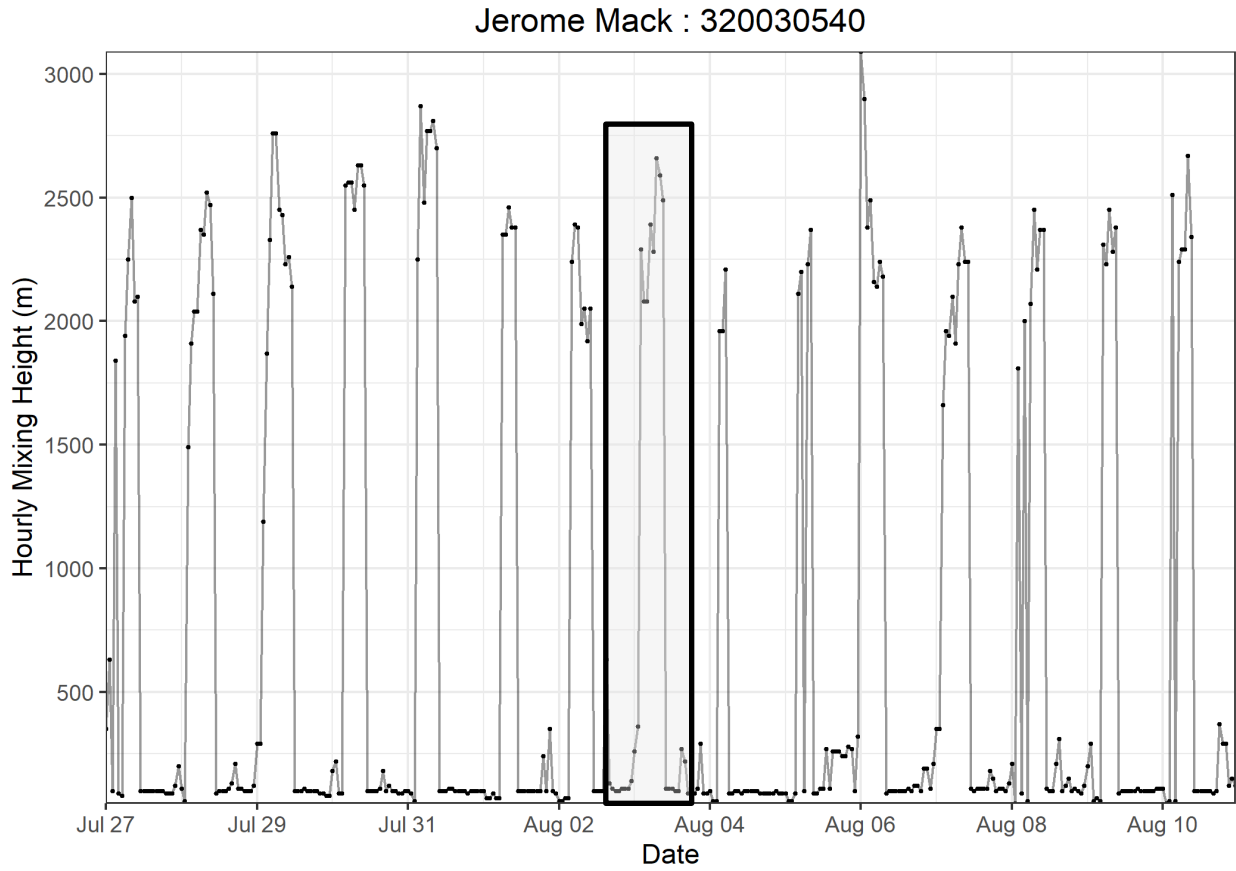
Figure 3-44. Time series of mixing heights derived from the Jerome Mack (NCore Site) ceilometer for two weeks before and after the August 3 exceptional event day. The mixing heights on August 3 are indicated by the box with the black outline.
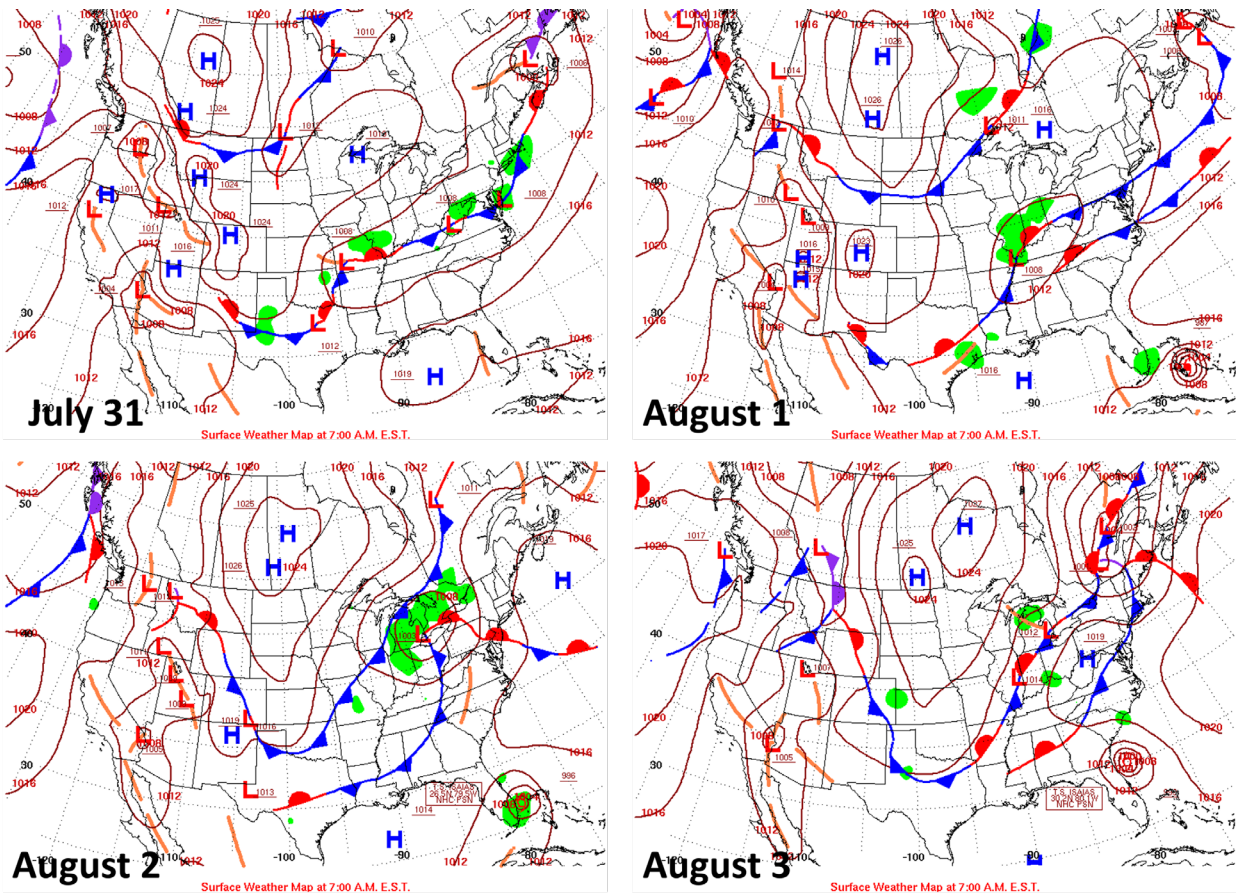
Figure 3-45. Daily surface meteorological maps for the three days leading up to the exceptional event and during the August 3 exceptional event.

In addition to the ceilometer-based measurements of mixing heights, vertical temperature profiles (Skew-T diagrams) can be used to estimate mixing heights. The vertical temperature profile at Las Vegas from July 31 to August 3 shows the vertical atmospheric profile becoming drier, with wind directions consistently from the south and southwest (**Figures 3-46 and 3-47**), indicating smoke present in the lower troposphere would be transported from the Apple Fire into Clark County. Enhanced vertical mixing from July 31 and August 1 to August 2 and August 3 can be seen from a more pronounced, very large mixed layer—as indicated by temperatures decreasing with height roughly along the dry adiabat up to at least 600 hPa—with associated warm temperatures and very dry air. The upper-level and surface weather maps, ceilometer data, and vertical temperature and wind profiles provide evidence that smoke plumes from the Apple Fire could have been transported in the free troposphere and/or within the deep mixed layer to Clark County and mixed to the surface on August 3.
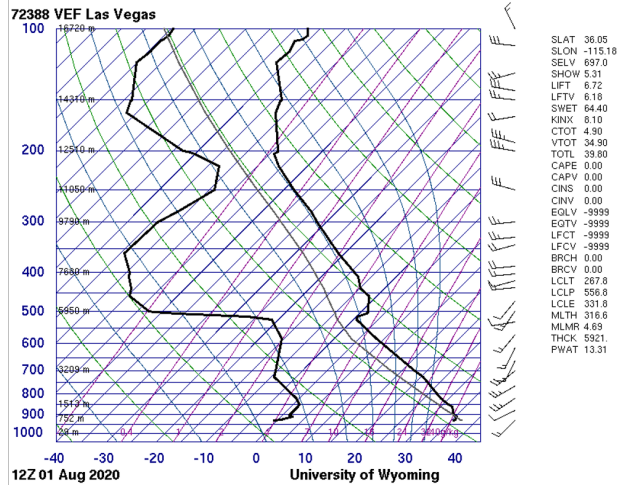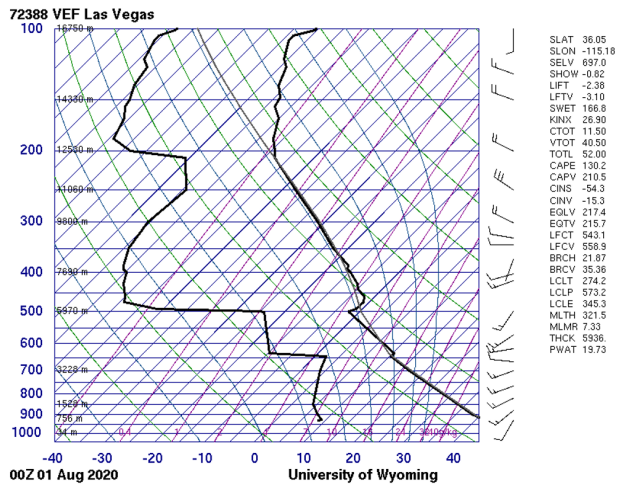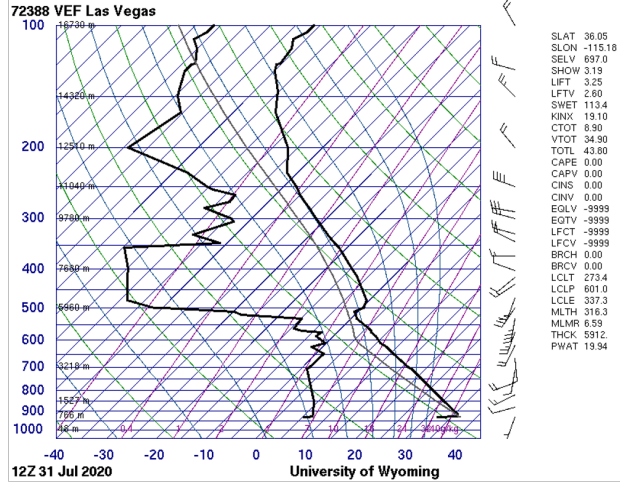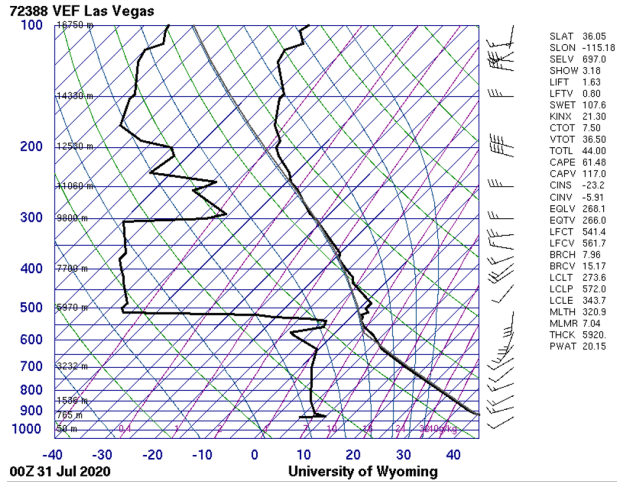
Figure 3-46. Skew-T diagrams from July 31 and August 1, 2020, in Las Vegas, Nevada.
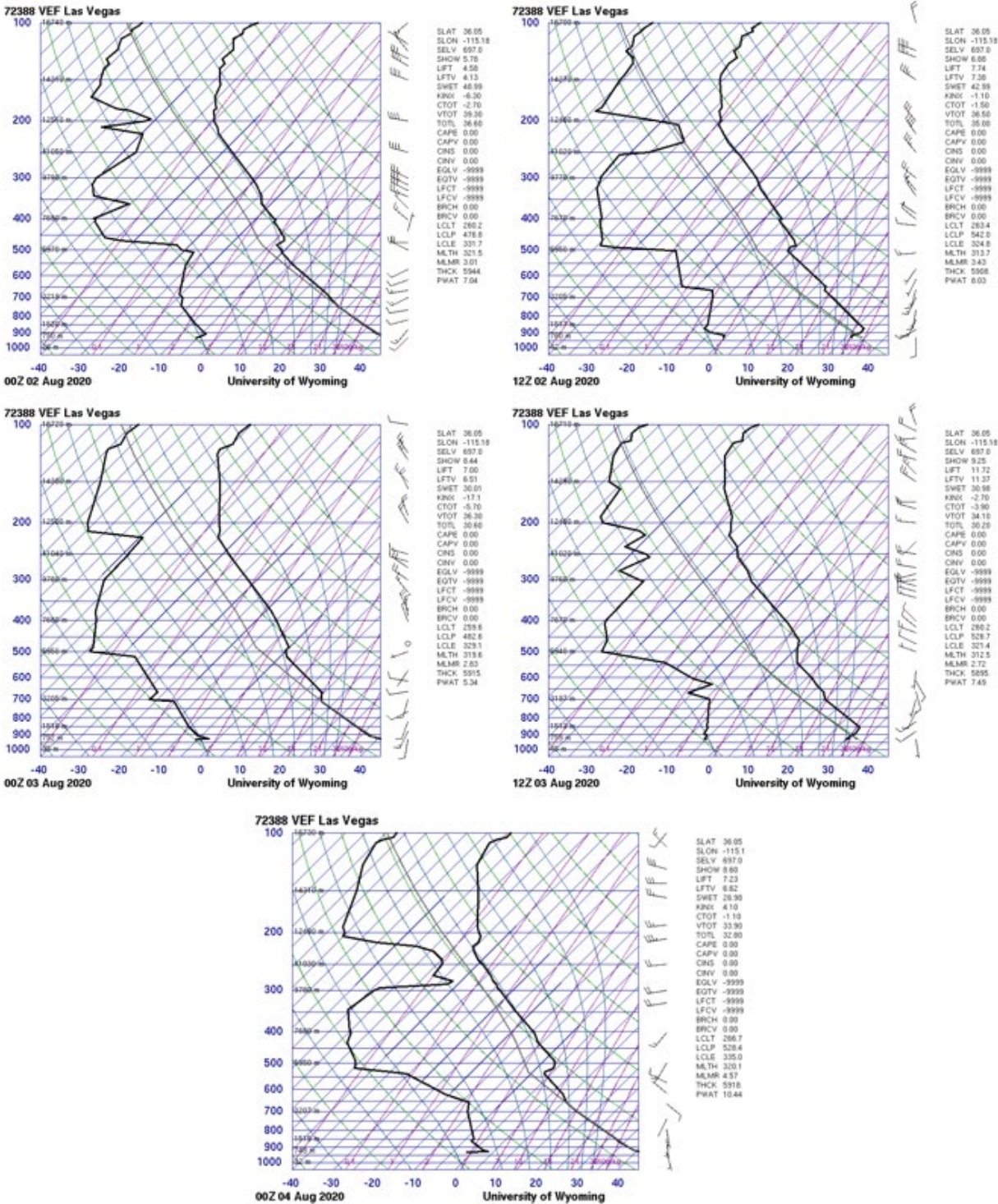
Figure 3-47. Skew-T diagrams from August 2 and 3, 2020 (LT), in Las Vegas, Nevada.

3.3.2 Matching Day Analysis

Ozone production and transport strongly depend on regional and local meteorological conditions. A comparison of ozone concentrations on suspected exceptional event days with non-event days that share similar meteorology can help identify periods when ozone production was affected by an atypical source. Given that similar meteorological days are likely to have similar ozone concentrations, noticeable differences in levels of ozone between the event date and meteorologically similar days can lend evidence to a clear causal relationship between wildfire smoke and elevated ozone concentration.

Identify Meteorologically Similar Days

In order to identify the best matching meteorological days, both synoptic and local conditions were examined from ozone-season days (April 1 through September 30) between 2014 and 2020. Excluded from this set are days with suspected EEs in the 2018 and 2020 seasons, as well as dates within five days of the event date, to ensure that lingering effects of smoke transport or stratospheric intrusion did not appear in the data.

To best represent similar air transport, twice-daily HYSPLIT trajectories (initiated at 18:00 and 22:00 UTC) from Clark County for 2014-2020 were clustered by total spatial variance. The calculation, based on the difference between each point along a trajectory, provides seven distinct pathways of airflow into Clark County (see Section 3.3.3 for more details). The cluster that best represents the trajectory on the EE day was chosen, and ozone-season days within the cluster were then subset for regional meteorological comparison to the EE day.

For the meteorological comparison, a correlation score was assigned to each day from the cluster subset. The National Centers for Environmental Prediction (NCEP) reanalysis data were compiled for the ozone seasons in 2014-2020. Daily average wind speed, geopotential height, relative humidity, and temperature were considered at 1,000 mb and 500 mb. At the surface, daily average atmospheric pressure, maximum temperature, and minimum temperature were utilized. Pearson product-moment coefficient of linear correlation (pattern correlation) was calculated between the EE date and each cluster-subset ozone-season day in 2014-2020 for each parameter. The pattern correlation calculates the similarity between two mapped variables at corresponding grid locations within the domain. The statistic was calculated using a regional domain of 30°N-45°N latitude and 125°W-105°W longitude. The correlation score for each day was defined as the average pattern correlation of all parameters at each height level. The correlation scores were then ranked by the highest correlation for 1,000 mb, the surface, and finally at 500 mb. Dates within five days of the EE were removed from the similar day analysis to ensure the data are mutually exclusive. The 50 dates with the highest rank correlation scores were then chosen as candidate matching days for further analysis.

Local meteorological conditions for the subset of candidate matching days were then compared to conditions on August 3, 2020, and filtered to identify five or more days that best matched the event date. Meteorological maps at the surface and 500 mb, along with local meteorological data describing temperature, wind, moisture, instability, mixing layer height, and cloud cover were examined. The data source for each parameter is summarized in Table 3-16.

Table 3-16. Local meteorological parameters and their data sources.

Meteorological Parameter	Data Source
Maximum daily temperature	Jerome Mack - NCore Monitoring Site
Average daily temperature	Jerome Mack - NCore Monitoring Site
Resultant daily wind direction	Jerome Mack - NCore Monitoring Site (calculated vector average)
Resultant daily wind speed	Jerome Mack - NCore Monitoring Site (calculated vector average)
Average daily wind speed	Jerome Mack - NCore Monitoring Site
Average daily relative humidity (RH)	Jerome Mack - NCore Monitoring Site
Precipitation	Jerome Mack - NCore Monitoring Site
Total daily global horizontal irradiance (GHI)	UNLV Measurement and Instrumentation Data Center (MIDC) in partnership with NREL (https://midcdmz.nrel.gov/apps/daily.pl?site=UNLV&start=20060318&yr=2021&mo=4&dy=29)
4:00 p.m. LST mixing layer mixing ratio	Upper air soundings from KVEF (http://weather.uwyo.edu/upperair/sounding.html)
4:00 p.m. LST lifted condensation level (LCL)	Upper air soundings from KVEF (http://weather.uwyo.edu/upperair/sounding.html)
4:00 p.m. LST convective available potential energy (CAPE)	Upper air soundings from KVEF (http://weather.uwyo.edu/upperair/sounding.html)
4:00 p.m. LST 1,000-500 mb thickness	Upper air soundings from KVEF (http://weather.uwyo.edu/upperair/sounding.html)
Daily surface meteorological map	NOAA's Weather Prediction Center Daily Weather Maps (https://www.wpc.ncep.noaa.gov/dailywxmap/index.html)
Daily 500 mb meteorological map	NOAA's Weather Prediction Center Daily Weather Maps (https://www.wpc.ncep.noaa.gov/dailywxmap/index.html)

Matching Day Analysis

The meteorological conditions on August 3, 2020, were normal for the region at this time of year. Table 3-17 displays that the percentile ranking of each examined meteorological parameter other than relative humidity at the Jerome Mack-NCore site falls within the 5th to 95th percentile range

among seven years of observations for the 30-day period surrounding August 3 (July 19 through August 18). Measurement summaries over this 30-day period best represent the expected conditions on the event date. The maximum temperature on August 3 was above the median for this time of year, which is reflected in the abnormally low relative humidity. The relative humidity is at the 1st percentile. As is typical for Clark County during this period, there was no precipitation.

The subset of synoptically similar days identified according to the methodology above was further filtered based on parameters listed in Table 3-16 to match local meteorological conditions that existed on the event date. Table 3-18 shows the 14 days that best match the meteorological conditions that existed on August 3, 2020, as well as the MDA8 ozone concentration at each site that experienced an ozone exceedance on August 3, 2020. One identified matching day, June 23, 2015, was omitted from this analysis due to evidence of smoke impact in Clark County on this date (see Appendix D). Weather maps for August 3, 2020, and each date listed in Table 3-18 show highly consistent conditions, with a surface low-pressure system and an upper-level region of low-gradient, relatively high pressure over Clark County. Most dates also had a surface high to the east. Surface and upper-level maps are included in Appendix D.

Table 3-18 shows the average MDA8 ozone concentration across these 14 days with a range defined by one standard deviation, a conservative estimate given the small sample size. The expected MDA8 ozone concentration, given similar meteorological conditions to those on the event date, is well below the 70-ppb ozone standard at each site, ranging from 55 to 61 ppb. Further, the upper end of the provided range at each site also falls below the ozone NAAQS. Several similar dates with higher photochemical potential than August 3 (lower wind speeds, higher average temperatures, and greater solar irradiance) did not exceed the ozone NAAQS. Thus, an ozone exceedance on August 3, 2020, was unexpected based on meteorological conditions alone. If meteorology were the sole cause of the ozone exceedance on August 3, 2020, we would expect to see similarly high ozone levels on each of the similar days listed in Table 3-18, especially those with even warmer average temperatures than experienced on August 3, alongside other similar conditions.

Table 3-17. Percentile rank of meteorological parameters on August 3, 2020, compared to the 30-day period surrounding August 3 over seven years (July 19 through August 18, 2014-2020). The percentile ranking of precipitation is marked NA because a vast majority of examined days recorded 0 inches. The percentile ranking of a directional degree value is irrelevant and has been marked NA.

Date	Max Temp (°F)	Avg Temp (°F)	Resultant Wind Direction (°)	Resultant Wind Speed (mph)	Avg Wind Speed (mph)	Avg RH (%)	Precip (in)	Total GHI (kWh/m²)	Mixing Layer Mixing Ratio (g/kg)	LCL (mb)	CAPE (J/kg)	500-1,000 mb Thickness (m)
2020-08-03	89	67	NA	30	27	1	NA	68	15	8	33	82

Table 3-18. Top fourteen matching meteorological days to August 3, 2020. PM, WJ, JN, GV, BC, J, and IS refer to monitoring sites Paul Meyer, Walter Johnson, Joe Neal, Green Valley, Boulder City, Jean, and Indian Springs respectively. Average MDA8 ozone concentration of meteorologically similar days is shown plus-or-minus one standard deviation rounded to the nearest ppb.

Date	Max Temp (°F)	Avg Temp (°F)	Resultant Wind Direction (°)	Resultant Wind Speed (mph)	Avg Wind Speed (mph)	Avg RH (%)	Precip (in)	Total GHI (kWh/m²)	Mixing Layer Mixing Ratio (g/kg)	LCL (mb)	CAPE (J/kg)	500-1,000 mb Thickness (m)	MDA8 Ozone Concentration (ppb)						
													PM	WJ	JN	GV	BC	J	IS
2020-08-03	111	97.33	141.8	1.74	2.89	4.38	0	7.95	4.57	528.46	0	5918	78	82	81	72	72	73	71
2017-07-01	111	97.54	156.49	3.1	4.2	8.04	0	8.7	4.35	518.7	161.96	5906	64	68	67	60	59	60	66
2017-07-28	109	98.42	134.76	2.93	3.58	18.62	0	8.1	7.48	592.49	146.7	5902	60	64	67	54	51	57	60
2019-07-21	108	96.71	122.07	2.36	3.45	12.46	0	8.42	5.54	554.05	69.03	5912	49	52	52	50	45	45	51
2019-08-14	111	96.62	178.14	0.44	1.43	11.12	0	7.87	5.81	564.95	78.16	5890	59	59	61	63	56	51	48
2019-08-17	107	96.08	193.57	5.16	5.88	8.71	0	8.11	3.42	511.13	0	5889	58	59	59	59	59	60	56
2019-08-20	107	93.83	133.03	0.74	2.12	9.92	0	7.77	5.08	550.84	0	5906	53	57	59	59	51	49	55
2019-08-21	110	94.88	104.27	1.03	2.45	9.33	0	7.69	5.31	543.33	0	5914	64	63	64	56	52	60	53
2019-08-31	110	95.71	137.44	0.93	3.04	9.96	0	7.22	5.4	542.99	0	5922	58	62	62	60	56	55	55
2019-09-01	110	95.79	141.53	1.72	3.6	11.79	0	7.17	6.8	572.29	175.85	5910	60	61	57	55	50	57	59
2020-07-06	109	97.5	158.73	1.69	3.32	6.08	0	8.79	4.8	533.86	0	5912	61	60	60	57	55	58	59
2020-07-10	110	97.29	115.69	1.14	2.44	6.46	0	8.62	6.13	565.7	0	5917	68	68	66	65	61	58	68
2020-08-04	107	96.25	143.24	3.1	4.29	5	0	8.03	5.21	550.72	0	5896	62	64	67	63	60	60	68
2020-08-05	105	94.46	192.71	3.35	4.44	9.12	0	8.13	4.28	544.19	0	5868	59	61	62	59	62	58	61
2020-08-06	103	93	160.51	4.96	5.26	10.67	0	8.16	4.82	563.92	0	5852	58	60	59	58	56	57	56
Average MDA8 Ozone Concentration of Meteorologically Similar Days													59± 4	61 ± 4	61± 4	58± 4	55± 5	56± 4	58± 6

These findings show that an external source of ozone contributed to the ozone exceedance on August 3, 2020. All examined meteorological parameters besides relative humidity fall between the 10th and 90th percentile. Our analysis expanded on methods shown in the EPA guidance and a previously concurred EE to identify 14 days that are meteorologically similar to August 3, 2020 (Arizona Department of Environmental Quality, 2018). The expected MDA8 ozone concentration at each site is over 10 ppb below the concentrations measured at each site on August 3, 2020. Based on this evidence, it is unlikely that meteorology alone enhanced photochemical production of ozone enough to cause an exceedance on August 3, 2020. This validates the existence of an extrinsic ozone source on August 3, 2020.

3.3.3   GAM Statistical Modeling

Generalized additive models (GAM) are a type of statistical model that allows the user to predict a response based on linear and non-linear effects from multiple variables (Wood, 2017). These models tend to provide a more robust prediction than Eulerian photochemical models or simple comparisons of similar events (Simon et al., 2012; Jaffe et al., 2013; U.S. Environmental Protection Agency, 2016). Camalier et al. (2007) successfully used GAM modeling to predict ozone concentrations across the eastern United States using meteorological variables with r^2 values of up to 0.8. Additionally, previous concurred exceptional event demonstrations and associated literature, i.e., Sacramento Metropolitan Air Quality Management District (2011), Alvarado et al. (2015), Louisiana Department of Environmental Quality (2018), Arizona Department of Environmental Quality (2016), and Pernak et al. (2019) used GAM modeling to predict ozone events that exceed the NAAQS standards, some in EE cases. By comparing the GAM-predicted ozone values to the actual measured ozone concentrations (i.e., residuals), we can determine the effect of outside influences, such as wildfires or stratospheric intrusions, on ozone concentrations each day (Jaffe et al., 2004). High, positive residuals suggest a non-typical source of ozone in the area but cannot specifically identify a source. Gong et al. (2017) and McClure and Jaffe (2018) used GAM modeling, in addition to ground and satellite measurements of wildfire pollutants, to estimate the enhancement of ozone during wildfire smoke events. Similar to other concurred EE demonstrations, we used GAM modeling of meteorological and transport variables to estimate the MDA8 ozone concentrations at multiple sites across Clark County for 2014-2020. To estimate the effect of wildfire smoke on ozone concentrations, we can couple the GAM residual results (observed MDA8 ozone–GAM-predicted MDA8 ozone) with the other analyses to confirm that the non-typical enhancement of ozone is due to wildfires on August 3, 2020.

Using the same GAM methodology as prior concurred EE demonstrations and the studies mentioned above, we examined more than 30 meteorological and transport predictor variables, and through testing, compiled the 16 most important variables to estimate MDA8 ozone each day at eight monitoring sites across Clark County, Nevada (Paul Meyer, Walter Johnson, Joe Neal, Green Valley,

Boulder City, Jean, Indian Springs, and Jerome Mack). As suggested by EPA guidance (U.S. Environmental Protection Agency, 2016), we used meteorological variables measured at each station (the previous day's MDA8 ozone, daily min/max temperature, average temperature, temperature range, wind speed, wind direction, or pressure), if available (see Table 2-1). If meteorological variables were not available at a specific site, we supplemented the data with National Centers for Environmental Prediction (NCEP) reanalysis meteorological data to fill any data gaps. We also tested filling data gaps with Jerome Mack meteorological data and found results had no statistical difference. We used sounding data from KVEF (Las Vegas Airport) to provide vertical meteorological components; soundings are released at 00:00 and 12:00 UTC daily. Variables such as temperature, relative humidity, wind speed, and wind direction were averaged over the first 1,000 m above the surface to provide near-surface, vertical meteorological parameters. Other sounding variables, such as Convective Available Potential Energy (CAPE), Lifting Condensation Level (LCL) pressure, mixing layer potential temperature, mixed layer mixing ratio, and 500-1,000 hPa thickness provided additional meteorological information about the vertical column above Clark County. We also initiated HYSPLIT GDAS 1°x1° 24-hour back trajectories from downtown Las Vegas (36.173°N, -115.155°W, 500 m agl) at 18:00 and 22:00 UTC (10:00 a.m. and 2:00 p.m. LST) each day to provide information on morning and afternoon transport during critical ozone production hours. We clustered the twice-per-day back trajectories from 2014-2020 into seven clusters. **Figure 3-48** shows the clusters, percentage of trajectories per cluster, and heights of each trajectory cluster. We identified a general source region for each cluster: (1) Northwest U.S., (2) Stagnant Las Vegas, (3) Central California, (4) Long-Range Transport, (5) Northern California, (6) Southern California, and (7) Baja Mexico. Within the GAM, we use the cluster value to provide a factor for the distance traveled by each back trajectory. Additionally, day of year (DOY) was used in the GAM to provide information on season and weekly processes. The year (2014, 2015, etc.) was used a factor for the DOY parameter to distinguish interannual variability.
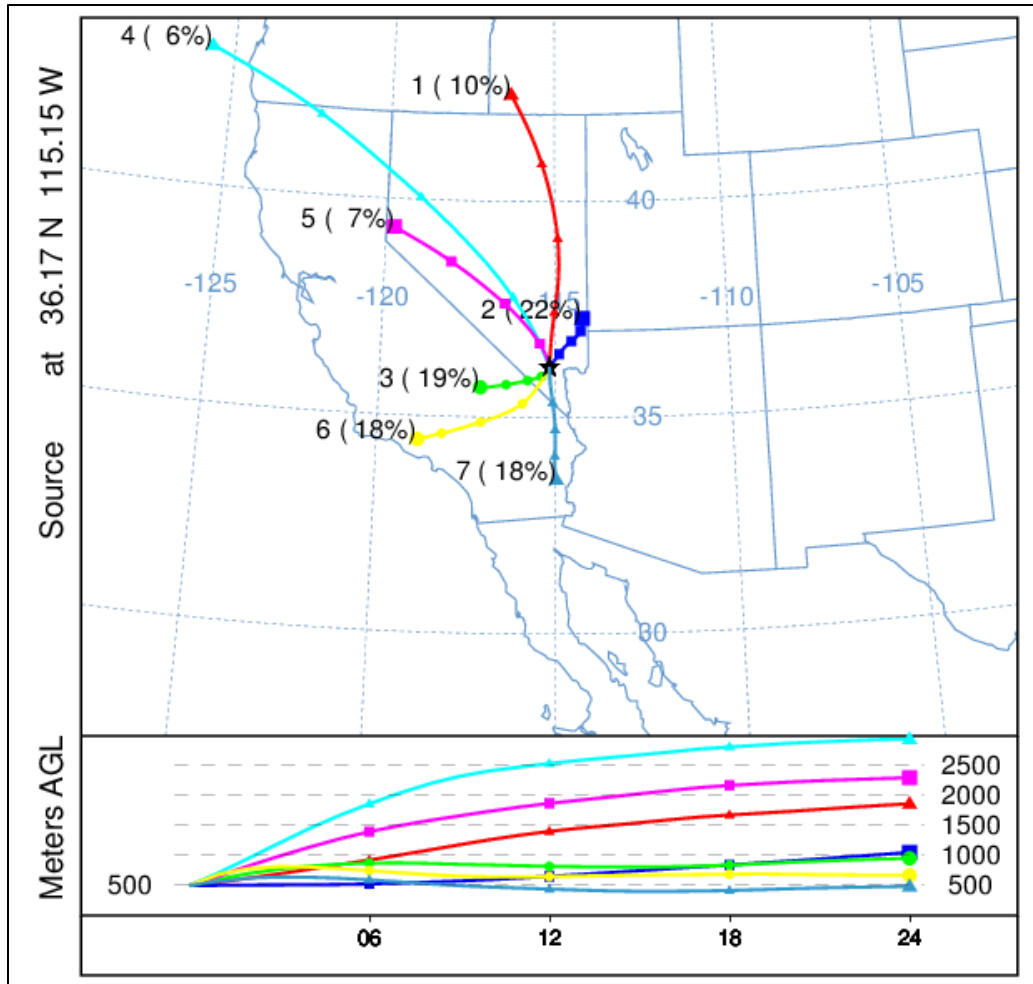
Figure 3-48. Clusters for 2014-2020 back trajectories. Seven unique clusters were identified for the twice daily (18:00 and 22:00 UTC) back-trajectories for 2014-2020 initiated in the middle of the Las Vegas Valley. The percentage of trajectories per cluster is shown next to the cluster number, and the height of each cluster is shown below the map.

Once all the meteorological and transport variables were compiled, we inserted them into the GAM equation to predict MDA8 ozone:

$$g\big(MDA8\ O_{3,i}\big) = f_1(V1_i) +\ f_2(V2_i) +\ f_3(V3_i) + \cdots + residual_i$$

where f_i are fit functions calculated from penalized cubic regression splines of observations (allowing non-linearity in the fit), V_i are the variables, and i is the daily observation. All variables were given a cubic spline basis except for wind direction, which used a cyclic cubic regression spline basis. For DOY and back trajectory distances, we used year factors (i.e., 2014-2020) and cluster factors (i.e., 1-7) to distinguish interannual variability and source region differences. The factors provide a different smooth function for each category (Wood, 2017). For example, the GAM smooth of DOY for 2014 can

be different than 2015, 2016, etc. In order to optimize the GAM, we first must adjust knots or remove any variables that are over-fitting or under-performing. We used the "mgcv" R package to summarize and check each variable for each monitoring site (Wood, 2020). A single GAM equation (using the same variables) was used for each monitoring site for consistency. During the initial optimization process, we removed the proposed 2018 and 2020 EE days from the dataset. We also ran 10 cross-validation tests by randomly splitting data 80/20 between training/testing for each monitoring site to ensure consistent results. All cross-validation tests showed statistically similar results with no large deviations for different data splits. We used data from each site during the April -September ozone seasons for 2014 through 2020, which is consistent with other papers modeling urban ozone (e.g., Pernak et al., 2019; McClure and Jaffe, 2018; Solberg et al., 2019; Solberg et al., 2018) and ozone concentrations during the periods with exceptional events are within the representative range of ozone in the GAM model.

Table 3-19 shows the variables used in the GAM and their F-value. The F-value suggests how important each variable is (higher value = more important) when predicting MDA8 ozone. Any bolded F-values had a statistically significant correlation ($p < 0.05$). R^2, the positive 95th quantile of residuals, and normalized mean square residual values for each monitoring site are listed at the bottom of the table.

Table 3-19. GAM variable results. F-values per parameter used in the GAM model are shown for each site. Units and data sources for each parameter in the GAM model are shown on the right of the table. The 95th quantile, R^2, and normalized mean square residual information are shown at the bottom of the table.

Parameters	Paul Meyer	Walter Johnson	Joe Neal	Green Valley	Jerome Mack	Boulder City	Jean	Indian Springs	Unit	Source
Day of Year (DOY) factored by Year (2014-2020)	8.11	7.09	7.65	11.8	7.94	7.11	8.68	7.53	--	--
Previous Day MDA8 Ozone	37.9	22.7	41.5	18.1	27.9	31.3	105.5	123.8	ppb	Monitor Data
Average Daily Temperature	1.92	2.90	4.80	0.05	1.83	2.13	0.12	1.83	K	
Maximum Daily Temperature	1.37	2.74	2.48	0.16	0.38	0.02	1.30	1.52	K	
Temperature Range (TMax - TMin)	4.12	2.13	1.38	1.74	1.77	1.51	0.50	0.54	K	Monitor Data/NCEP Reanalysis
Average Daily Pressure	5.54	6.42	6.74	4.64	2.94	0.22	2.17	0.24	hPa	
Average Daily Wind Speed	11.1	5.03	7.49	5.02	15.3	0.07	0.49	2.19	knots	
Average Daily Wind Direction	0.47	1.04	0.24	1.35	2.43	0.69	0.11	2.48	deg	
18 UTC HYSPLIT Distance factored by Cluster	1.70	1.82	1.69	0.92	2.52	2.97	1.66	1.03	km	HYSPLIT Back-Trajectories
22 UTC HYSPLIT Distance factored by Cluster	1.03	0.74	1.47	1.47	1.20	1.26	1.19	0.50	km	
00 UTC Convective Available Potential Energy	3.50	0.13	0.37	1.17	1.16	0.57	5.71	6.49	J/kg	
00 UTC Lifting Condensation Level Pressure	1.36	2.78	2.29	2.41	3.76	0.38	1.43	0.38	hPa	
00 UTC Mixing Layer Potential Temperature	0.65	0.79	1.72	0.10	1.23	0.97	1.09	2.53	K	Sounding Data
00 UTC Mixed Layer Mixing Ratio	2.10	2.76	2.85	3.09	3.07	2.42	0.69	1.04	g/kg	
00 UTC 500-1000 hPa Thickness	2.91	0.43	1.70	1.60	1.69	4.11	2.18	1.83	m	
12 UTC 1km Average Relative Humidity	12.4	14.6	17.8	21.3	37.5	26.0	11.1	2.18	%	
95th Quantile of Positive Residuals (ppb)	10	10	10	10	9	9	9	10		
R^2	0.55	0.58	0.60	0.58	0.61	0.58	0.57	0.55		
Normalized Mean Square Residual	3.6E-06	7.3E-04	6.1E-05	1.3E-04	3.1E-05	1.3E-04	1.2E-04	1.5E-04		

Table 3-20 provides GAM residual and fit results for all sites for the ozone seasons of 2014 through 2020. Overall, the residuals are low for all data points, and similarly low for all non-EE days. However, the 2018 and 2020 EE day residuals are significantly higher than the non-EE day results, meaning there are large, atypical influences on these days. **Figure 3-49** shows non-EE vs EE median residuals with the 95th confidence intervals denoted as notches in the boxplots. We show the data in both ways to provide specific values, as well as illustrate the difference in non-EE vs EE residuals. Since the 95th confidence intervals for median EE residuals are above and do not overlap with those for non-EE residuals at any site in Clark County, we can state that the median residuals are higher and statistically different ($p<0.025$). The R^2 for each site ranged between 0.55 and 0.61, suggesting a good fit for each monitoring site, and similar to the results in prior studies and EE demonstrations mentioned previously (r^2 range of 0.4-0.8). We also provide the positive 95th quantile MDA8 ozone concentration, which is used to estimate a "No Fire" MDA8 ozone value based on the EPA guidance (U.S. Environmental Protection Agency, 2016). We also provide the median residuals (and confidence interval) for all non-EE days with observed MDA8 at or above 60 ppb; this threshold was needed to build a sufficient sample size with a representative distribution, and derive the median and 95% confidence interval. It should be noted that four out of the seven years modeled by the GAM were high wildfire years, and these values likely include a significant amount of wildfire days. We were not able to systematically remove wildfire influence by subsetting the Clark County ozone data based on HMS smoke, HMS smoke and $PM_{2.5}$ concentrations, and low wildfire years. These methods produced a significant number of false positives and negatives, and yielded datasets that were still affected by wildfire smoke. Therefore, these values should be considered an upper estimate of residuals for high ozone days. We see that the median residuals for 2018 and 2020 EE days are significantly higher than those on non-EE high observed ozone days since their confidence intervals do not overlap (or are comparable for the Jerome Mack station). The non-EE day residuals on days where observed MDA8 was at or above 60 ppb were determined to be normally distributed with a slight positive skew (median skewness = 0.39).

Table 3-20. Overall 2014-2020 GAM median residuals and 95% confidence interval range in square brackets for each site modeled. Sample size is shown in parentheses below the residual statistics. For sample sizes of less than ten, we include a range of residuals in square brackets instead of the 95% confidence interval. Residual results are split by non-EE days and the 2018 and 2020 EE days. R^2 for each site is also shown along with the positive 95th quantile result.

Site Name	All Residuals (ppb)	Non-EE Day Residuals (ppb)	2018 & 2020 EE Day Residuals (ppb)	R^2	Positive 95th Quantile (ppb)	Non-EE Day Residuals when MDA8 ≥ 60 ppb (ppb)
Boulder City	0.22 [-0.04, 0.48] (1,132)	0.22 [-0.04, 0.48] (1,130)	12.05 [10.38-13.72] (2)	0.58	9	4.05 [3.55, 4.55] (200)
Green Valley	0.17 [-0.15, 0.48] (948)	0.10 [-0.21, 0.41] (934)	7.38 [5.40, 9.36] (14)	0.58	10	3.76 [3.28, 4.23] (271)
Indian Springs	0.13 [-0.18, 0.44] (1,014)	0.08 [-0.22, 0.38] (1,010)	12.30 [9.37-17.19] (4)	0.55	10	4.79 [4.26, 5.32] (201)
Jean	0.21 [-0.06, 0.48] (1,149)	0.20 [-0.07, 0.47] (1,146)	12.57 [9.59-13.90] (3)	0.57	9	3.40 [2.94, 3.85] (290)
Jerome Mack	0.09 [-0.19, 0.36] (1,152)	0.05 [-0.22, 0.32] (1,141)	6.83 [4.21, 9.45] (11)	0.61	9	3.83 [3.32, 4.33] (242)
Joe Neal	0.23 [-0.08, 0.54] (1,113)	0.17 [-0.13, 0.47] (1,097)	7.77 [5.79, 9.75] (16)	0.60	10	3.32 [2.92, 3.71] (377)
Paul Meyer	0.21 [-0.08, 0.50] (1,159)	0.10 [-0.19, 0.39] (1,137)	8.11 [6.34, 9.88] (22)	0.55	10	3.58 [3.19, 3.97] (388)
Walter Johnson	0.27 [-0.03, 0.57] (1,163)	0.19 [-0.10, 0.48] (1,141)	7.16 [5.11, 9.21] (22)	0.58	10	3.53 [3.13, 3.93] (379)
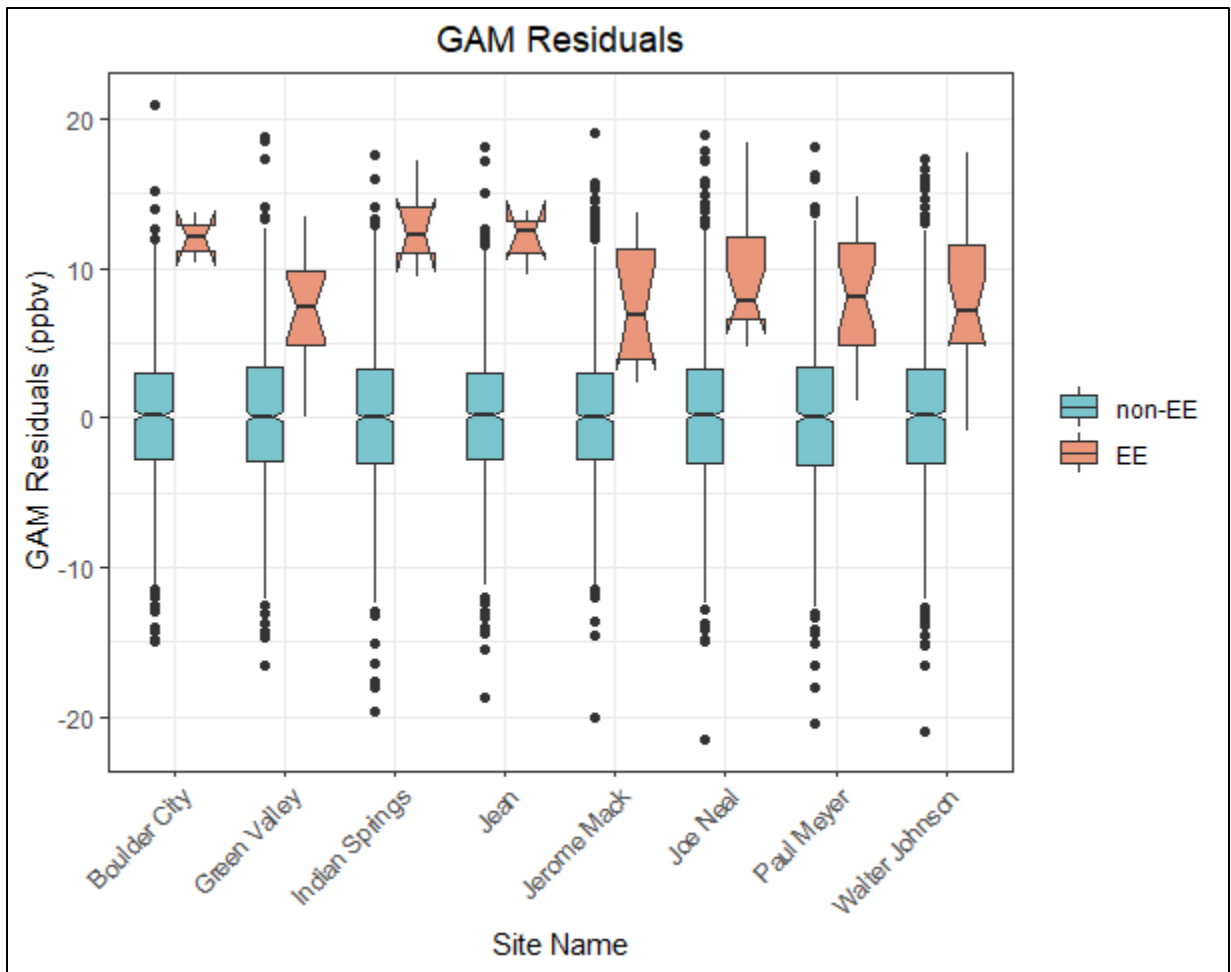
Figure 3-49. Exceptional event vs. non-exceptional event residuals. Non-exceptional events (non-EE in blue) and exceptional events (EE in orange) residuals are shown for each site modeled in Clark County. The notches for each box represent the 95th confidence interval. This figure illustrates the information in Table 3-20.

Overall, the GAM results show low bias and consistently significantly higher residuals on EE days compared with non-EE days. We also evaluated the GAM performance on verified high ozone, non-smoke days by looking at specific case studies. This was done to assess whether high-ozone days, such as the EE days, have a consistent bias that is not evident in the overall or high ozone day GAM performance. Out of the seven years used in the GAM model, four were high wildfire years in California (2015, 2017, 2018, and 2020). Since summer winds in Clark County are typically out of California (44% of trajectories originate in California according to the cluster analysis [not including transport through California in the Baja Mexico cluster]), wildfire smoke is likely to affect a large portion of summer days and influence ozone concentrations in Clark County. We identified specific case studies where most monitoring sites in Clark County had an MDA8 ozone concentration greater than or equal to 60 ppb and had no wildfire influence; "no wildfire influence" was determined by

inspecting HMS smoke plumes and HYSPLIT back trajectories for each day and confirming no smoke was over, near, or transported to Clark County. We found one to two examples from each year used in the GAM modeling, and required that at least half of the case study days needed to include an exceedance of the ozone NAAQS. Table 3-21 shows the results of these case studies. Most case study days, including NAAQS exceedance days, show positive and negative residuals even when median ozone is greater than or equal to 65 ppb in Clark County, similar to the results for the entire multi-year dataset. GAM residuals on non-EE days when MDA8 is at or above 60 ppb have a median of 3.69 [95% confidence interval: 3.47, 3.88] (see Table 3-20). The high ozone, non-smoke case study days all show median residuals within or below the confidence interval of the high ozone residuals (from Table 3-20, meaning that the GAM model is able to accurately predict high ozone, non-smoke days within a reasonable range of error. Two additional factors indicate the GAM has good performance on normal, high ozone days: (1) the median residuals for the case studies are mostly lower than the 95% confidence interval of high ozone residuals (i.e., includes non-EE wildfire days), and (2) the case study days were verified as non-smoke days, Thus, residuals above the 95th confidence interval of the median residuals, such as those on the EE days, are statistically higher than on days with comparable high ozone concentrations, and not biased high because of the high ozone concentrations on these days.

Table 3-21. GAM high ozone, non-smoke case study results. Median GAM residuals for ten days in 2014-2020 are shown where most monitoring sites had MDA8 ozone concentrations of 60 ppb or greater. Sites used to calculate the MDA8 and GAM residual median/range are listed in the Clark County AQS Site Number column by site number.

Date	Clark County AQS Site Number	Median (Range) of Observed MDA8 Ozone (ppb)	Median (Range) GAM Residual (ppb)
5/17/2014	0601, 0075, 1019, 0540, 0043, 0071	66 (64-71)	1.66 (-0.53-4.28)
6/4/2014	0601, 0075, 0540, 1019, 0043, 0071	69 (66-72)	3.46 (1.70-4.80)
6/3/2015	1019, 0043, 0075, 0540, 7772, 0601, 0071	71 (65-72)	3.01 (-0.34-5.77)
6/20/2015	0601, 0298, 7772, 1019, 0540, 0075, 0043, 0071	65 (63-70)	1.40 (-6.20-5.28)
6/3/2016	0298, 1019, 0075, 0540, 0043, 0071	65 (63-71)	3.89 (1.89-5.26)
7/28/2016	0075, 0071, 0298, 0540, 0043	70 (63-72)	0.24 (-5.95-3.67)
6/17/2017	0601, 0075, 0071, 1019, 0540, 0298, 0043	66 (63-72)	1.85 (-1.94-7.01)
6/4/2018	0601, 0298, 7772, 1019, 0540, 0075, 0043, 0071	65 (60-67)	3.06 (-0.91-3.60)
5/5/2019	0601, 0298, 7772, 1019, 0540, 0075, 0043, 0071	65 (62-67)	1.28 (-2.00-3.42)
5/15/2020	0298, 0043, 0075, 0071	63 (63-65)	1.52 (1.09-3.49)

We also evaluate the bias of GAM residuals versus predicted MDA8 ozone concentrations in **Figure 3-50**. Residuals (i.e., observed ozone minus GAM-predicted MDA8 ozone) should be independent of the GAM-predicted ozone value, meaning that the difference between the actual ozone concentration on a given day and the GAM output should be due to outside influences and not well described by meteorological or seasonal values (i.e., variables used in the GAM prediction). Therefore, in a well-fit model, positive and negative residuals should be evenly distributed across all

GAM-predicted ozone concentrations and on average zero. In Figure 3-50, we see daily GAM residuals at all eight monitoring sites in Clark County from 2014-2020, the residuals are evenly distributed across all GAM-predicted ozone concentrations, with no pattern or bias at high or low MDA8 fit concentrations. This evaluation of bias in the model is consistent with established literature and other EE demonstrations (Gong et al., 2018; McVey et al., 2018; Texas Commission on Environmental Quality, 2021; Pernak et al., 2019), and indicate a well-fit model. In **Figure 3-51**, we also provide a histogram of the residuals at each monitoring site modeled in Clark County. This analysis shows that residuals at each site are distributed normally around a median near zero, and none of the distributions shows significant tails at high or low residuals (median skew = 0.05 with 95% confidence interval [-0.03, 0.12]). This analysis of error in the model and our results are consistent with previously concurred EE demonstrations (Arizona Department of Environmental Quality, 2016) and previous literature (Jaffe et al., 2013; Alvarado et al., 2015; Gong et al., 2017; McClure and Jaffe, 2018; Pernak et al., 2019). **Appendix E** provides GAM residual analysis from the concurred ADEQ and submitted TCEQ demonstrations that compare well with our GAM residual results. Based on these analysis methods, bias in the model is low throughout the range of MDA8 prediction values and confirms that the GAM can be used to predict MDA8 ozone concentrations in Clark County.
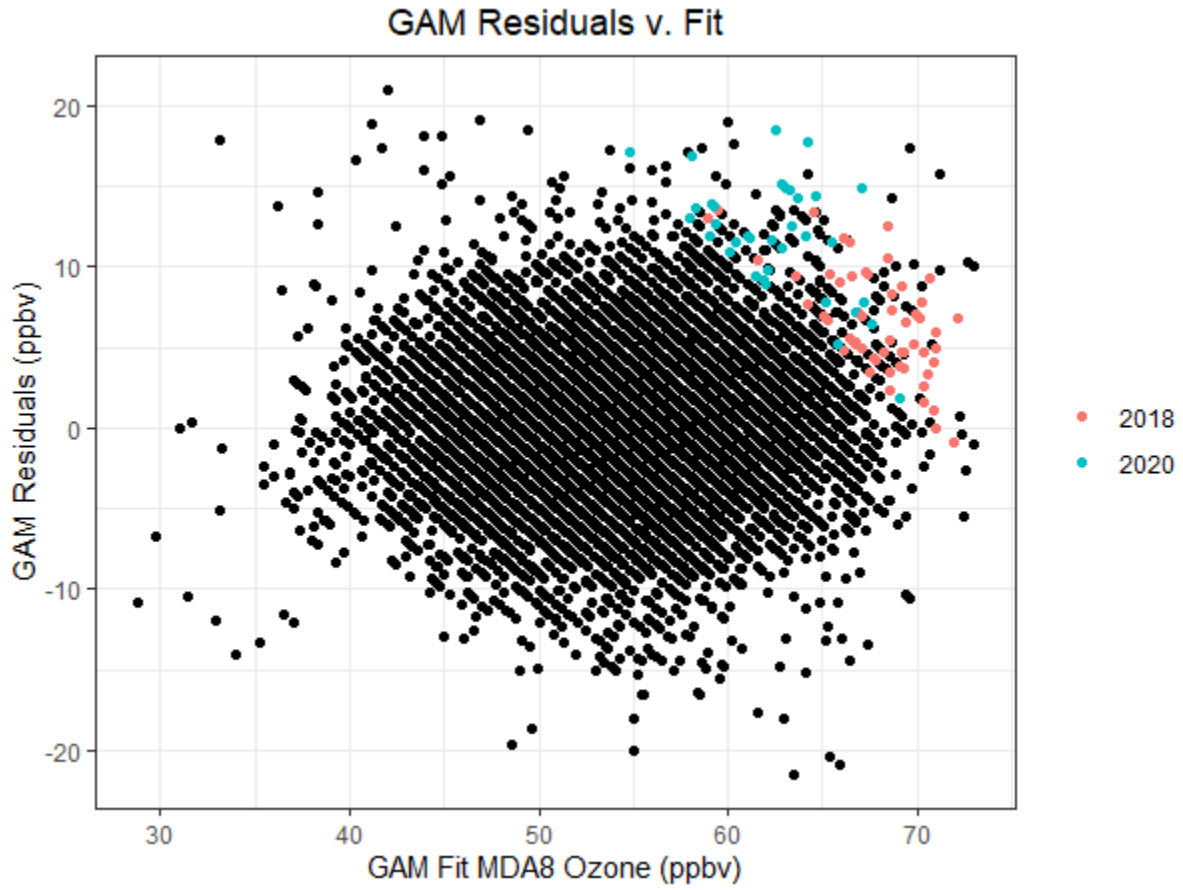
Figure 3-50. Daily GAM residuals for 2014-2020 vs GAM Fit (Predicted) MDA8 Ozone values. 2018 and 2020 exceptional events residuals are shown in red and blue.
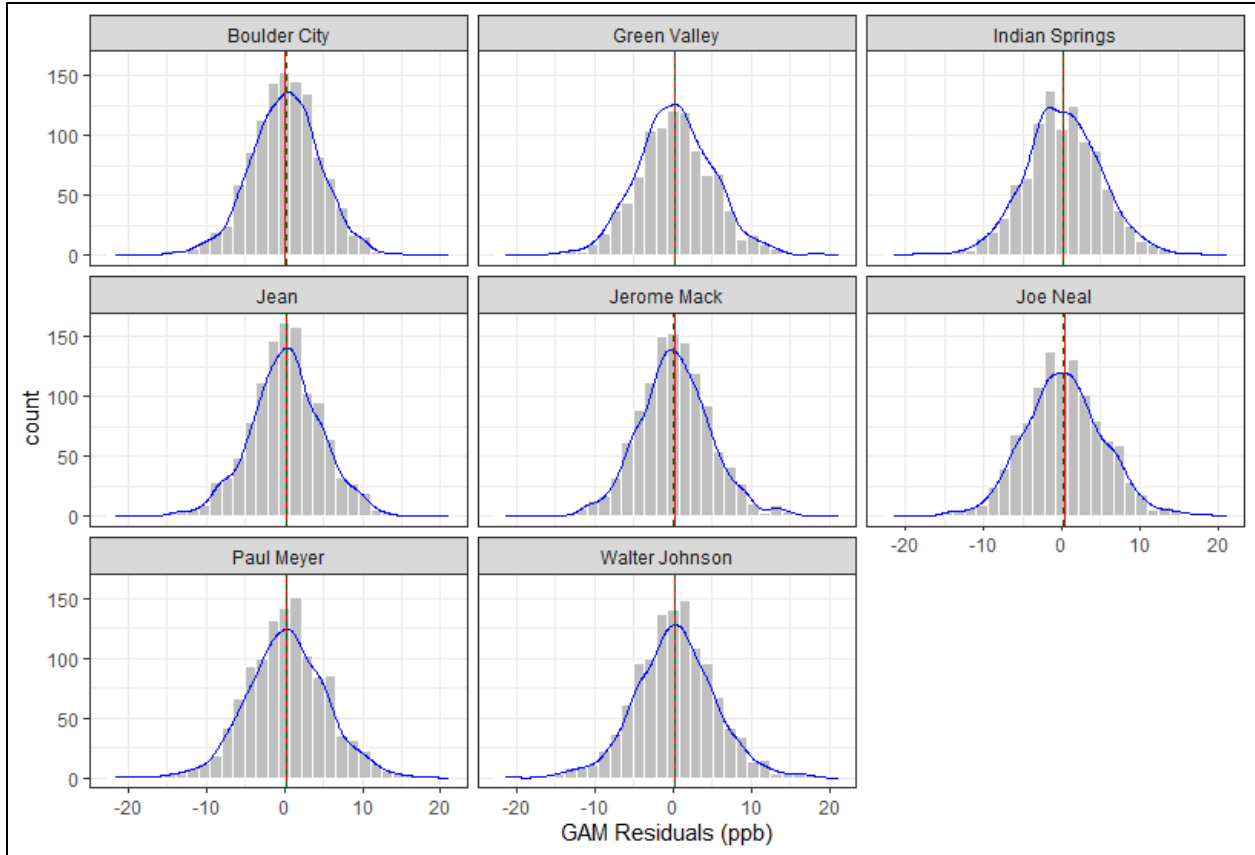
Figure 3-51. Histogram of GAM residuals at all modeled Clark County monitoring sites. The red line indicates the mean and the green dashed line indicates the median. The blue line provides the density distribution.

Within the GAM model, we include HYSPLIT 24-hour distance values, which are factored by cluster, to provide source region and stagnation information into the algorithm. A major upwind pollution source for Las Vegas is the Los Angeles Basin (see the Southern California cluster), which is around 400 km away. Since the GAM model uses source region and distance traveled information to help predict daily MDA8 ozone concentrations, contributions from LA should be accounted for in the algorithm. Based on this, we can assess whether GAM residuals on LA-source region days were significantly different from other source regions. In **Figures 3-52 and 3-53**, we subset the GAM results by removing any potential EE days. From these results, we find that both morning (18:00 UTC) and afternoon (22:00 UTC) trajectory data have similar distributions for all clusters. The notches in the box plots (representing the 95th confidence interval) provide an estimate of statistical difference, and show that the median of residuals is near zero for all clusters. The Northwest U.S. cluster at 18:00 UTC shows slightly negative residuals, while the Long-Range Transport cluster shows slightly positive residuals for both 18:00 and 22:00 UTC. The Southern California cluster shows a median residual of around zero for both 18:00 and 22:00 UTC trajectories, with significant overlap between the 95th confidence intervals of most other clusters (not statistically different). Additionally, the number of data points per cluster (bottom of each figure) corresponds well with transport from California being

dominant for the April through September time frame. Overall, this analysis provides evidence that even when the Los Angeles Basin (Southern California cluster) is upwind of Las Vegas, the GAM model performs well (low median residuals), and the results are statistically similar to most of the other clusters. This implies that when residuals are large, the Los Angeles Basin's influence is unlikely to be the only contributor to enhancements in MDA8 ozone.
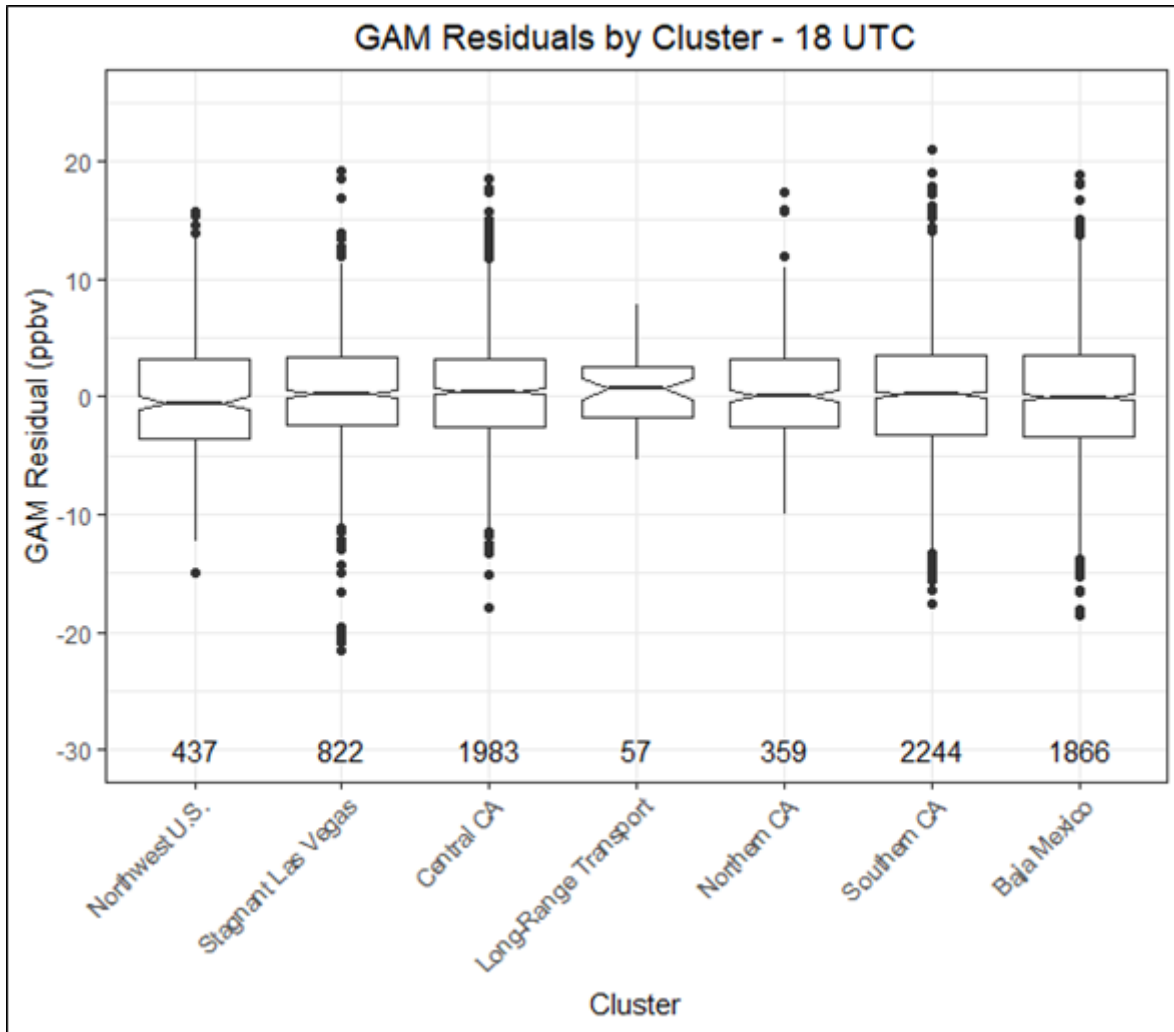
Figure 3-52. GAM cluster residual results for 18:00 UTC. The cluster is determined by grouping 24-hour back trajectories from Las Vegas based on their path. Clusters were created by using back trajectory results from Clark County between 2014 and 2020 (EE days were removed).
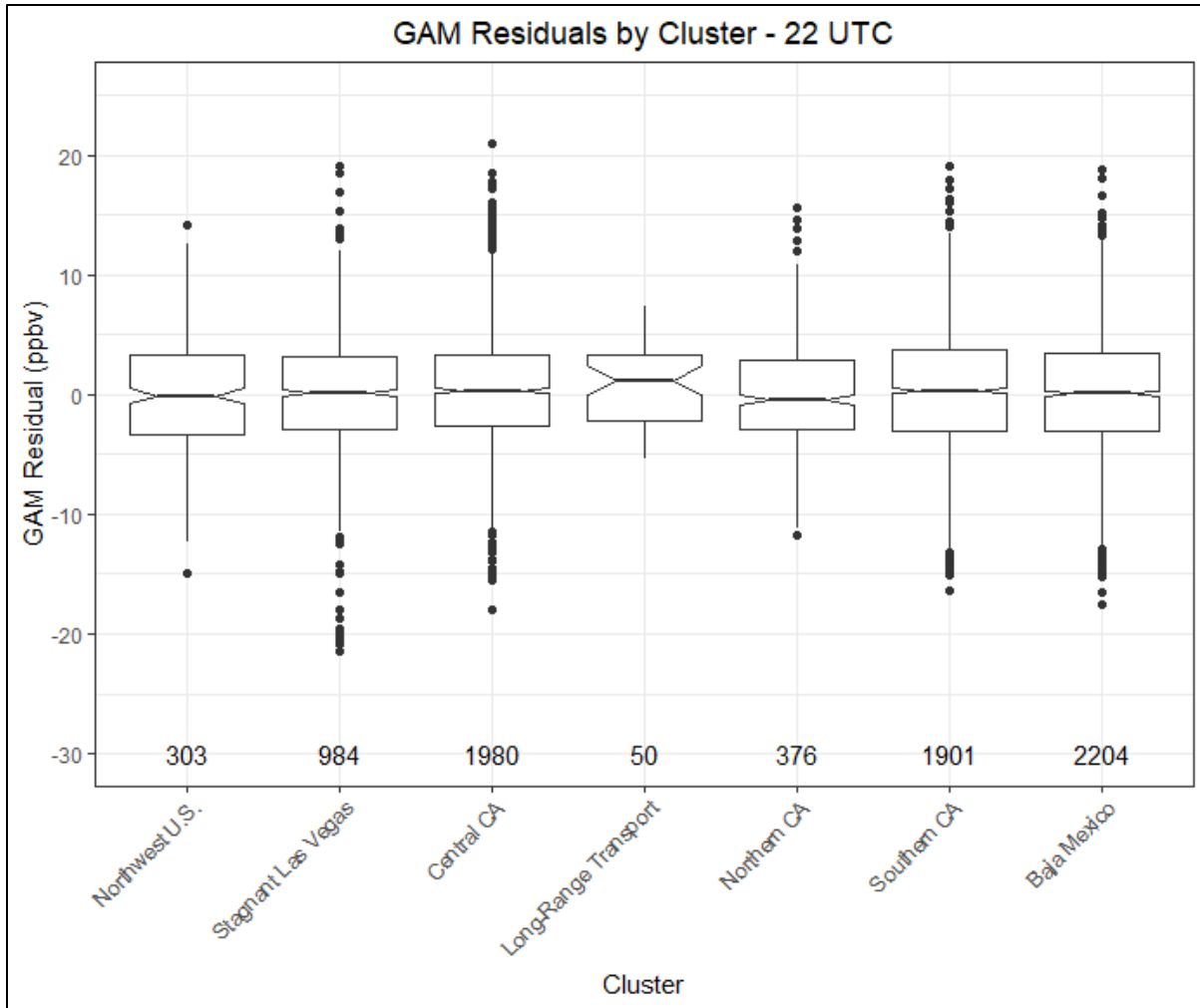
Figure 3-53. GAM cluster residual results for 22:00 UTC. The cluster is determined by grouping 24-hour back trajectories from Las Vegas based on their path. Clusters were created by using back trajectory results from Clark County between 2014 and 2020 (EE days were removed).

Mobile emissions sources decreased throughout the U.S. after COVID restrictions went into place in March 2020. Based on emission inventories from Las Vegas, on-road emissions make up a significant portion of the NO_x emissions inventory (see Section 2.3 for more details). Based on traffic data from the Nevada Department of Transportation, on-road traffic in Clark County in 2020 was significantly different than 2019 through early to mid-June (depending on the area where traffic volume was measured; see Appendix F for more details). Figure 3-54 provides a scatter plot of MDA8 ozone observed versus GAM fit for all eight monitoring sites, separated by year. The linear regression fit, slope, and intercept do not show large difference between 2020 and other modeled years. Figure 3-55 provides a more in-depth look at the most heavily affected months due to COVID restrictions and traffic changes (April – May 2020). The 95th confidence interval (shown as a notch in the box plots) show overlap between 2020 and most other years (except 2015 and 2016). The May 6, 9, and 28 EE days are included in the 2020 box. This analysis shows that there was not a statistically

different GAM response in 2020 compared with other years; this is confirmed in the COVID analysis section (Appendix F), where we show that MDA8 ozone during April – May 2020 in Las Vegas was not statistically different from previous years. While the reduction in traffic emissions due to COVID restrictions did not affect the August 3 event, we thought it was important to address the effects of COVID restrictions on the 2020 GAM results. Overall, ozone in Clark County did not change significantly and, similarly, GAM results were not significantly affected.
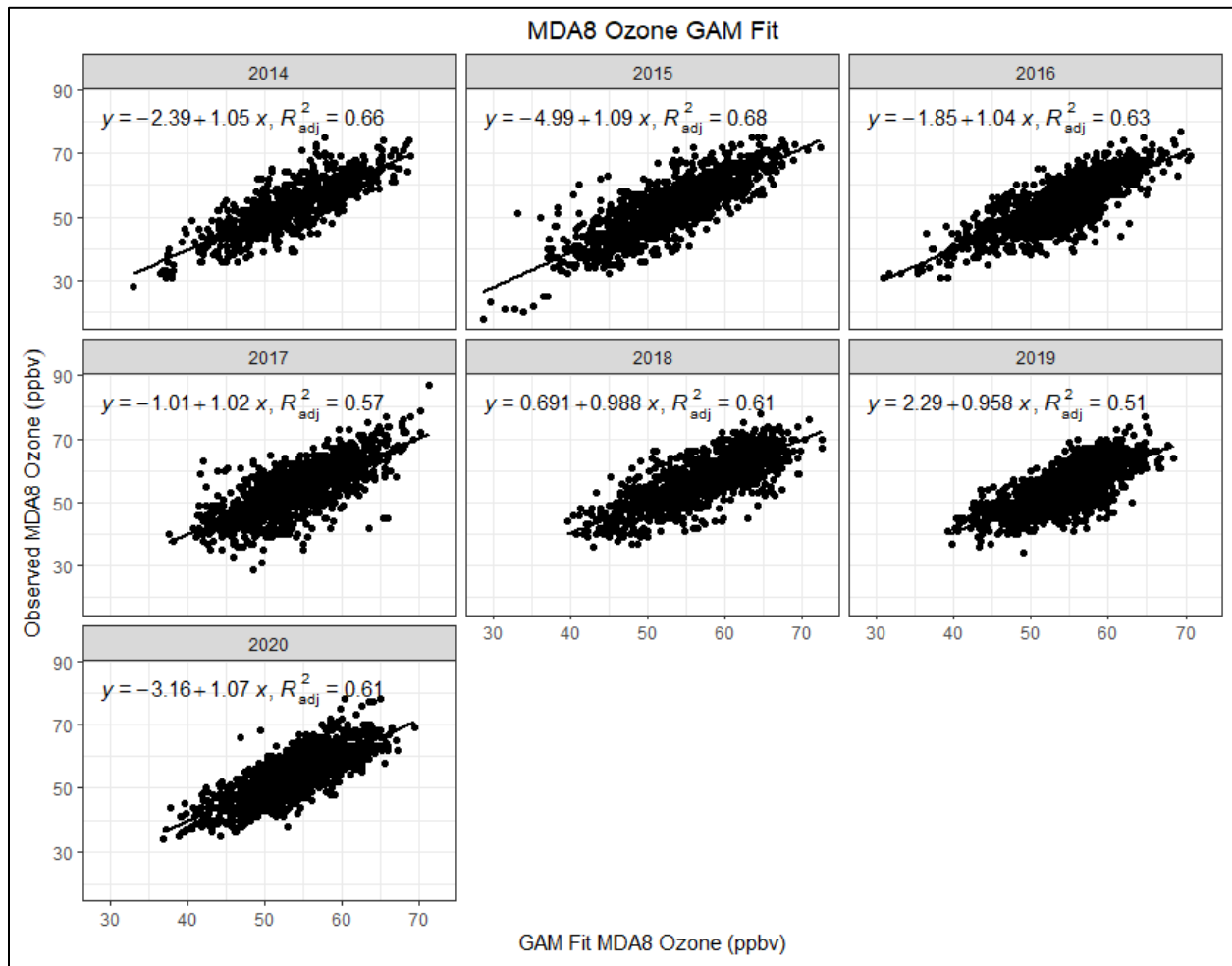
Figure 3-54. Observed MDA8 ozone vs. GAM fit ozone by year. The relationship between observed MDA8 ozone and GAM fit ozone at all eight modeled monitoring sites in Clark County is broken out by year, with linear regression and fit statistics shown (slope, intercept, and r^2). EE days are not included in the regression equations.
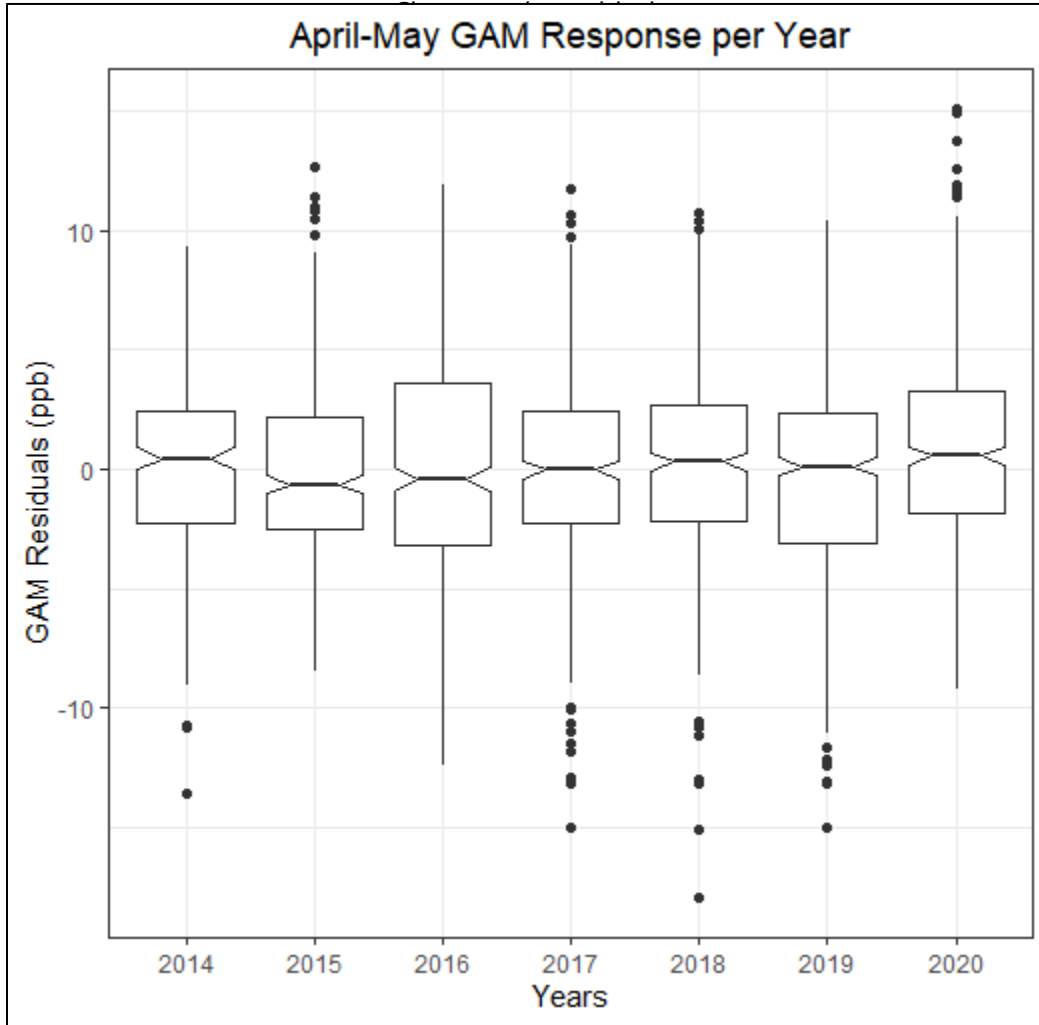
Figure 3-55. April–May Interannual GAM Response. April–May residuals per year from 2014–2020 are plotted for all eight modeled monitoring sites in Clark County. The potential EE days of May 6, 9, and 28 are included.

Figure 3-56 provides the observed MDA8 ozone versus GAM Fit MDA8 from 2014 through 2020 for the sites affected on August 3 (Boulder City, Green Valley, Indian Springs, Jean, Joe Neal, Paul Meyer, and Walter Johnson). We marked the possible 2020 (red), 2018 (blue), and other (purple) EE days to show that observed MDA8 ozone on these days is higher than those predicted by the GAM. The other (purple) points are from 2014–2016 and are suspected wildfire events, as indicated in the EPA AQS record. We also highlight the August 3, 2020, EE day as a large red triangle in each figure. Linear regression statistics (slope, intercept, and r^2) are also provided for context. All linear regressions show a slope near unity, and a low intercept value (around 1-4 ppb) with a good fit r^2 value.
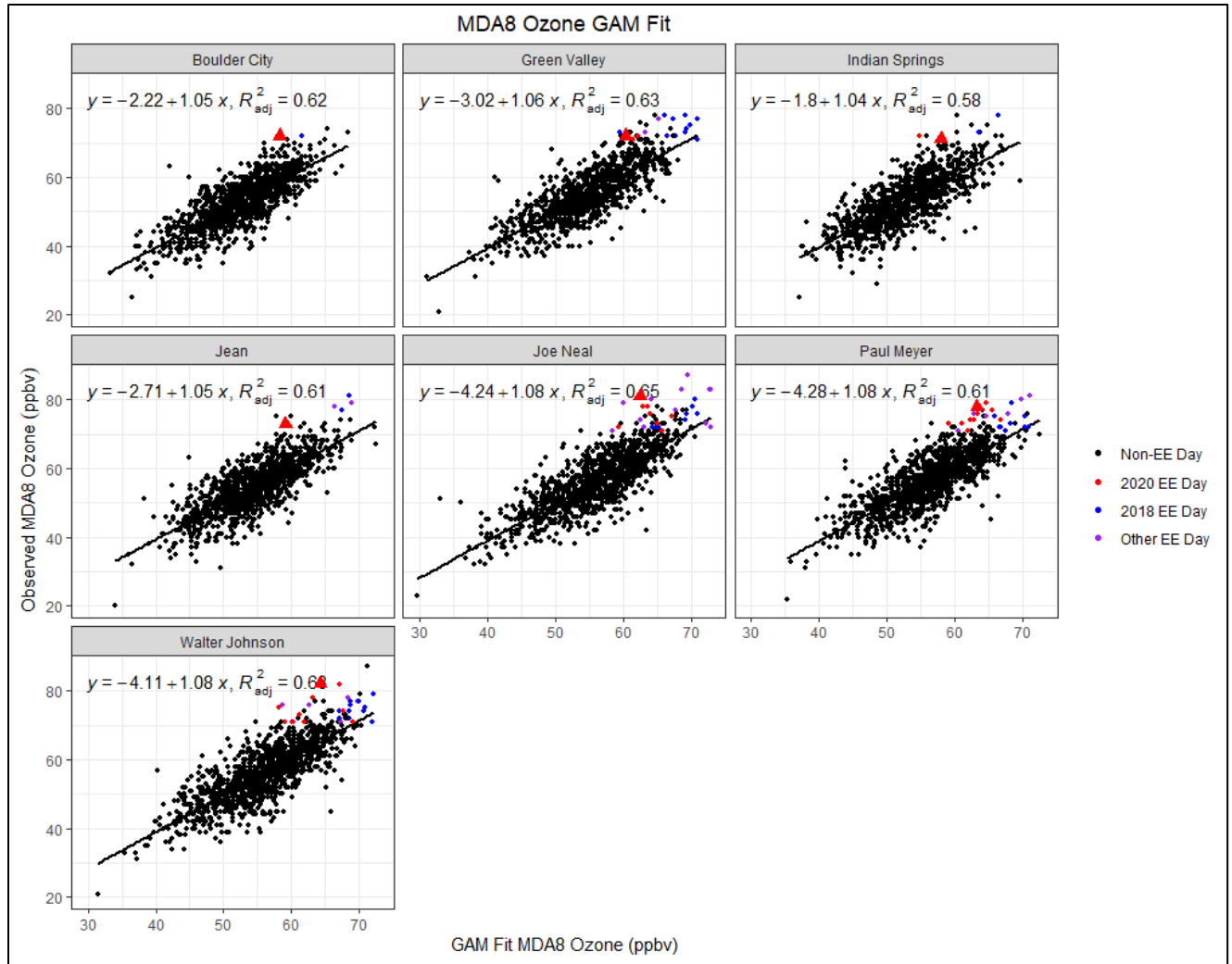
Figure 3-56. GAM MDA8 Fit versus Observed MDA8 ozone data from 2014 through 2020 for the EE affected sites on August 3, 2020. Black circles indicate data not associated with the 2018 or 2020 EE days, red circles indicate 2020 EE days, blue circles indicate 2018 EE days, and purple circles indicate 2014-2016 EE days. August 3 is shown as a red triangle. The black line is the linear regression of the data, and statistics (equation and r² value) are shown in the top of each sub-figure.

Table 3-22 provides the GAM results for August 3, 2020, at each monitoring site affected by the EE. GAM residuals show a modeled wildfire impact between 12 and 19 ppb for all monitoring sites, with MDA8 GAM prediction values well below the 0.070 ppm standard. EPA guidance requires a further level of investigation. By adding the GAM MDA8 Prediction value and the Positive 95th quantile of residuals, we calculated the "No Fire" MDA8 ozone value. The difference between the observed and "No Fire" MDA8 ozone value (2 to 9 ppb) is a conservative estimate of the influence of wildfire smoke at each site. Due to the large number of wildfires affecting Clark County during the 7-year modeling period, we also calculate the "No Fire" and minimum predicted fire influence given the 75th percentile (7 to 13 ppb). This provides a range of minimum smoke enhancement (2 to 13 ppb). The

actual enhancement due to wildfire smoke likely lies between the minimum smoke enhancement estimate and the GAM residual. Previous studies and concurred EE demonstrations show and discuss the limitations of the 95th positive percentile evaluation (Miller et al., 2014; Arizona Department of Environmental Quality, 2016). Additionally, production of ozone is an extremely complex process that can only be predicted by meteorological variables in a GAM model with a 50%-80% correlation based on previously cited papers (our GAM model shows a 55%-61% correlation). In our case, this leaves exceptional events, wildfire influence during high wildfires years, stratospheric intrusions, non-normal emissions, non-normal meteorology, etc., which make up the other 39%-45%. Due to the large number of high wildfires years used in the GAM model, we assert that the minimum predicted fire influence value (as determined by the positive 95th quantile) should not be used as a strict guideline for actual fire influence. Based on the values from the GAM model, we see a significant, non-typical enhancement in MDA8 ozone concentrations at the affected Clark County monitoring sites on August 3, 2020.

Table 3-22. August 3 GAM results and residuals for each site. The GAM residual is the difference between observed MDA8 ozone and the GAM Prediction. We also estimate the minimum predicted fire influence based on the positive 95th quantile and GAM prediction value.

Site Name	MDA8 O$_3$ Concentration[a] (ppm)	MDA8 GAM Prediction[b] (ppm)	GAM Residual (ppm)	Positive 75th-95th Quantile[c] (ppm)	"No Fire" MDA8[b+c] (ppm)	Minimum Predicted Fire Influence[a-(b+c)] (ppm)
Paul Meyer	0.078	0.063	0.015	0.005-0.010	0.068-0.073	0.005-0.010
Walter Johnson	0.082	0.064	0.018	0.005-0.010	0.069-0.074	0.008-0.013
Joe Neal	0.081	0.062	0.019	0.006-0.010	0.068-0.072	0.009-0.013
Green Valley	0.072	0.060	0.012	0.005-0.010	0.065-0.070	0.002-0.007
Boulder City	0.072	0.058	0.014	0.005-0.009	0.063-0.067	0.005-0.009
Jean	0.073	0.059	0.014	0.005-0.009	0.064-0.068	0.005-0.009
Indian Springs	0.071	0.057	0.014	0.005-0.010	0.062-0.067	0.004-0.009

Finally, **Figure 3-57** shows a 2-week time series of observed MDA8 ozone values across Clark County and the GAM prediction values at those sites. August 3, 2020 (and August 7, 2020 – another EE date), shows the large gap between observed MDA8 ozone and the GAM-predicted values. Outside of the possible EE day, the GAM prediction values are very close to the observed values, suggesting that immediately before and after the event, we are able to accurately predict typical fluctuations in ozone on non-event days.
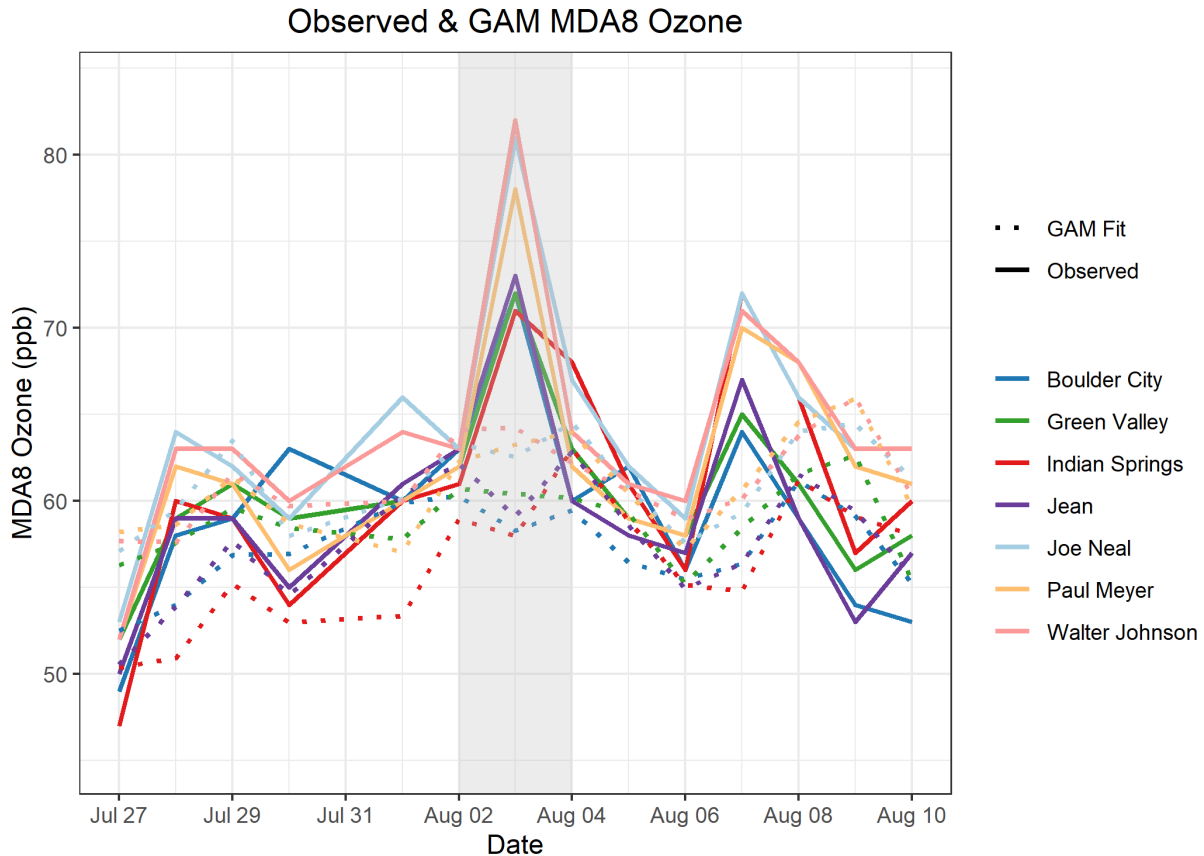
Figure 3-57. GAM time series showing observed MDA8 ozone for two weeks before and after the August 3 EE (solid lines). The GAM MDA8 ozone fit value is also shown for two weeks before and after September 2 (dotted line).

Overall, the GAM evidence clearly demonstrates that a non-typical source of ozone significantly impacted concentrations all EE-affected Clark County sites on August 3, 2020. Coupled with wildfire smoke evidence from all other tiers of analyses, we can conclude by weight of evidence that the enhancement in ozone concentration was due to smoke from the Apple Fire in southern California that was transported to Clark County, Nevada.

3.4   Clear Causal Relationship Conclusions

The analyses conducted in this report support the impact of smoke from the Apple Fire in southern California on ozone concentrations in Clark County, Nevada, on August 3, 2020. We find that:

1. Visible satellite imagery, news articles, and back trajectories support the conclusion of smoke transport from the Apple Fire to Clark County.

2. A large mixing layer, back trajectories starting aloft near the fire and ending at the surface in Clark County, and surface enhancements of wildfire-related pollutants in Clark County support the conclusion that smoke was mixed down to the surface in Clark County.

3. Comparisons with non-event concentrations, meteorologically similar matching day analysis, and GAM statistical modeling support the conclusion that the ozone concentrations seen in Clark County were well above typical summer concentrations.

The analyses presented in this report fulfill the requirements for a Tier 3 exceptional event demonstration, and all conclusions for each type of analysis are summarized in Table 3-23. The effect of the Apple Fire in Clark County caused ozone exceedances at the Paul Meyer, Walter Johnson, Joe Neal, Green Valley, Boulder City, Jean, and Indian Springs monitoring stations. Based on the evidence shown that the Apple Fire was a natural event and unlikely to recur, as well as the clear causal relationship between the wildfire event and the monitored exceedances, we conclude that the ozone exceedance event on August 3, 2020, in Clark County was not reasonably controllable or preventable.

Table 3-23. Results for each tier analysis for the August 3 exceptional event.

Tier	Requirements	Finding
1	- Comparison of fire-influenced exceedance with historical concentrations - Key factor: Evidence that fire and monitor meet one of the following criteria: - Seasonality differs from typical season, or - Ozone concentrations are 5-10 ppb higher than non-event related concentrations - Evidence of transport of fire emissions to monitor: - Trajectories of fire emissions (reaching ground level), or - Satellite Images and supporting evidence from surface measurements - Media coverage and photographic evidence of smoke	- The August 3, 2020, ozone exceedance occurred during a typical ozone season, but event concentrations were significantly higher than non-event concentrations. - Trajectories, satellite images, media coverage, and ground images support smoke transport from the Apple Fire into Clark County.
2	- All Tier 1 requirements - Key Factor #1: Fire emissions and distance of fires - Key Factor #2: Comparison of the event-related ozone concentration with non-event-related high ozone concentrations (high percentile rank over five years/seasons) - Annual and Seasonal Comparison - Evidence that fire emissions affected the monitor (at least one of the following): - Visibility impacts - Changes in supporting measurements - Satellite enhancements of fire-related species (i.e., NOx, CO, AOD, etc.) - Fire-related enhancement ratios and/or tracer species - Differences in spatial/temporal patterns	- Q/d values for the Apple Fire were well below 100. - Ozone concentrations at all sites showed high percentile rank over the past five years and ozone seasons. - Surface concentrations of supporting pollutants show enhanced concentrations and changes in typical diurnal profiles, consistent with smoke. - Satellite measurements also show enhanced levels of fire-related species. - Levoglucosan, a wildfire tracer, showed a positive detection during this event.
3	- All Tier 2 requirements - Evidence of fire emissions effects on monitor: - Multiple analyses from those listed for Tier 2 - Evidence of fire emissions transport to the monitor: - Trajectory or satellite plume analysis, and - Additional discussion of meteorological conditions - Additional evidence such as: - Comparison to ozone concentrations on matching (meteorologically similar) days - Statistical regression modeling - Photochemical modeling of smoke contributions to ozone concentrations	- Meteorology patterns during this event show transport from the Apple Fire area to Clark County. - Vertical profiles show potential for vertical mixing and suggest transport to the surface. - Meteorologically similar day analysis shows that average MDA8 ozone across similar days was well below the ozone NAAQS and 10 ppb lower than the August 3 exceedance at all affected sites. - GAM statistical modeling predicts ozone concentrations lower than observed, suggesting an impact from non-typical sources on ozone concentrations in Clark County during this event.

4.   Natural Event Unlikely to Recur

A wildfire is defined in 40 CFR 50.1(n) as "any fire started by an unplanned ignition caused by lightning; volcanoes; other acts of nature; unauthorized activity; or accidental, human-caused actions, or a prescribed fire that has developed into a wildfire. A wildfire that predominantly occurs on wildland is a natural event." Furthermore, a "wildland" is "an area in which human activity and development are essentially non-existent, except for roads, railroads, power lines, and similar transportation facilities. Structures, if any, are widely scattered." 40 CFR 50.1(o). As shown in Table 3-3, the fire that contributed to this event was caused by human-caused actions, and therefore meets the definition of wildfire. Based on the documentation provided in Section 3.2.1 of this submittal, the Apple Fire in California, which contributed to wildfire smoke in Clark County, predominately took place on wildlands designated as National Forests, as seen in Figure 3-29. Therefore, under 40 CFR §50.1, the fire listed in Table 3-3 can be classified as a natural event that is unlikely to recur. Accordingly, the Clark County Department of Environment and Sustainability has shown in this submittal that smoke from California wildfires, which led to an ozone exceedance in Clark County of August 3, 2020, may be considered for treatment as an EE.

5. Not Reasonably Controllable or Preventable

As shown by the documentation provided in Section 3.2.1 of this submittal, the wildfire listed in Table 3-3 burned predominantly on wildland. The Exceptional Events rule stated in 40 CFR 50.1(j) indicates that a wildfire that occurs on wildland is not reasonably controllable or preventable. Previous sections of this report have shown that each fire referenced in this report was a wildfire that occurred on wildland. The InciWeb report for the Apple Fire indicates that this wildfire burned across vast areas in generally inaccessible land, limiting firefighting efforts in each event (https://inciweb.nwcg.gov/incident/6902/). The Clark County Department of Environment and Sustainability is not aware of any evidence clearly demonstrating that prevention or control efforts beyond those made would have been reasonable. Therefore, the emissions that caused exceedances at monitors in Clark County on August 3 are neither reasonably controllable or preventable.

6.   Public Comment

This exceptional event demonstration will undergo a 30-day public comment period concurrent with EPA's review beginning September 3, 2021. A copy of the public notice, along with any comments received and responses to those comments, will be submitted to EPA after the comment period has closed, consistent with the requirements of 40 CFR 50.14(c)(3)(v). **Appendix G** contains documentation of the public comment process.

7.   Conclusions and Recommendations

The analyses conducted in this report support the conclusion that smoke from the Apple Fire in southern California impacted ozone concentrations in Clark County, Nevada, on August 3, 2020. This exceptional event demonstration has provided the following elements required by the EPA guidance for wildfire exceptional events (U.S. Environmental Protection Agency, 2016):

1. A narrative conceptual model that describes the Apple Fire in southern California and how the emissions from this wildfire led to ozone exceedances downwind in Clark County (Sections 1 and 2).

2. A clear causal relationship between the Apple Fire and the August 3 exceedance through ground and satellite-based measurements, trajectories, emission modeling, comparison with non-event concentrations, vertical profile analysis, and statistical modeling (Section 3).

3. Event ozone concentrations at or above the 99th percentile when compared with the last five years of observations at each site and among the four highest ozone days at each site (Section 3).

4. The Apple Fire was a human-caused accident due to a malfunctioning diesel engine near a wildland interface that grew rapidly and quickly beyond firefighting controls, which classifies this event as unlikely to recur (Section 4).

5. Demonstration that the emissions from the Apple Fire being transported to Clark County was neither reasonably controllable or preventable (Section 5).

6. This demonstration went through the public comment process via Clark County's Department of Environment and Sustainability (Section 6).

The major conclusions and supporting analyses found in this report are:

1. Visible satellite imagery, news articles, and back trajectories support the conclusion of smoke transport from the Apple Fire to Clark County.

2. A large mixing layer, back trajectories starting aloft near the fire and ending at the surface in Clark County, and surface enhancements of wildfire-related pollutants in Clark County support the conclusion that smoke was mixed down to the surface in Clark County.

3. Comparisons with non-event concentrations, meteorologically similar matching day analysis, and GAM statistical modeling support the conclusion that the ozone concentrations seen in Clark County were well above typical summer concentrations.

The analyses presented in this report fulfill the requirements for a Tier 3 exceptional event demonstration, and all conclusions for each type of analysis are summarized in Table 3-23. The effect of the Apple Fire in Clark County caused ozone exceedances at the Paul Meyer, Walter Johnson, Joe Neal, Green Valley, Boulder City, Jean, and Indian Springs monitoring stations. Based on the evidence

shown that the Apple Fire was a natural event and unlikely to recur, as well as the clear causal relationship between the wildfire event and the monitored exceedances, we conclude that the ozone exceedance event on August 3, 2020, in Clark County was not reasonably controllable or preventable.

8.   References

Alvarado M., Lonsdale C., Mountain M., and Hegarty J. (2015) Investigating the impact of meteorology on O_3 and $PM_{2.5}$ trends, background levels, and NAAQS exceedances. Final report prepared for the Texas Commission on Environmental Quality, Austin, TX, by Atmospheric and Environmental Research, Inc., Lexington, MA, August 31.

Arizona Department of Environmental Quality (2016) State of Arizona exceptional event documentation for wildfire-caused ozone exceedances on June 20, 2015 in the Maricopa nonattainment area. Final report, September. Available at https://static.azdeq.gov/pn/1609_ee_report.pdf.

Arizona Department of Environmental Quality (2018) State of Arizona exceptional event documentation for wildfire-caused ozone exceedances on July 7, 2017 in the Maricopa Nonattainment Area. Final report, May. Available at https://static.azdeq.gov/pn/Ozone_2017ExceptionalEvent.pdf.

Bhattarai H., Saikawa E., Wan X., Zhu H., Ram K., Gao S., Kang S., Zhang Q., Zhang Y., Wu G., Wang X., Kawamura K., Fu P., and Cong Z. (2019) Levoglucosan as a tracer of biomass burning: recent progress and perspectives. *Atmospheric Research*, 220, 20-33, doi: 10.1016/j.atmosres.2019.01.004. Available at http://www.sciencedirect.com/science/article/pii/S0169809518311098.

Brey S.J. and Fischer E.V. (2016) Smoke in the city: how often and where does smoke impact summertime ozone in the United States? *Environ. Sci. Technol.*, 50(3), 1288-1294, doi: 10.1021/acs.est.5b05218, 2016/02/02.

Bytnerowicz A., Cayan D., Riggan P., Schilling S., Dawson P., Tyree M., Wolden L., Tissell R., and Preisler H. (2010) Analysis of the effects of combustion emissions and Santa Ana winds on ambient ozone during the October 2007 southern California wildfires. *Atmospheric Environment*, 44, 678-687, doi: 10.1016/j.atmosenv.2009.11.014.

Camalier L., Cox W., and Dolwick P. (2007) The effects of meteorology on ozone in urban areas and their use in assessing ozone trends. *Atmospheric Environment*, 41, 7127-7137, doi: 10.1016/j.atmosenv.2007.04.061.

Clark County Department of Air Quality (2019) Ozone Advance program progress report update. August.

Clark County Department of Environment and Sustainability (2020) Revision to the Nevada state implementation plan for the 2015 Ozone NAAQS: emissions inventory and emissions statement requirements. September. Available at https://files.clarkcountynv.gov/clarknv/Environmental%20Sustainability/SIP%20Related%20Documents/O3/20200901_2015_O3%20EI-ES_SIP_FINAL.pdf?t=1617690564073&t=1617690564073.

Draxler R.R. (1991) The accuracy of rrajectories during ANATEX calculated using dynamic model analyses versus rawinsonde observations. *Journal of Applied Meteorology*, 30, 1446-1467, doi: 10.1175/1520-0450(1991)030<1446:TAOTDA>2.0.CO;2, February 25. Available at https://journals.ametsoc.org/doi/abs/10.1175/1520-0450%281991%29030%3C1446%3ATAOTDA%3E2.0.CO%3B2.

Finlayson-Pitts B.J. and Pitts Jr J.N. (1997) Tropospheric air pollution: Ozone, airborne toxics, polycyclic aromatic hydrocarbons, and particles. *Science*, 276, 1045-1051, (5315).

Gong X., Kaulfus A., Nair U., and Jaffe D.A. (2017) Quantifying O_3 impacts in urban areas due to wildfires using a generalized additive model. *Environ. Sci. Technol.*, 51(22), 13216-13223, doi: 10.1021/acs.est.7b03130.

Gong X., Hong S., and Jaffe D.A. (2018) Ozone in China: spatial distribution and leading meteorological factors controlling O_3 in 16 Chinese cities. *Aerosol and Air Quality Research*, 18(9), 2287-2300. Available at http://dx.doi.org/10.4209/aaqr.2017.10.0368.

Hennigan C.J., Sullivan A.P., Collett J.L., Jr., and Robinson A.L. (2010) Levoglucosan stability in biomass burning particles exposed to hydroxyl radicals. *Geophysical Research Letters*, 37(L09806), doi: 10.1029/2010GL043088. Available at https://www.firescience.gov/projects/09-1-03-1/project/09-1-03-1_hennigan_etal_grl_2010.pdf.

Hoffmann D., Tilgner A., Iinuma Y., and Herrmann H. (2009) Atmospheric stability of levoglucosan: a detailed laboratory and modeling study. *Environ. Sci. Technol.*, 44, 694–699.

Jaffe D., Chand D., Hafner W., Westerling A., and Spracklen D. (2008) Influence of fires on O₃ concentrations in the western U.S. *Environ. Sci. Technol.*, 42(16), 5885-5891, doi: 10.1021/es800084k.

Jaffe D.A., Bertschi I., Jaegle L., Novelli P., Reid J.S., Tanimoto H., Vingarzan R., and Westphal D.L. (2004) Long-range transport of Siberian biomass burning emissions and impact on surface ozone in western North America. *Geophys. Res. Let.*, 31(L16106).

Jaffe D.A., Wigder N., Downey N., Pfister G., Boynard A., and Reid S.B. (2013) Impact of wildfires on ozone exceptional events in the western U.S. *Environ. Sci. Technol.*, 47(19), 11065-11072, doi: 10.1021/es402164f, October 1. Available at http://pubs.acs.org/doi/abs/10.1021/es402164f.

Kimbrough S., Hays M., Preston B., Vallero D.A., and Hagler G.S.W. (2016) Episodic impacts from California wildfires identified in Las Vegas near-road air quality monitoring. *Environ. Sci. Technol.*, 50(1), 18-24. Available at https://doi.org/10.1021/acs.est.5b05038.

Lai C., Liu Y., Ma J., Ma Q., and He H. (2014) Degradation kinetics of levoglucosan initiated by hydroxyl radical under different environmental conditions. *Atmospheric Environment*, 91, 32-39, doi: 10.1016/j.atmosenv.2014.03.054, 2014/07/01/. Available at http://www.sciencedirect.com/science/article/pii/S1352231014002398.

Langford A.O., Senff C.J., Alvarez R.J., Brioude J., Cooper O.R., Holloway J.S., Lin M.Y., Marchbanks R.D., Pierce R.B., Sandberg S.P., Weickmann A.M., and Williams E.J. (2015) An overview of the 2013 Las Vegas Ozone Study (LVOS): impact of stratospheric intrusions and long-range transport on surface air quality. *Atmospheric Environment*, 109, 305-322, doi: 10.1016/j.atmosenv.2014.08.040, 2015/05/01/. Available at http://www.sciencedirect.com/science/article/pii/S1352231014006426.

Louisiana Department of Environmental Quality (2018) Louisiana exceptional event of September 14, 2017: analysis of atmospheric processes associated with the ozone exceedance and supporting data. Report submitted to the U.S. EPA Region 6, Dallas, TX, March. Available at https://www.epa.gov/sites/production/files/2018-08/documents/ldeq_ee_demonstration_final_w_appendices.pdf.

Lu X., Zhang L., Yue X., Zhang J., Jaffe D., Stohl A., Zhao Y., and Shao J. (2016) Wildfire influences on the variability and trend of summer surface ozone in the mountainous western United States. *Atmospheric Chemistry & Physics*, 16, 14687-14702, doi: 10.5194/acp-16-14687-2016.

McClure C.D. and Jaffe D.A. (2018) Investigation of high ozone events due to wildfire smoke in an urban area. *Atmospheric Environment*, 194, 146-157, doi: 10.1016/j.atmosenv.2018.09.021, 2018/12/01/. Available at http://www.sciencedirect.com/science/article/pii/S1352231018306137.

McVey A., Pernak R., Hegarty J., and Alvarado M. (2018) El Paso ozone and PM₂.₅ background and totals trend analysis. Final report prepared for the Texas Commission on Environmental Quality, Austin, Texas, by Atmospheric and Environmental Research, Inc., Lexington, MA, June. Available at https://www.tceq.texas.gov/assets/public/implementation/air/am/contracts/reports/da/582188176307-20180629-aer-ElPasoOzonePMBackgroundTotalsTrends.pdf.

Miller D., DeWinter J., and Reid S. (2014) Documentation of data portal and case study to support analysis of fire impacts on ground-level ozone concentrations. Technical memorandum prepared for the U.S. Environmental Protection Agency, Research Triangle Park, NC by Sonoma Technology, Inc., Petaluma, CA, STI-910507-6062, September 5.

National Weather Service Forecast Office (2020) Las Vegas, NV: general climatic summary. Available at https://www.wrh.noaa.gov/vef/lassum.php.

Pernak R., Alvarado M., Lonsdale C., Mountain M., Hegarty J., and Nehrkorn T. (2019) Forecasting surface O$_3$ in Texas urban areas using random forest and generalized additive models. *Aerosol and Air Quality Research*, 19, 2815-2826, doi: 10.4209/aaqr.2018.12.0464.

Sacramento Metropolitan Air Quality Management District (2011) Exceptional events demonstration for 1-hour ozone exceedances in the Sacramento regional nonattainment area due to 2008 wildfires. Report to the U.S. Environmental Protection Agency, March 30.

Simon H., Baker K.R., and Phillips S. (2012) Compilation and interpretation of photochemical model performance statistics published between 2006 and 2012. *Atmospheric Environment*, 61, 124-139, doi: 10.1016/j.atmosenv.2012.07.012.

Simoneit B.R.T., Schauer J.J., Nolte C.G., Oros D.R., Elias V.O., Fraser M.P., Rogge W.F., and Cass G.R. (1999) Levoglucosan, a tracer for cellulose in biomass burning and atmospheric particles. *Atmospheric Environment*, 33, 173-182.

Simoneit B.R.T. (2002) Biomass burning - a review of organic tracers for smoke from incomplete combustion. *Applied Geochemistry*, 17, 129-162.

Solberg S., Walker S.-E., Schneider P., Guerreiro C., and Colette A. (2018) Discounting the effect of meteorology on trends in surface ozone: development of statistical tools. Technical paper by the European Topic Centre on Air Pollution and Climate Change Mitigation, Bilthoven, the Netherlands, ETC/ACM Technical Paper 2017/15, August. Available at https://www.eionet.europa.eu/etcs/etc-atni/products/etc-atni-reports/etcacm_tp_2017_15_discount_meteo_on_o3_trends.

Solberg S., Walker S.-E., Guerreiro C., and Colette A. (2019) Statistical modelling for long-term trends of pollutants: use of a GAM model for the assessment of measurements of O$_3$, NO$_2$ and PM. Report by the European Topic Centre on Air pollution, transport, noise and industrial pollution, Kjeller, Norway, ETC/ATNI 2019/14, December. Available at https://www.eionet.europa.eu/etcs/etc-atni/products/etc-atni-reports/etc-atni-report-14-2019-statistical-modelling-for-long-term-trends-of-pollutants-use-of-a-gam-model-for-the-assessment-of-measurements-of-o3-no2-and-pm-1.

Texas Commission on Environmental Quality (2021) Dallas-Fort Worth area exceptional event demonstration for ozone on August 16, 17, and 21, 2020. April. Available at https://www.tceq.texas.gov/assets/public/airquality/airmod/docs/ozoneExceptionalEvent/2020-DFW-EE-Ozone.pdf.

U.S. Census Bureau (2010) State & County QuickFacts. Available at http://quickfacts.census.gov/qfd/states/.html.

U.S. Environmental Protection Agency (2016) Guidance on the preparation of exceptional events demonstrations for wildfire events that may influence ozone concentrations. Final report, September. Available at www.epa.gov/sites/production/files/2016-09/documents/exceptional_events_guidance_9-16-16_final.pdf.

U.S. Environmental Protection Agency (2020) Green Book: 8-hour ozone (2015) area information. Available at https://www.epa.gov/green-book/green-book-8-hour-ozone-2015-area-information.

Wigder N.L., Jaffe D.A., and Saketa F.A. (2013) Ozone and particulate matter enhancements from regional wildfires observed at Mount Bachelor during 2004–2011. *Atmospheric Environment*, 75, 24-31, doi: 10.1016/j.atmosenv.2013.04.026, August. Available at http://www.sciencedirect.com/science/article/pii/S1352231013002719.

Wood S. (2020) Mixed GAM computation vehicle with automatic smoothness estimation. Available at https://cran.r-project.org/web/packages/mgcv/mgcv.pdf.

Wood S.N. (2017) *Generalized additive models: an introduction with R*, 2nd edition, CRC Press, Boca Raton, FL.

Zhang L., Lin M., Langford A.O., Horowitz L.W., Senff C.J., Klovenski E., Wang Y., Alvarez R.J., II, Petropavlovskikh I., Cullis P., Sterling C.W., Peischl J., Ryerson T.B., Brown S.S., Decker Z.C.J., Kirgis G., and Conley S. (2020) Characterizing sources of high surface ozone events in the southwestern US with intensive field measurements and two global models. *Atmospheric Chemistry & Physics*, 20, 10379-10400, doi: 10.5194/acp-20-10379-2020. Available at https://acp.copernicus.org/articles/20/10379/2020/acp-20-10379-2020.pdf.